EGE UNIVERSITY
GRADUATE SCHOOL OF
NATURAL AND APPLIED SCIENCES

(Ph.D. THESIS)

DEVELOPMENT OF NEW OPTICAL SENSORS FOR METAL ION SENSING

Nur AKSUNER

Department of Chemistry

Code of discipline: 405.03.01

Date of presentation: 15.02.2008

Supervisor
Prof. Dr. Emür HENDEN

BORNOVA - İZMİR
2008

Nur AKSUNER tarafından **Doktora Tezi** olarak sunulan "**Development Of New Optical Sensors For Metal Ion Sensing"** başlıklı bu çalışma, E.Ü. Lisansüstü Eğitim ve Öğretim Yönetmeliği ile E.Ü. Fen Bilimleri Enstitüsü Eğitim ve Öğretim yönergesi'nin ilgili hükümleri uyarınca tarafımızdan değerlendirilerek savunmaya değer bulunmuş ve 15.01.2008 tarihinde yapılan tez savunma sınavında aday oybirliği / oy çokluğu ile başarılı bulunmuştur.

Jüri Üyeleri: **İmza**

Jüri Başkanı **:** Prof. Dr. Emür HENDEN ....

Üye **:** Prof. Dr. Berrin YENİGÜL ....

Üye **:** Prof. Dr. Ahmet EROĞLU ....

Üye **:** Prof. Dr. Ümran YÜKSEL ....

Üye **:** Doç.Dr. Kadriye ERTEKİN ....

ÖZET

METAL İYONU DUYAR OPTİK SENSÖR GELİŞTİRİLMESİ

AKSUNER, Nur

Doktora Tezi, Kimya Anabilim Dalı

Danışman: **Prof. Dr. Emür HENDEN**

Ocak 2008, 144 sayfa

Bu çalışmanın birinci bölümünde, sensör tanımı ve sınıflandırılması yapılarak, sensörlerin avantaj ve dezavantajları açıklanmıştır. Sensör teknolojisinde kullanılan indikatörler, polimerler ve immobilizasyon yöntemleri anlatılmıştır. Ayrıca çalışılan ağır metallerin insan sağlığı ve çevre açısından önemleri vurgulanmıştır.

Çalışmanın ikinci bölümünde, kullanılan cihazlar, kimyasal reaktifler gibi deneysel parametreler üzerinde durulmuştur. Sensör film hazırlama yöntemleri ve kuantum verimi hesaplanma yöntemi açıklanmıştır.

Çalışmanın üçüncü bölümünde, 4-(1-fenil-1-metilsiklobütil-3-yl)-2-(2-hidroksi-1-naftadien)thiazol (LH) schiff bazı ilk kez PVC filmlere immobilize edilerek Cu^{2+} iyonuna duyar ve seçimli optik sensor geliştirilmiştir. LH ligantının üç farklı çözgen ve PVC matriksdeki fotofiziksel ve fotokimyasal özellikleri araştırılmıştır. Sensörün ortalama yanıt süresinin 2.5 dakika olduğu, 5.0×10^{-8} - 1.0×10^{-4} M aralığında Cu^{2+}'ye doğrusal yanıt verdiği saptanmıştır. Çalışma dalga boyunda diğer metallerin girişim yapmadığı tespit edilmiştir. 5.0-8.0 pH aralığında sensör yanıtında önemli değişiklik olmadığı gözlenmiştir.

Dördüncü bölümde, yine ilk kez 4-(1-fenil-1-metilsiklobüten-3-yl)-2-(2-hidroksi-5-bromobenzildien) aminothiazol (PMC) schiff bazı ve etil selüloz matrikse immobilize edilerek, 1.0 x 10^{-8} M - 5.7 x 10^{-4} M derişim aralığında Cu^{2+} iyonunun tayini gerçekleştirilmiştir. Sensör yanıtında 4.5 – 8.5 pH aralığında önemli değişiklik olmadığı gözlenmiştir. Sensör yaklaşık 2 dakikada dengeye ulaşmakta, 0.01 M HCl ile rejenerasyon işlemi başarıyla yapılmaktadır. Belirtme sınırı 8.8 x 10^{-9} M (0.56 µg L^{-1}) olarak hesaplanmıştır.

Çalışmanın beşinci bölümünde, 2-(2-hidroksi-5-kloro)benzaldehit-[4-(3-metil-3-siklobütil)-1,3-thiazol-2yl]hidrazon (HCB) ligantının verdiği floresansın Zn^{2+} ile kompleks oluşması sonucu sönümünden yararlanarak Zn^{2+} tayini gerçekleştirilmiştir. Bu ligant da ilk kez sensör çalışmasında kullanılmıştır. Sensor 5.0 x 10^{-7} to 9.6 x 10^{-5} M derişim aralığında doğrusal yanıt vermektedir ve belirtme sınırı 2.2 x 10^{-7} M (14.4 µg L^{-1}) olarak hesaplanmıştır. Rejenerasyon işlemi 0.1 M EDTA çözeltisi ile yapılmıştır.

Çalışmanın son bölümünde ise, etil selüloz ve sol-gel matrikse morin immobilizasyonuna dayalı Al^{3+} sensörü geliştirilmiştir. pH 4.8'de etil selüloz matrikse dayalı sensörün çalışma aralığı 1.0 x 10^{-7}-5.0 x 10^{-4} M ve sol-gel matrikse dayalı sensörün çalışma aralığı 2.0 x 10^{-6} - 2.0 x 10^{-3} M olarak saptanmıştır.

Anahtar Sözcükler: Schiff bazı; PVC matriks; Etil selüloz matriks; Sol-gel matriks; Fluoresans spektroskopisi; Optik sensör; Bakır(II); Çinko(II); Aluminyum(III).

ABSTRACT

DEVELOPMENT OF NEW OPTICAL SENSORS FOR METAL ION SENSING

AKSUNER, Nur
Ph. D. in Chemistry
Supervisor: **Prof. Dr. Emür HENDEN**
January 2008, 144 pages

In the first chapter of this study, definition and classification of the sensors were made and their advantages and disadvantages were given. The indicators and polymers used in sensors were given and immobilization techniques used in sensor technology were explained. The importance of the heavy metals used in this study in human health and environment were summarized.

The second part of the thesis is about experimental. In this section apparatus and chemicals used in this study were given and procedure of the sensor film preparation was given. The way of quantum yield calculation was also explained.

In the third chapter of this study, a highly sensitive and selective determination of Cu(II) was accomplished by using a new sensor prepared by embedding a cyclobutane-substituted schiff base ligand into PVC films. The photophycial and photochemical characteristics of a thiazole derivative 4-(1-phenyl-1-methylcyclobutyl-3-yl)-2-(2-hydroxy-1-naphtylidene)thiazole

(LH) in three different solvents and plasticized PVC matrix were determined. The membrane respond was sensitive to Cu^{2+} in the 5.0 x 10^{-8} - 1.0 x 10^{-4} M range for an average exposure time of 2.5 min. No significant effect of interferents was observed at the working wavelength. It has a reproducible response and provides an inexpensive and quick method for the determination of Cu^{2+}. It has also been shown that the response of this sensor does not vary significantly in the pH range 5.0 – 8.0.

The newly prepared optode described in the fourth chapter of the study proved that the immobilized 4-(1-phenyl-1-methylcyclobutane-3-yl)-2-(2-hydroxy-5-bromobenzylidene) aminothiazole (PCT) dye can be used for Cu^{2+}sensing in the concentration range of 1.0 x 10^{-8} - 5.7 x 10^{-4} M. It has a reproducible response and provides an inexpensive and quick method for the determination of Cu^{2+}. It has been shown that the response of this sensor does not vary significantly in the pH range 4.5 – 8.5. The approximate response time was measured as 2 min. The sensor can easily be regenerated by treatment with 0.01 M HCl. A very low LOD, 8.8 x 10^{-9} M (0.56 μg L^{-1}) was reached.

In the fifth chapter of the study, a new optical sensor has been developed for the selective determination of Zn^{2+} ions. The reversible sensing system was prepared by embedding 2-(2-hydroxy-5-chloro)benzaldehyde-[4-(3-methyl-3-mesitylcyclobutyl)-1,3-thiazol-2yl]hydrazone (HCB) in plasticized PVC membrane. The response of the sensor is based on the fluorescence quenching of HCB by Zn^{2+} ions. The proposed sensor displays a calibration response for Zn^{2+} over a wide concentration range of 5.0 x 10^{-7} to 9.6 x 10^{-5} M with a detection limit of 2.2 x 10^{-7} M (14.4 μg L^{-1}). The sensor can readily be regenerated with 0.1 M EDTA solution.

In the last chapter of the study, an optical sensor has been proposed for the determination of aluminum. These sensors developed were based on immobilization of morin in ethyl cellulose matrix and sol-gel matrix. The response to the concentration of Al^{3+} at pH 4.8 is linear in ethyl cellulose and sol-gel matrix in the range of 1.0 x 10^{-7}-5.0 x 10^{-4} M, and 2.0 x 10^{-6} to 2.0 x 10^{-3} M respectively.

Key Words: Schiff base; PVC matrix; Ethyl cellulose matrix; Sol-gel matrix; Fluorescence spectroscopy; Optical sensor; Copper(II); Zinc(II); Aluminum(III)

ACKNOWLEDGEMENT

I would like to present my gratitude to my supervisor, Prof. Dr. Emür HENDEN, for his kind supervision, precious support and patience.

I am very thankful to Prof. Dr. Berrin YENİGÜL, member of Ph. D. thesis committee for her suggestions during my study. I present my gratitude to Prof. Dr. Ahmet EROĞLU, member of Ph. D. thesis committee for his suggestions during my study.

I also thank to Doç. Dr. Kadriye ERTEKİN for her valuable contribution during the preparation of this thesis.

I would like to thank The Scientific and Technological Research Council of Turkey and Ege University Research Found for financial support during this study.

I also thank to all of the members of the chemistry department and especially to the members of the analytical chemistry division for providing the conditions and support throughout my studies. I would like to thank to my friends who have encouraged and helped me throughout my work.

Finally, I would like to thank and present my gratitude to my family and especially to my mother Ülkü ERDEM, my father M. Kemal ERDEM, my dear husband Hakan AKSUNER and my dear daughter Bade AKSUNER for their encouragement, understanding, support and patience during the study.

CONTENTS

Page

CONTENTS (CONTINUE)

CONTENTS (CONTINUE)

CONTENTS (CONTINUE)

CONTENTS (CONTINUE)

CONTENTS (CONTINUE)

LIST OF FIGURES

LIST OF TABLES

ABBREVIATIONS

Abbreviations	**Explanations**
EC	Ethyl cellulose
PVC	Polyviniyl chloride
DOP	bis-(2-ethylhexyl)phtalate
DOS	bis(2-ethylhexyl)sebecate
DOA	bis-(2-ethylhexyl)adipate
PTCPB	potassiumtetrakis-(4chlorophenyl)borate
THF	tetrahydrofuran
TEOS	tetraethyl ortosilicate
LH	4-(1-phenyl-1-methylcyclobutyl-3-yl)-2-(2-hydroxy-1-naphtylidene) thiazole
PCT	4-(1-phenyl-1-methylcyclobutane-3-yl)-2-(2-hydroxy-5-bromobenzylidene) aminothiazole
HCB	2-(2-hydroxy-5-chloro)benzaldehyde-[4-(3-methyl-3-mesitylcyclobutyl)-1,3-thiazol-2yl]hydrazone

1. CHAPTER ONE – INTRODUCTION

1.1. Analytical Aspects of Sensors

A sensor is a device capable of continuously and reversibly recording a physical parameter or the concentration of a chemical or biochemical species. Typical examples for a mechanical, electrochemical, and optical sensor, respectively, are the mercury thermometer, the pH glass electrode, and a nonbleeding pH paper strip. Ideally, such a sensor can be stuck directly into the sample, and the result of the measurement is displayed within a few seconds. No sampling, addition of reagent, or dilution is required. This is a most distinct feature of sensors, since these operations are known to introduce errors into all kinds of analytical assays (Wolfbeis, Vol.1, 1991).

Continuous sensing of chemical analytes is a matter of growing interest by virtue of the real-time nature of most sensors. Increasing concern about environmental quality, and – in a more and more cost-conscious world – considerable personnel savings in comparison to manual off-line methods contribute to the desirability of sensors. Hence, tremendous effort has been devoted to the development of various sensing devices which, partially in combination with lab rotobic systems, will enable analyses to be performed fully automatically or on-line, e.g., in product and food control, in the clinical lab, and in many other fields of routine analysis.

Certain devices, which do not act fully reversibly but are suitable for single use, have also been called sensors. It is suggested that, instead, the word probe be used for these in order to make a rough differentiation, although the borderline between sensors and probes is vanishing. Another differentiation may be made between sensors (or probes) and so-called dosimeters, which are designed for cumulative assay. Dosimeters, in contrast to sensors and probes, do not give real-time data and are not reversible.

A great variety of transducers sensitive to heat, light, anions and cations, gases, electron transfer, mass changes, conductance, and light depolarization are known and compete successfully with each other. Among these, the electrochemical sensing method is potentiometry, and pH-sensing glass electrodes have been used over decades for the determination of pH as such, but also for carbon dioxide which reversibly changes the pH of a bicarbonate buffer, and ammonia, which affects the pH of an ammonium ion buffer. pH electrodes have been applied as transducers for bioprocesses in which protons are produced or consumed (Turner, 1987).

Different definitions of sensors are given in the literature and discussion about the features and the requirements of sensors is still going on. The chemical sensor descriptions from an IUPAC commission on sensors are given below;

“A chemical sensor is a device that transforms chemical information ranging from the concentration of a specific sample component to total composition analysis into analytical useful signal. The chemical information mentioned above may originate from a chemical reaction of the analyte or from a physical property of the system investigated. A chemical sensor is an essential component of an analyzer. In addition to the sensor, the analyzer may contain that perform the following functions: sampling, sample transport, signal processing, data processing” (Wolfbeis, Vol. 1, 1991).

1.2. Sensor Classification

Sensors can be classified in many different ways (Figure 1.1). They may be classified according to the principle of operation of transducer in two main groups as “physical” and “chemical” sensors. They also can be divided into sub groups as optical, electrochemical, electrical, mass sensitive, magnetic and thermometric devices. They can also be classified as direct and indirect sensors or as reversible or non-reversible and respect of their applications or sizes.

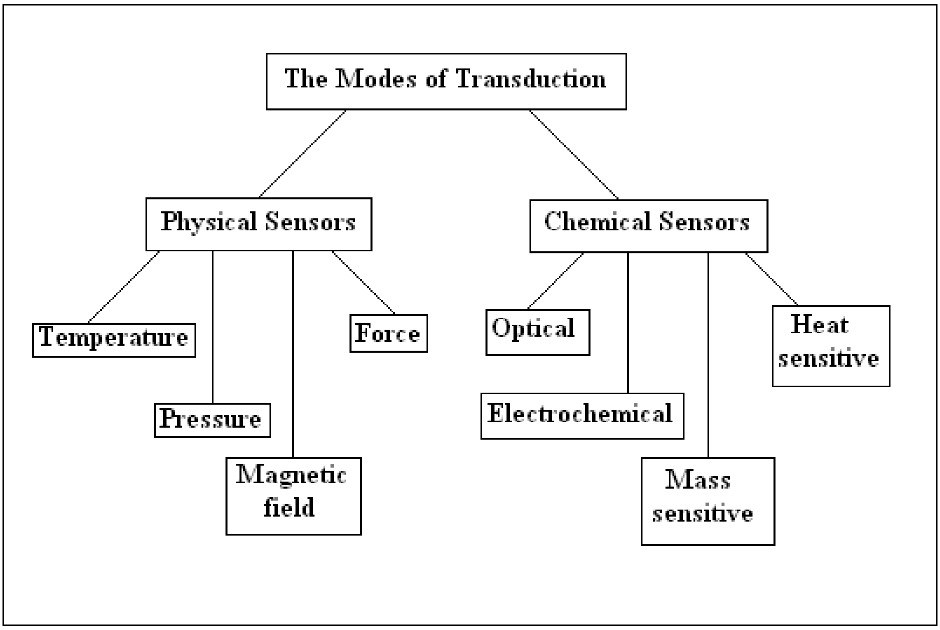

Figure 1.1. General classification of sensors

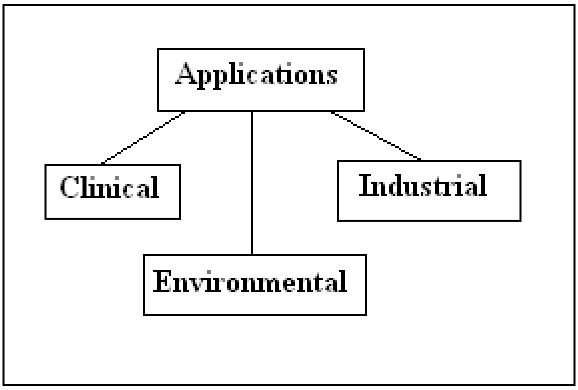

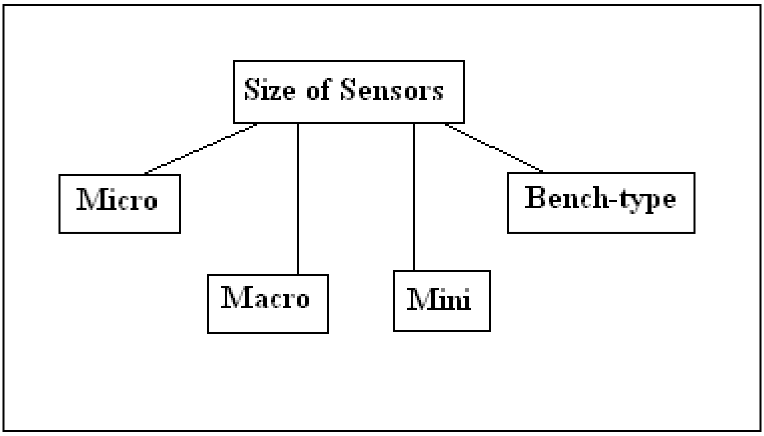

Figure 1.1. General classification of sensors

So many different kinds of sensors are commercially available; some of them are described below.

1.2.1. Semiconducting oxide sensors

The heated metal oxide sensor is probably the most investigated and widely produced chemical sensor. The working principle of this type of sensor is that the resistance of metal oxide semiconductor changes when it is exposed to the target gas reacts with the metal oxide surface and changes its electronic properties. New materials such as the rare earth oxides or gallium oxide are being used as the active sensor elements. Recent reviews include many examples of this type of gas sensors (Gopel and Schierbaum, 1995; Shimizu et al., 1999).

1.2.2. Electrochemical sensors (liquid electrolyte)

There are two major sensor classes that use liquid electrolytes: amperometric and potentiometric sensors. The earliest example of an amperometric gas sensor, the Clark oxygen sensor used for the measurement of oxygen in the blood is more than 40 years old. The amperometric sensor produces current signal, which is related to the concentration of the analyte by Faraday's law and laws of mass transport (Cao et al., 1992).

1.2.3. Ion-selective electrodes

Ion-selective electrodes (ISEs) belong to potentiometric chemical sensor group and are most often based on the measurement of the interfacial potential at an electrode surface caused by a selective ion exchange reaction. The well known glass pH electrode is a typical ISE (Galster, 1991).

1.2.4. Solid electrolyte sensors

Using a solid electrolyte to replace the liquid electrolyte in an electrochemical sensor, one can construct a solid electrolyte electrochemical sensor. Solid electrolyte sensors are typically designed to operate at high temperature and can operate in either a potentiometric or amperometric mode. Over the past ten years, two potentiometric designs have evolved: surface-modifed solid electrolyte gas sensors and mixed potential gas sensors (Yamazoe and Miura, 1996; Göpel et al., 2000; Mukundan et al., 1999).

1.2.5. Optical chemical sensors

They have become an important area of research since their introduction two decades ago. Optical sensors are compact and ideally suited to miniaturization while at the same time they are resisting to electrical interference and utilize the simplicity of photometric measurements. Many optical chemical sensors utilize color complexing or redox reagents immobilized in suitable polymeric membrane (Ensafi and Bakhshi, 2003; Ensafi and Aboutalebi, 2005). Optical chemical sensors can be classified in three groups: Probes, fiber-optic chemical sensors and non fiber optic chemical sensors. Sensors which produce an irreversible response to the presence of analytes are referred to as ‘probes’. If the signal is reversible and continuous then it as called as sensor. Fiber optic sensors are based on optical spectroscopy performed on sites inaccessible to conventional spectroscopy, over large distances, or even on several spots along the fiber.

1.2.5.1. Advantages of optical sensing

Depending on the field of application, optical sensing can offer one or more of the following advantages over other sensor types:

❖ Optrodes do not require a reference signal as in potentiometry, where the difference of two absolute potentials is measured. The need for reference electrodes makes potentiometric sensors, particularly those intended for use in disposable probes, relatively costly. Moreover, the liquid-liquid junction between the two electrolytes is prone to perturbations and can be considered to be weakest "link" in all potentiometers (Christiansen, 1986).

❖ The ease of miniaturization allows the development of very small, light, and flexible sensors. This is of great utility in case of minute sample volumes and in designing small catheters for invasive sensing in clinical chemistry and medicine.

❖ Low loss optical fibers allow transmittance of optical signals over wide distances. Remote sensing makes it possible to perform analyses when samples are hard to reach, dangereous, too hot or too cold, in harsh environments or radioactive.

❖ Because the primary signal is optical, it is not subject to electrical interferences by static electricity of the body, strong magnetic fields, or surface potentials of the sensor head. On the other hand, fibers do not present a risk to patients since there are no electrical connections to the body.

❖ Analyses can be performed in almost real time without any need of sampling.

❖ Since several fiber sensors placed in different sites can be coupled to one fluorimeter, the method allows multiple analyses with a single control instrument.

❖ Coupling of small sensors for different analytes to produce a sensor bundle of small size allows simultaneous monitoring of various analytes by hybrid sensors without crosstalk of the single strands.

❖ In many cases the sensor head does not consume the analyte in a measurable rate as, for instance, in the case of polarographic electrodes. This fact is of particular advantage in case of extremely small sample volumes.

❖ Fiber optical sensing is non-destructive analytical method.

❖ Fibers are manufactured from nonrusting materials, so that they have excellent stability. They are also resistant to radiation.

❖ Especially sensors based on dynamic fluorescence quenching have a useful dynamic range often larger than that of electrochemical sensors.

❖ Most fiber sensors can be employed over a wider temperature range than electrodes and some have a smaller temperature dependence.

❖ Many oxygen and pH sensors are steam-strerilizable.

1.2.5.2. Disadvantages of optical sensing

Notwithstanding a number of advantages, optical sensors exhibit the following disadvantages:

❖ Ambient light can interfere. Therefore optical sensors must either be used in dim or dark surroundings or the optical signal must be encoded so that it can be resolved from ambient background light or it must be covered with an optically tight layer.

❖ Sensors with indicator phases are likely to have limited long term stability because of photobleaching or wash out.

❖ Since in indicator phase sensor analyte and indicator are in different phases, there is a mass transfer necessary before a steady-state equilibrium and consequently a constant response is established. This, in turn, limits response time for analytes with small diffusion coefficients. This situation makes it desirable to keep the volume of the analyte accessible indicator phase much smaller than that of the sample in order not to dilute sample volume.

❖ Sensors with immobilized pH indicators as well as chelating reagents have limited dynamic ranges as compared to electrodes.

❖ The fiber optics used at present have impurities of a spectral nature that can give background absorption or emission.

❖ More selective indicators have to be found for various important analytes and the immobilization chemistry has to be improved for better selectivity and sensitivity.

Despite several limitations, optical sensors have the potential of becoming an attractive alternative to other sensing methods and to perform diagnostic, environmental, or clinical functions better, faster, more accurately, or less expensively than existing approaches.

1.2.5.3. Optical measurement techniques

❖ Amplitude change based ones
– absorption
– fluorescence, luminescence
– spectral-dependent variations of absorption/fluorescence
– refractive index
– scattering
❖ Time resolved changes (luminescence, absorption)
❖ Polarization changes
❖ Phase changes – interferometry

Spectroscopic methods (Absorption and fluorescence method): Most optical sensors are based on absorption and fluorescence methods. Absorption method is simple and easy to use but it is not very sensitive, requiring the use of a high concentration of the indicator and/or a thick sensing layer. Fiber-optic sensors based on absorption method are difficult to miniaturize, especially for transmission mode in which a sensing element has to be placed between two face to face fibers. Reflection configuration, sometimes using a reflector, is often employed to overcome this problem (Motellier et al., 1993). In addition, evanescentwave (EW) or attenuated total reflection modes can also be used (Egami et al., 1997; Yang and Saavedra, 1995). In contrast, fluorescence method is more sensitive and can be used for small-size sensors and/or low concentration of indicators (Tan et al., 1992).

1.2.6. Fiber optic chemical sensors

Over the past 20 years two major product revolutions have taken place due to the growth of the optoelectronics and fiber optic communications industries. The optoelectronics industry has brought about such products as compact disc players, laser printers, bar code scanners, and laser pointers. The fiber optic communications industry has literally revolutionized the telecommunications industry by providing higher-performance, more reliable telecommunication links with ever-decreasing bandwidth cost. This revolution is bringing about the benefits of high-volume production to component users and a true information superhighway built of glass.

In parallel with these developments, fiber optic sensor (Culshaw, 1996; Grattan, 1998) technology has been a major user of technology associated with the optoelectronic and fiber optic communications industry. Many of the components associated with these industries were often developed for fiber optic sensor applications. Fiber optic sensor technology, in turn, has often been driven by the development and subsequent mass production of components to support these industries. As component prices have fallen and quality improvements have been made, the ability of fiber optic sensors to displace traditional sensors for rotation, acceleration, electric and magnetic field measurement, temperature, pressure, acoustics, vibration, linear and angular position, strain, humidity, viscosity, chemical measurements, and a host of other sensor applications has been enhanced. In the early days of fiber optic sensor technology, most commercially successful fiber optic sensors were squarely targeted at markets where existing sensor technology was marginal or in many cases nonexistent. The inherent advantages of fiber optic sensors, which include (1) their ability to be lightweight, of very small size, passive, low-power, resistant to electromagnetic interference, (2) their high sensitivity, (3) their bandwidth, and (4) their environmental ruggedness, were heavily used to offset their major disadvantages of high cost and end-user unfamiliarity.

The situation is changing. Laser diodes that cost $3000 in 1979 with lifetimes measured in hours now sell for a few dollars in small quantities, have reliability of tens of thousands of hours, and are widely used in compact disc players, laser printers, laser pointers, and bar code readers. Single-mode optical fiber that cost $20/m in 1979 now costs less than $0.10/m, with vastly improved optical and mechanical properties. Integrated optical devices that were not available in usable form at that time are now commonly used to support production models of fiber optic gyros. Also, they could drop in price dramatically in the future while offering ever more sophisticated optical circuits. As these trends continue, the opportunities for fiber optic sensor designers to product competitive products will increase and the technology can be expected to assume an ever more prominent position in the sensor marketplace. In the following sections the basic types of fiber optic sensors being developed are briefly reviewed followed by a discussion of how these sensors are and will be applied (Francis and Shizhuo, 2002).

Fiber optic sensors which rely on a change in the light of transmission characteristics of fiber caused by an alteration in a specific physical property of a medium being sensed are classified as intrinsic sensors. In extrinsic fiber optic sensors, any kind of optical spectroscopy is coupled with fiber optic technique. They may be subdivided into three as first, second and third generation sensors. In the first type, the fiber simply acts as a light guide. It allows remote spectrometric analysis of the analyte having an intrinsic optical property. These sensors are also called bare-ended fiber sensors or plain fiber sensors. Due to the variety of chemical species does not have an analytically useful intrinsic optical property, in a second group the analytical information of interest is mediated by some sort of indicator chemistry. However for a variety of analytes there are no indicators known or they do not fulfill certain requirements such as react without addition of reagents or being highly specific. In order to perform the analysis of these species, third order generation sensors have been developed. In this type a biocatalytic process is usually coupled to either plain fiber sensors or an indicator mediated sensor. The term biosensors can be applied to all kinds of sensors suitable for sensing biological systems (Wolfbeis, Vol. 1, 1991).

1.3. Optical Chemical Sensors for the Determination of Heavy Metal Ions

Recent years, chemical sensors for heavy metal ions have seen an increasing interest. A ‘metal sensor’ is described as a device which is capable of responding to the presence of a heavy metal ion in a reversible and continuous manner. Sensors which produce an irreversible response to the presence of heavy metal ions are referred to as ‘metal probes’. The optical properties of a material may be measured by the conventional methods of absorbance, fluorescence and reflectance spectroscopy, and in various formats such as test strips and disposable tips, while employing optical waveguides such as optical fibers, integrated optics and capillary type devices (Oehme and Wolfbeis, 1997).

1.3.1. Sensors based on intrinsic optical properties

So far, the optical sensors discussed have been based on an immobilized reagent which acts as a chemical transducer for the desired analyte. However, there are sensors which rely on the intrinsic optical properties of heavy metal ions. In this case, quantification is achieved via the measurement of the absorbance or luminescence of the sample solution. Suitable analytes for this mode of measurement include the transition metal ions Fe (II), Co (II), Cu (II), Cr (III), Ni (II) (Andrew and Worsfold, 1994), the lanthanide ions europium and terbium, and the radionuclides uranium and plutonium. Such sensors lack specificity since they are subject to interference from any species absorbing at the same wavelength as the analyte, and sample turbidity and changes in refractive index will also have a significant effect. Absorbance based analysis is applicable only at relatively high concentrations of heavy metal ions because their molar absorptivities are low, typically 10-100 mol^{-1} dm^3 cm^{-1}.

1.3.2. Sensors based on chromophores

The majority of heavy metal ion sensors are based on the use of an indicator dye which undergoes a binding reaction with the ions. This reaction is accompanied by a change in the absorbance or fluorescence of such chelators. In other words, an indicator acts as a transducer for the chemical species that can not be determined directly by optical means. This has an important implication in that it is the concentration of the indicator species that is quantified rather than the analyte itself.

Many indicators can not be used in optical sensors because of unfavorable analytical wavelengths, poor photostability, low molar absorptivity or the need for additional reagents. Most of them bind with the metal ion irreversibly or only at low or high pH so they can not be used for continuous sensing at near neutral pH. Upon binding with the metal ion, most indicators undergo a change in colour, with one band appearing as the other disappears, rather than an intensity change of one single band.

1.3.3. Sensors based on fluorophores

In contrast to chromogenic reagents, fluorescent indicators are of the yes/no type in that only one of the species (the complexed or the noncomplexed) is fluorescent. Fluorescent indicators frequently provide improved sensitivity (which is important in miniature sensors) and also selectivity because it is unlikely that an interfering species would have the same absorbance and emission as the analyte complex. Fluorimetry (and luminescence spectrometry in a wider sense) also offers a broad variety of spectroscopic techniques including the measurement of lifetime, polarization and energy transfer. An important group of indicators is based on quenching of luminescence by heavy metals and transition metals. In the case of static quenching, the quencher interacts with the fluorophore in its ground state. In dynamic (collisional) quenching, the interaction between the metal ion (quencher) and the fluorophore occurs in the excited state only and leads to a reduction in both the emission intensity and the decay time. The photophysical process of dynamic quenching is fully reversible, that is, the indicator is not consumed. Hence, quenching efficiency of many transition metals, in particular Fe(III), Co(II) and Ni(II) are thought to be due to their numerous unpaired spins.

1.3.4. Sensors based on ionophores

Due to limitations of conventional reagents (mainly caused by their high stability constants) there has been an increase in the use of ionophores in optical chemical sensors. Ionophores are non-coloured ion-complexing organic molecules, or lipophilic ion carriers, which are capable of reversibly binding to ions and transporting them across organic membranes by carrier translocation. Their most widespread application so far is in ion-selective membranes for alkali and alkaline earth metal ions, the best example being valinomycin, highly specific neutral carrier for potassium ions (Wolfbeis and Schaffar, 1987; Hisamoto et al., 1995). Several sensing schemes are used in which ionophore selectivity is combined with an optical readout, namely (a) the introduction of chromoionophores or fluorogenic moieties into ionophores to obtain so-called chromoionophores or fluoroionophores, (b) the combination of ionophores with potentially sensitive indicators, (c) the extraction of ions into membranes using neutral ion carriers (ion exchange), and (d) the extraction of an ion along with a counter ion into a membrane phase (coextraction). Recognition of heavy metals is accomplished by neutral ionophores capable of binding the metal ion, while the optical signal is provided by a proton selective chromoionophore. On extraction of a heavy metal ion (of charge n) into the membrane, n protons are released by the chromoionophore, resulting in a change in its colour or fluorescence. The interesting feature of this approach is that it is only the carrier for a specific heavy metal ion that needs to be varied, while the chromoionohore can remain the same.

1.4. Sensor Chemistry - Indicators

All kinds of extrinsic second generation optical sensors require some sort of indicator chemistry which converts the analyte concentration into an optical signal. In other words, an indicator acts as a transducer for the chemical species that cannot be determined directly by optical means. Consequently, it is the concentration of the indicator species that is determined rather than the analyte itself.

Indicators can be categorized as either absorbance and fluorescence based. Most absorbance based indicators undergo a color change rather than an intensity change of one band only. Usually, both the complexed and uncomplexed species have an absorption of comparable intensity in the visible.

Fluorescence indicators, in contrast, are frequently of the yes/no type in that only one of the species (the complexed or the uncomplexed one) is fluorescent. Hence, absolute fluorescence intensity can be measured with no background from a second species. However, internal two-wavelength referencing is sometimes more difficult. Another disadvantage of fluorescent indicators results from the fact that they are prone to quenching by species other than the analyte. Finally, most fluorophores have lower molar absorbance (as compared to color indicators) and cannot be excited by green, yellow, or red LEDs, or by semiconductor lasers. On the other hand, fluorescence indicators provide distinctly improved sensitivity (which is important in case of minute sensor size) and selectivity because it is unlikely that an interfering species has the same absorption and emission as the indicator. Finally, fluorimetry offers a broad variety of additional techniques including dynamic quenching, lifetime measurements, energy transfer, and combinations of them (Wolfbeis, Vol. 1, 1991).

1.4.1. pH indicators

Sensors for physiological pHs are of greatest importance. Indicators may be classified according to their chemical structures in order to demonstrate the influence of substituents on pK_a values and spectral properties. But although a great variety of both colored and fluorescent pH indicators are known, only a few meet the requirements of an ideal pH sensor for measurement in the physiological pH range (Bistop, 1972; Kotyk and Slavik, 1988; Fernandez-Guttierez and Munoz de la Pena, 1985).

1.4.1.1. Absorbance-based indicators

Among the great variety of organic chromophores such as azo dyes, nitrophenols, phthaleins, sulfophthaleins, aniline- sulfophthaleins, triphenylmethane dyes, polymethines, and others, only a few have so far been considered to be useful and applied to sensor technology. These dyes are phenol red (Peterson et al., 1980; Suidan et al., 1983), chlorophenol red and bromothymol blue (Bacci et al., 1988; Kirkbright, 1984), and alizarin (Suidan et al., 1983).

1.4.1.2. Fluorescent indicators

Fluorescent indicators have been applied more often than absorbance based indicators in optrodes, such as,

❖ Coumarins

❖ Fluoresceins

❖ Naphthyl and pyrene derivatives

❖ Lipophilic pH indicators

1.4.2. Metal indicators

There are many types of compounds that form colored complexes with metal ions and therefore can be employed as indicators in optical sensors provided that the experimental conditions are suitably chosen. Metal indicator chemistry is fairly well established (Cheng et al., 1982; Fernandez-Guttierez and Munoz de la Pena, 1985) and a number of textbooks and rewievs are available for long-known indicators so that there is no need to go into detail.

Crown ether dyes have found particular attention (Katayama et al., 1988; Van Gent et al., 1988). These compounds are designed to bring about specific color changes on the interaction with metal cations such as alkali and alkaline earth metals, thus serving as probes or photometric reagents selective for these metal ions.

1.4.3. Redox indicators

Fluorescent redox dyes where color depends on oxidation state have been useful in biochemical studies in conjunction with microscopic or flow cytofluorometric techniques, but await their application to optical sensors for the redox state of systems such as biofermenters. The change from the oxidized to the reduced form should be accompanied by a marked color change and fully reversible. The redox potential of the indicator may then be chosen appropriately so to provide some selectivity for the redox process to be monitored in the system under investigation.

1.4.4. Potential-sensitive dyes

These comprise a quite different class of dyes which respond to an electrical potential (V/cm) created at an interface. Thus, they do not directly report the concentration or an activity of a chemical species, but rather an electromagnetic parameter. They provide an interesting alternative to sensors based on conventional chromogenic chelators. Most of the work with potential-sensitive dyes (PSDs) so far is on measurement of membrane potential of cells and tissue (Szöllösi et al., 1987). PDSs are usually placed directly at the site where an electrical voltage is applied or where such a potential is created in a fashion similar to ion-selective electrodes, using an ion carrier incorporated into a lipid membrane.

Various reasons have given for the response of PSDs towards electrolytes. Changes in membrane potential can occur as a result of

(1) charge separation across the membrane (caused, for instance, by an added ionophore),

(2) streaming potentials at the membrane surface caused by the sample solution passing by,

(3) possibly, the formation of diffusional potentials.

These changes in potential result in optical changes which, in turn, may be due to a variety of effects (Wolfbeis and Schaffar, 1987).

1.4.4.1.Cationic potential-sensitive dyes

Positively charged carbocyanines are membrane-permeant and distribute across the membrane according to the membrane potential. Fluorescence changes as large as 80 % associated with a redistribution of the dyes between cells and the extracellular medium during hyperpolarization have been monitored (Beeler et al., 1981). The rhodamine dyes comprise another class of cationic PSDs. Among these, rhodamine 6G (Dietzman et al., 1987), rhodamine 123, and rhodamine B octadecyl ester (Zhujun and Seitz, 1988) have been found to be useful for measurements of membrane potential in sensors. The rhodamine esters are nontoxic, highly fluorescent dyes which do not form aggregates or display binding-dependent changes in fluorescence efficiency.

1.4.4.2. Anionic potential-sensitive dyes

Oxonol dyes undergo slow potential dependent absorpsion changes without alteration in the state of dye aggregation (Zhujun and Seitz, 1988). The voltage-dependent partitioning between water and the membrane is usually measured by differential absorption changes rather than fluorescence. The lipophilic fluorescent pH indicator, 7-hydroxy-4-tridecylcoumarin, also has found use as a PDS (Fromherz and Kotulla, 1984).

1.4.4.3. Neutral potential-sensitive dyes

Styryl dyes containing an (aminostyryl)pyridinium chromophore are fast-responding PSDs. The fast-response is the result of a direct potential-sensitive change in the electronic distribution within the dye that results in spectral shifts (Fluhler et al., 1985).

1.5. Materials and Polymers in Optical Sensing

1.5.1. Requirements for sensor polymers/materials

- Solubility of indicator chemistry in polymer matrix
- Selectivity and sensitivity (solubility of the analyte, free analyte diffusion)
- Good operational lifetime and shelf-life
- No crystallisation/migration/reorientation of components
- No ageing effects
- Stability at elevated temperatures (sterilisability)
- Stability against ambient light
- Stability against chemicals (acids, bases, oxidants)
- Mechanical stability
- Transparency for light
- No intrinsic colour/luminescence of the polymer matrix
- Biocompatibility (no toxicity of components)

1.5.2. Types of polymers used in optical sensing

1.5.2.1. Lipophilic polymers and plasticizers

Polymers that have a high glass transition temperature (Tg) are brittle (Figure 1.2). They require plasticizers to make them flexible. Furthermore, the high density/rigidity of the polymer chains (without plasticizers) hinders diffusion of ions and gases in the polymer matrix. Therefore, plasticizer to polymer ratios of up to 2:1 are required (Figure 1.3). While PVC is soluble in tetrahydrofuran and cyclopentanone, polymers such as PMMA, PS and PVAc are also soluble in ethyl acetate, ethylmethyl ketone, dichloromethane, etc.

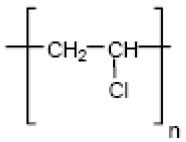

poly(vinyl chloride) PVC
(Tg ~90° C)

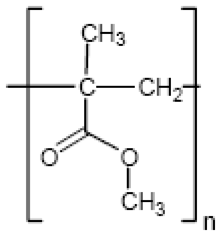

poly(methyl methacrylate)
PMMA (Tg ~100° C)

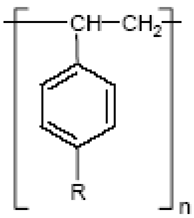

polystyrene-derivatives
PS (Tg 100-140° C)

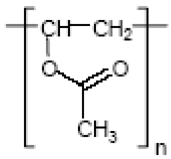

poly(vinyl acetate
PVAc (Tg ~30° C)

Figure 1.2. Lipophilic polymers that have a high glass transition temperature
(taken from http://www2.uni-jena.de/~c1moge/Mohr/ASCOS2002.pdf)

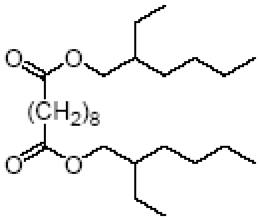

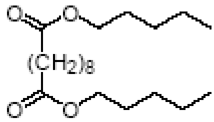

bis(2-ethylhexyl) sebacate DOS

Dibutyl sebacate DBS

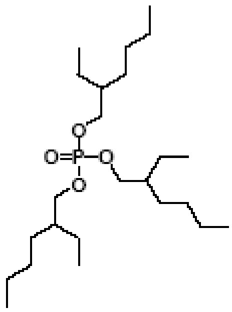

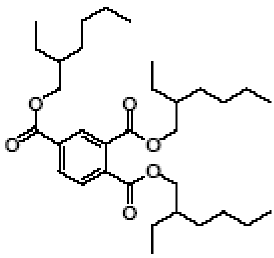

tris(2-ethyl-hexyl) phosphate TOP

tris(2-ethylhexyl) trimmelitate

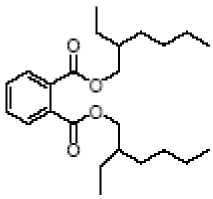

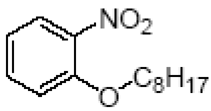

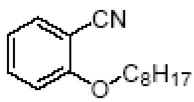

bis(2-ethylhexyl) phthalate DOP

2-nitrophenyl octyl ether NPOE

2-cyanophenyl octyl ether CPOE

Figure 1.3. Lipophilic plastizers

(taken from http://www2.uni-jena.de/~c1moge/Mohr/ASCOS2002.pdf)

Polymers with low glass transition do not require plasticizers (Figure 1.4). However, these compounds are often unpolar and, consequently, bad solvents for polar ligands, ionophores, dyes, and analytes.

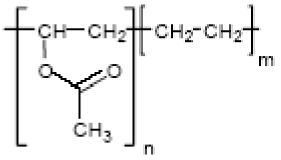

poly(ethylene vinyl acetate) PEVA

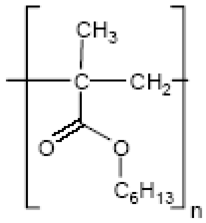

poly(hexyl methacrylate) PHMA (Tg -4° C)

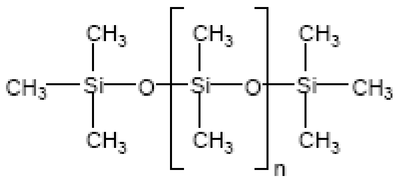

poly(dimethyl siloxane) (ε ~ 3, Tg -80 to -40° C)

cis-polybutadiene (ε ~ 2, Tg -100° C)

Figure 1.4. Polymers with low glass transition
(taken from http://www2.uni-jena.de/~c1moge/Mohr/ASCOS2002.pdf)

Reinhoudt et al. have presented siloxane copolymers with reactive methacrylate groups and polar substituents which exhibit a behaviour and polarity similar to plasticized PVC but have the advantage that all components can be covalently linked to the polymer matrix (by copolymerisation) (Reinhoudt et al., 1994).

1.5.2.2. Hydrophilic polymers

Hydrophilic polymers (Figure 1.5) provide a matrix which corresponds to an aqueous environment. Ions can diffuse quite freely, but the possible water uptake (10-1000%) can cause significant swelling of the polymer. Swelling of the matrix affects the optical properties of the sensors and, consequently, the signal changes.

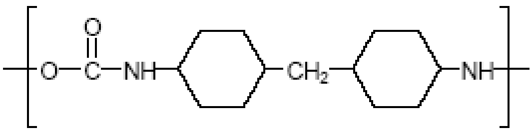

polyurethane PU

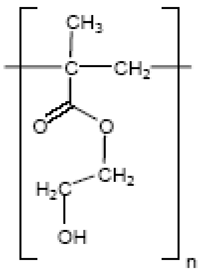

poly(2-hydroxyethyl methacrylate) PHMA

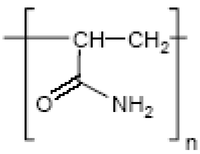

poly(acryl amide) PAA

Figure 1.5. Hydrophilic polymers
(taken from http://www2.uni-jena.de/~c1moge/Mohr/ASCOS2002.pdf)

1.5.2.3. Ionic polymers (Polyelectroytes)

Polyelectrolytes exhibit a large amount of dissociable groups (Figure 1.6). These compounds are often used for ion-exchange chromatography. They can also be used to exchange their counterions with indicator ions.

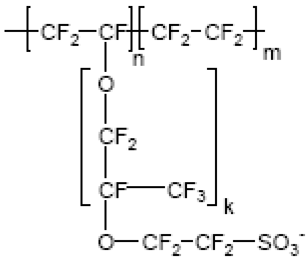

Nafion™

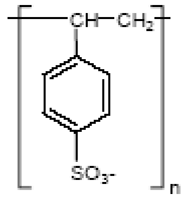

polystyrene sulfonates

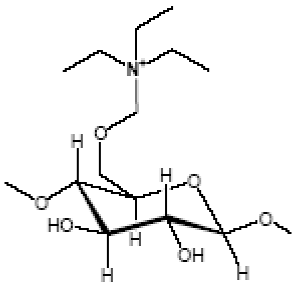

triethylammonium-methylcellulose

TEAE-C

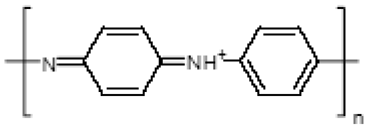

polyaniline

Figure 1.6. Ionic polymers

(taken from http://www2.uni-jena.de/~c1moge/Mohr/ASCOS2002.pdf)

1.5.2.4. Molecularly imprinted polymers (MIPs)

Molecular imprinting can be accomplished in two ways: the self assembly approach and the preorganisation approach. The first involves host guest complexes produced from weak intermolecular interactions (such as ionic or hydrophobic interaction, hydrogen bonding) between analyte and the functional monomers. The self assembled complexes are spontaneously formed in the liquid phase and are sterically fixed by polymerisation. After extraction of the analyte, vacant recognition sites specific for the imprint are established. Monomers used for self assembly are methacrylic acid, vinylpyridine and dimethylamino methacrylate.

The preorganisation approach involves formation of strong reversible covalent arrangements (boronate esters, imines, ketals) of the monomers with the print molecule before polymerisation. Thus, the print molecule has to be chemically derivatised with the monomers before actual imprinting is performed. After cleaving the covalent bonds and removal of the print molecules, recognition sites complementary to the analyte are obtained again.

Optical sensors based on molecular imprints can be obtained by co-polymerising indicator dyes that respond to the analyte by changing their colour. Another approach is to label the analyte with small dye molecules, perform imprinting, and then measure the competitive release of the labeled molecule when the MIP is exposed to the actual analyte (Mohr, 2006).

1.6. Immobilization Techniques

Following the choice of indicator and polymeric support, the next step is immobilization of the dye on the support to give the sensing scheme. Three methods are important for the preparation of sensing chemistries namely mechanical, electrostatic and covalent immobilization. Fluorescent indicators should not be covalently bond to polymers by azo – coupling because most azo dyes do not fluorescence except for certain metal complexes of orto-hydroxy azo compounds. However, certain indicators nonfluorescent in bulk solution exhibit fluorescence when adsorbed on a solid support or contained in a rigid polymer. Immobilization of most dyes result in a small change of their spectral characteristics. In addition there are frequently considerably shifts in pKa values, binding constants and in particular dynamic quenching constants. The changes reflect the various interactions between neighbor dye molecules and polymer surface and also electronic effects on covalent bonds.

1.6.1. Mechanical Immobilization

Mechanical (physical) immobilization involves adsorption and encapsulation of molecules in a sphere which they can not leave. The capsulation method is usually confined to large molecules which react with low molecular weight analyts that can permeate the membrane. Surface adsorption or deposition is favored way in case of gaseous samples which do not present the risk of washing out the indicator dye.

1.6.2. Electrostatic Immobilization

When the surface of a rigid support is fitted with charged groups such as sulfo groups or quarternerized ammonium groups, the material is capable of binding ions having opposite charge. For example sulfonated polystyrene binds cations with varying binding strength. This effect is widely used to separate anions or cations from a solution and for enrichment of trace amounts of ions. They may be displaced from the solid phase with strong acid or base. The charged functional groups at the polymer surface are also capable of binding oppositely charged indicators. Numerous ion exchange materials are commercially available and may be classified “strong” and “weak” ion exchangers. This refers to the binding strength of the material to the respective cation or anion. Both membrane and bead type ion exchange materials are available. In order to firmly bind organic dye ions, the use of strong ion exchangers is advisable so to prevent washout of the dye with time. The major advantages of electrostatic immobilization are to ease of procedure and its reproducibility. Loading can be easily governed by the time of immobilization.

1.6.3. Chemical (covalent) Immobilization

Chemical immobilization can be accomplished by creating a covalent bond between indicator and the polymer surface. Covalent immobilization of enzymes, antigens, antibodies, and even whole bacteria can be achieved by both surface immobilization on a solid support and by cross-linking the material with protein like albumin.

In order to covalently bond between indicator to polymer surface one or two activation steps are usually required to make reagents undergo to facilitate room temperature reaction. The first step usually involves the modification of the polymer to provide it with a sufficiently reactive function. A similar procedure may be required when the indicator does not possess chemical functions suitable for immobilization. Numerous methods of surface modification of polymers exist but, as noted earlier, the fluorescent indicators should not be covalently bond to polymers by azo-coupling with a few exceptions.

Covalent surface modification of quartz, kieselgel, silicagel, conventional glass and metals such as iron and platinium can be achived with reagents of the type $(RO)_3Si\text{-}R'$ (R=ethyl or methyl, R'= aminopropyl, 3-chloropropyl, 3-glicidyloxy, vinyl or a long chain amine).

Cellusose can be modified by reaction with cyanogen bromide followed by a treatment with long chain diamine.

Carboxymethylcellulose (CMC) and aminoethyl cellulose are commercially available in various modifications. Polyacrylamide (PAA) is low of reactivity but can be activated by surface saponification with strong alkaline hydroxide. Subsequent acidification yields a material having carboxy groups which are capable of covalent binding to amines. Carboxy modified polyacrylamid, crosslinked polyacrilic acid, and carboxy modified PVC are commercially available and capable of coupling to amine type indicators.

Polymers such as polyvinyl alcohols, polyglycols or the strongly basic polyethylene offer alternatives but tend to swell or dissolve in water (Wolfbeis, Vol I, 1991).

1.7. The Sol-gel Process

The sol-gel process allows the preparation of glass films where indicator chemistry can be incorporated. The production of ceramic materials and glassy networks is based on the polymerisation of suitable precursors at low temperature. The increasing popularity of sol-gels in sensor applications results from the processing versatility.

There are a number of variables which affect the hydrolysis and condensation rates and hence the microstructure of the sol-gel glass. The detailed microstructure of sol-gel glasses depends on parameters such as nature and concentration of the catalyst, water sol-gel precursor ratio (R), precursor type, nature of the solvent, ageing time, ageing temperature, drying time and drying temperature. The process can be adapted for formation of thin sensor layers. At the sol stage, thin glass films can be formed by dip-coating or spin-coating. These films are porous and are used for sensor applications.

Components of the sol-gel cocktail are the sol-gel precursor, water, a catalyst, the indicator and a solvent such as ethanol. The sol-gel precursors are mostly low molecular weight alkoxysilanes such as tetramethoxysilanes (TMOS) and tetraethyl ortosilicate (TEOS). Mixing these components causes hydrolysis of the ester, silanol-ester condensation, and silanol-silanol condensation of the precursors. In this process, the alkoxy groups hydrolyze and the hydroxy groups condense.

The sol-gel process involves the preparation of inorganic matrices via three steps. This general reaction scheme can be seen in Equations 1.1, 1.2 and 1.3.

$Si(OR)_4 + H_2O \rightarrow Si(OR)_3OH + ROH$ (hydrolysis) (1.1)

$Si(OR)_3OH + Si(OR)_4 \rightarrow Si(OR)_3\text{-O-}Si(OR)_3 + ROH$ (condensation) (1.2)

$R\text{-}Si\text{-}OH + HO\text{-}Si\text{-}R \rightarrow R\text{-}Si\text{-}O\text{-}Si\text{-}R + H_2O$ (condensation) (1.3)

1.7.1. Hydrolysis and condensation reactions

The hydrolysis reaction (Eq. 1.1), through the addition of water, replaces alkoxide groups (-OR) with hydroxyl groups (-OH). Subsequent condensation reactions (Eq 1.2 and 1.3) involving the silanol groups (Si-OH) produce siloxane bonds (Si-O-Si) plus the by-products water or alcohol. Under most conditions, condensation begins before hydrolysis is complete. However, conditions such as pH, H_2O/Si molar ratio (R), and catalyst can force completion of hydrolysis before condensation begins (Keefer, 1990). Additionally, because water and alkoxides are immiscible, a mutual solvent such as an alcohol is utilized. With the presence of this homogenizing agent, alcohol, hydrolysis is facilitated due to the miscibility of the alkozide and water (Prassas and Hench, 1988).

The first phase in the process is the formation of the “sol”. A sol is a colloidal suspension of solid particles in a liquid. Colloids are solid particles with diameters of 1-100 nm. As the number of siloxane bonds increases, the individual molecules are bridged and jointly aggregate in the sol. After a certain period, the colloidal particles and condensed silica species link to form a “gel”- an interconnected, rigid network with pores of submicrometer dimensions and polymeric chains whose average length is greater than micrometer. After the sol-gel transition, the solvent phase is removed from the interconnected pore network. If removed by conventional drying such as evaporation, so-called “xerogel” are obtained, if removed via supercritical evacuation; the product is an “aerogel” (Figure 1.7).

“Ageing” is the process that take place after mixing precursor, water, solvent and catalyst to form a sol, but before coating, in the case of coating sols. Ageing or pre-polymerisation of the sol causes aggregation due to hydrolysis and condensation reactions, and consequently an increase in viscosity. During this step, the sol is allowed to stand either at room temperature or at a higher temperature for a period of time during which hydrolysis and condensation reactions cause aggregation and cross-linking.

The “gel point” is defined as the point at which the entire solid mass becomes interconnected. The physical characteristics of the gel network depends upon the size of particles and extent of cross-linking prior to gelation. Acid-catalysis leads to a more polymeric form of gel with linear chains as intermediates. Base catalysis yields colloidal gels where gelation occurs by cross-linking of the colloidal particles.

Sol-gel glass is ion-permeable due to residual hydroxy groups and its porosity, and can be used to optically measure pH by entrapping (caging) conventional pH indicator dyes in the material. Often, water soluble indicator dyes do not have to be chemically modified for immobilisation because due to their size they are retained in the pores of the sol-gel glass and do not wash out.

Ormosils (organically modified siloxanes) represent hybrid systems in which several precursor types such as organotrialkoxysilanes or diorganodialkoxysilane precursors ($R'Si(OR)_3$ or $R'_2Si(OR)_2$, respectively) are combined in which R′ represents a non-hydrolyzable organic substituent (e.g. methyl or phenyl). The substituent R′ can also be a reactive aminopropyl group which allows subsequent covalent binding of indicators. Ormosils are not as hydrophilic and brittle as conventional sol-gel glass. If the content of alkyl chains R′ increases, then the material turns hydrophobic and ion-impermeable. Nevertheless, due to its gas permeability, it can be used for sensing acidic or basic gases which permeate the material and react with indicator dyes (e.g. by protonation/deprotonation of pH indicators).

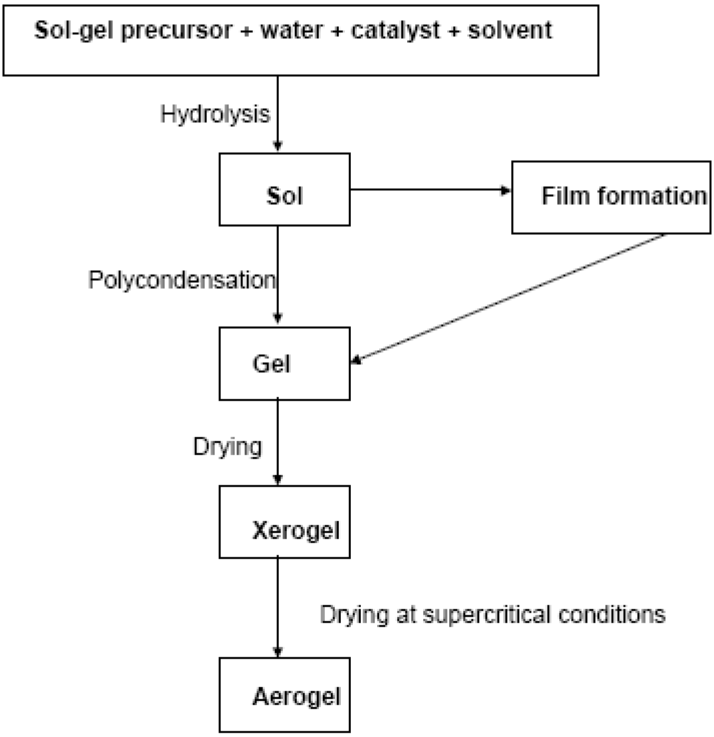

Figure 1.7. Sol-gel process
(taken from http://www2.uni-jena.de/~c1moge/Mohr/ASCOS2002.pdf)

1.7.1.1. Hydrolysis

Although hydrolysis can occur without addition of an external catalyst, it is most rapid and complete when they are employed. Mineral acids (HCl) and ammonia are mostly used, however, other catalysts are acetic acid, KOH, amines, KF, and HF (Brinker and Scherer, 1990).

With weaker bases such as, ammonium hydroxide and pyridine, measurable speeds of reaction were produced only if large concentrations were present. Therefore, compared to acidic conditions, base hydrolysis kinetics is more strongly affected by the nature of the solvent (Aelion et al., 1950). Figure 1.8 shows the pH rate profile for hydrolysis reaction in aqueous solution.

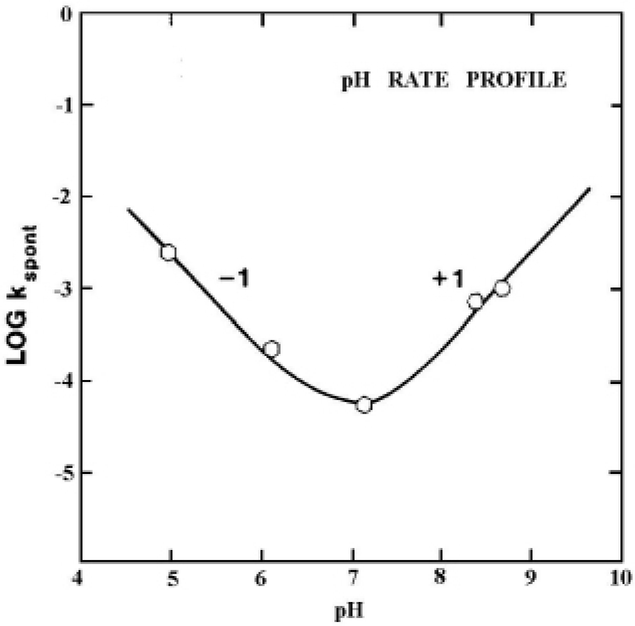

Figure 1.8. pH rate profile for hydrolysis in aqueous solution
(taken from http://www.psrc.usm.edu/mauritz/solgel.html)

1.7.1.1.1. Acid-catalyzed mechanism

Under acidic conditions, it is likely that an alkoxide group is protonated in a rapid first step. Electron density is withdrawn from the silicon atom, making it more electrophilic and thus more susceptible to attack from water. This results in the formation of a penta-coordinate transition state with significant SN2-type character (Brinker and Scherer, 1990). The transition state decays by displacement of an alcohol and inversion of the silicon tetrahedron, as seen in Figure 1.9.

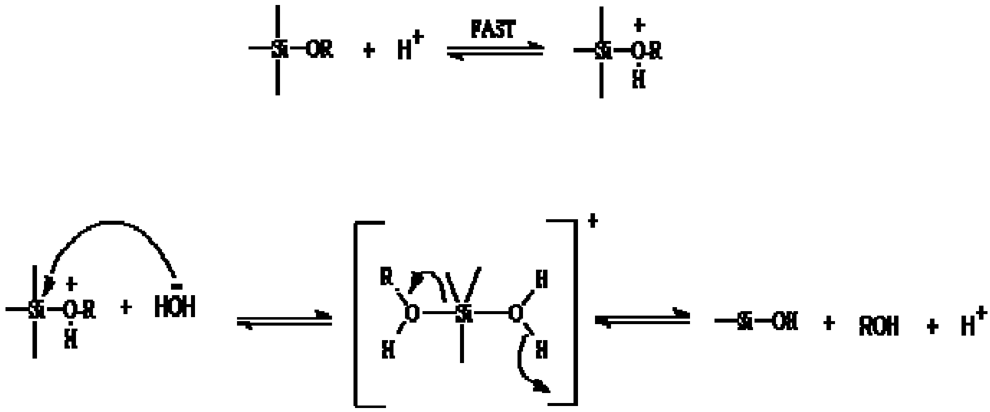

Figure 1.9. Acid-catalyzed hydrolysis
(taken from http://www.psrc.usm.edu/mauritz/solgel.html)

H_2O/Si Molar Ratio (R)

From equation 1.1, an increased value of R is expected to promote the hydrolysis reaction. Additionally, higher values of R caused more complete hydrolysis of monomers before significant condensation occurs. Differing extents of monomer hydrolysis should affect the relative rates of the alcohol- or water-producing condensation reactions. Generally, with under stoichiometric additions of water ($R << 2$), the alcohol producing-condensation mechanism is favored, whereas, the water-forming condensation reaction is favored when $R \geq 2$ (Assink and Kay, 1998).

Although increased values of R generally promote hydrolysis, when R is increased while maintaining a constant solvent:silicate ratio, the silicate concentration is reduced. This in turn reduces the hydrolysis and condensation rates, resulting in longer gel times. This effect is evident in Figure 1.10 which shows gel times for acid-catalyzed TEOS systems as a function of R and the initial alcohol: TEOS molar ratio (Klein, 1985). Finally, since water is the by-product of the condensation reaction (Eq. 1.3), large values of R promote siloxane bond hydrolysis (reverse of Eq. 1.3).

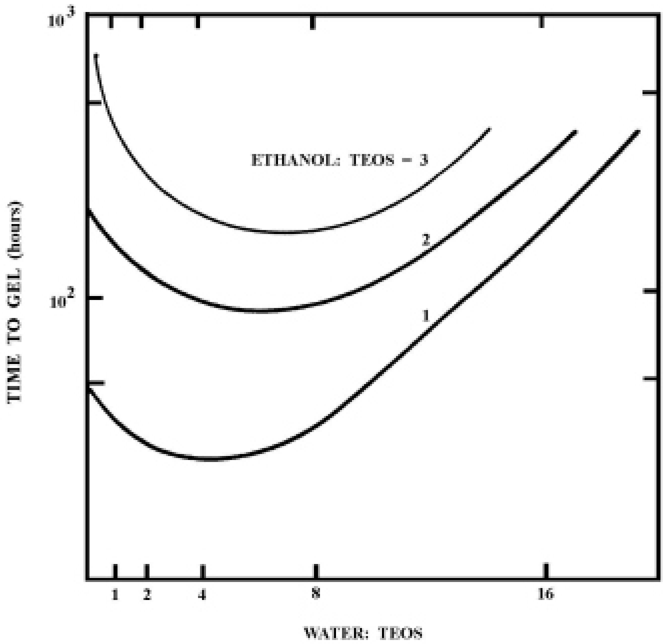

Figure 1.10. Gel times as a function of H_2O:TEOS ratio, R.
(taken from http://www.psrc.usm.edu/mauritz/solgel.html)

1.7.1.1.2. Based-catalyzed mechanism

Base-catalyzed hydrolysis of silicon alkoxides proceeds much more slowly than acid-catalyzed hydrolysis at an equivalent catalyst concentration. Basic alkoxide oxygens tend to repel the nucleophile, -OH. However, once an initial hydrolysis has occurred, following reactions proceed stepwise, with each subsequent alkoxide group more easily removed from the monomer then the previous one (Kelts et al., 1986). Therefore, more highly hydrolyzed silicones are more prone to attack. Additionally, hydrolysis of the forming polymer is more sterically hindered than the hydrolysis of a monomer. Although hydrolysis in alkaline environments is slow, it still tends to be complete and irreversible. Thus, under basic conditions, it is likely that water dissociates to produce hydroxyl anions in a rapid first step. The hydroxyl anion then attacks the silicon atom. Again, an SN2-type mechanism has been proposed in which the -OH displaces -OR with inversion of the silicon tetrahedron. This is seen in Figure 1.11.

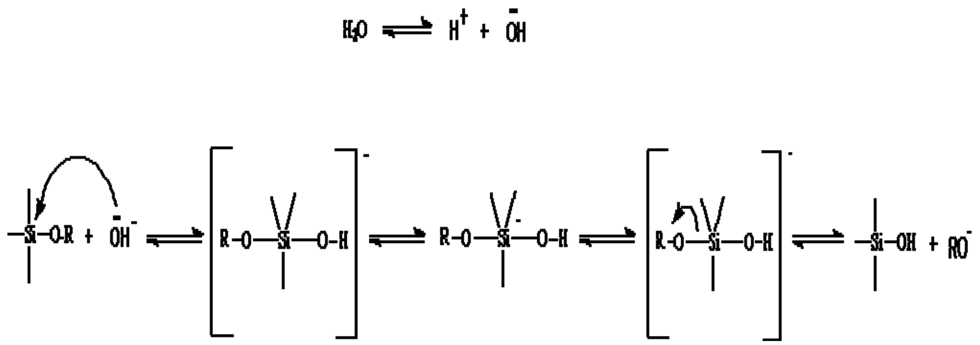

Figure 1.11. Base-catalyzed hydrolysis
(taken from http://www.psrc.usm.edu/mauritz/solgel.html)

1.7.1.2. Condensation

Polymerization to form siloxane bonds occurs by either an alcohol-producing or a water-producing condensation reaction. It has been shown by Engelhardt et al. that a typical sequence of condensation products is monomer, dimer, linear trimer, cyclic trimer, cyclic tetramer, and higher order rings (Engelhardt et al., 1977; Brinker and Scherer, 1990).

As with hydrolysis, condensation can proceed without catalyst, however, their use in organosiloxanes is highly helpful. It has been shown that condensation reactions are acid and base specific (Pohl and Osterholtz, 1985). In addition, Iler has shown that under more basic conditions, gel times are observed to increase (Iler, 1979). Condensation reactions continue to proceed, however, gelation does not occur.

1.7.1.2.1. Acid-catalyzed mechanism

It is generally believed that the acid-catalyzed condensation mechanism involves a protonated silanol species. Protonation of the silanol makes the silicon more electrophilic and thus susceptible to nucleophilic attack. The most basic silanol species (silanols contained in monomers or weakly branched oligomers) are the most likely to be protonated. Therefore, condensation reactions may occur preferentially between neutral species and protonated silanols situated on monomers, end groups of chains, etc. (Brinker and Scherer, 1990).

1.7.1.2.2. Base-catalyzed mechanism

The most widely accepted mechanism for the base-catalyzed condensation reaction involves the attack of a nucleophilic deprotonated silanol on a neutral silicic acid (Iler, 1979).

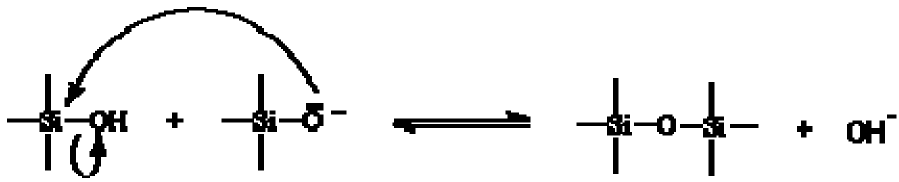

Figure 1.12. Nucleophilic attack to form siloxane bond
(taken from http://www.psrc.usm.edu/mauritz/solgel.html)

1.8. Luminescence

1.8.1. Mechanism of luminescence

Luminescence means emission of light by electronically excited atoms or molecules. Electronic excitation requires the supply of energy. Various kinds of luminescence, such as electroluminescence, chemi luminescence, themoluminescence and photoluminescence, are known and called by the source from which energy is derived (Lakowicz, 1999). In the case of photoluminescence (fluorescence and phosphorescence) the energy is provided by the absorption of infra-red, visible or ultra-violet light. Two models are necessary to describe the interaction of light with matter: in the one light is regarded as a succession of waves, in the other as a collection of particles. The latter was introduced by Planck, who showed that radiant energy can only be absorbed in definite units or quanta. The energy quantum E, is defined as

$$E = h\nu = h\frac{c}{\lambda}$$

Where ν is the frequency, h is Planck's constant (6.626×10^{-34} Js), λ the wavelength, and c the constant velocity of light in vacuum (2.998×10^{8} ms^{-1}).

The adsorption and emission of light is illustrated by Jablonski level diagram, shown in Figure 1.13. According to the Boltzman distribution, at room temperature the valence electrons are in the lowest vibration level ($\nu = 0$) of the ground electronic state. A transition of these electrons from the ground state (level 0 of S_0) to higher energy levels takes place on absorption of light. The Frank-Condon principle states that there is approximately no change in nuclear position and spin orientation, because absorption of light occurs in about 10^{-15} s. Therefore, the electronic transition is represented by a vertical line. Molecules excited to an upper vibrational level of any excited state rapidly lose their excess of vibrational energy by collision with solvent molecules, and falls to the lowest vibrational level. Molecules in the upper excited states (S_2, S_3, …) relax by internal conversion (IC), radiationless to the lowest excited singlet state (S_1) within 10^{-12} s. Transition from this level to the vibration levels of the ground state can take place by emitting photons. A portion of the excited molecules may return to the ground sate by other mechanisms, such as electron transfer, collision, intersystem crossing (ISC), internal conversion or chemical reaction. Fluorescence emission occurs spontaneously, again in accordance with the Franck-Condon principle, if the radiationless transition lifetime is sufficiently long. The radiative lifetime of fluorescence between 10^{-9} s for spin allowed transitions ($\pi^{*} \rightarrow \pi$) to 10^{-6} for less probable transitions ($\pi^{*} \rightarrow n$). Molecules in the lowest excited state (S_1) can also undergo conversion to the first triplet state (T_1) by intersystem crossing (ISC).

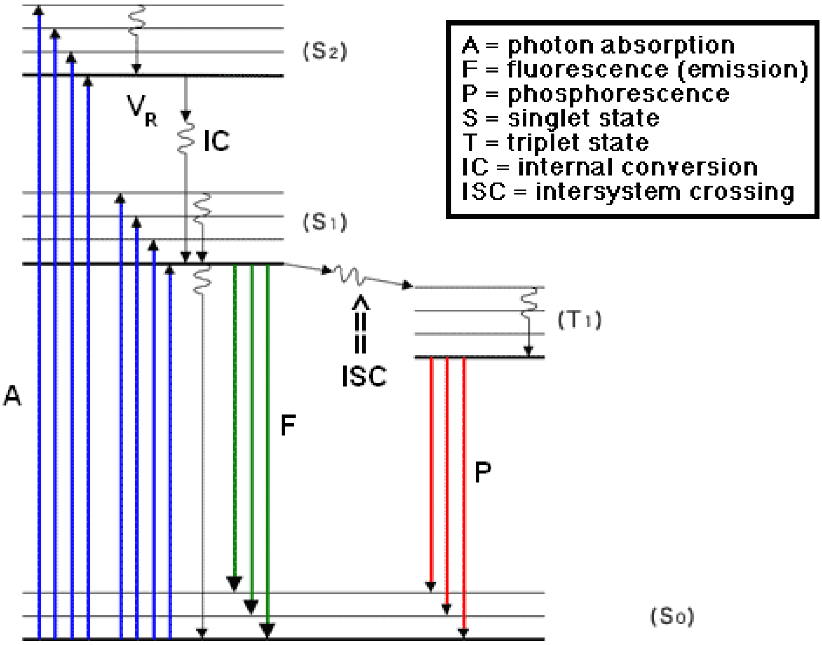

Figure 1.13. Jablonski diagram

1.8.2. Stokes shift

The law of Stokes states that the fluorescence and phosphorescence is shifted to higher wavelengths relative to absorption (Stokes shift). The explanation is provided by the Jablonski diagram. As already mentioned, emission usually occurs form the lowest excited state, but higher excited state are reached by absorption. The radiationless vibrational relaxation (V_R) and internal conversion (IC) involves a loss of energy which is reflected in a shift to emission bands of lower energy. Furthermore, molecules generally decay to excited vibrational levels of S_0 (Lakowicz, 1999).

1.8.3. Quantum yield

A molecule in the relaxed state S_1 (the lowest excited state) can return to the ground state, radiationless or by the emission of fluorescence. The fluorescence quantum yield is the ratio of the number of photons emitted to the number absorbed expressed by the rate constants Γ and k, respectively. Hence, the quantum yield can be written as

$$\Phi = \frac{\Gamma}{\Gamma \oplus k}$$

The quantum yield can be close to unity if the radiationless rate of deactivation (k) is much smaller than the rate of radiative emission ($k << \Gamma$) (Lakowicz, 1999).

1.9. Heavy Metals

Heavy metal ions play an important role in many biological and environmental processes (Trautwen, 1997; Merian, 1991). Depending on the abiotic environment and/or the organisms of interest, the physiological, ecological and toxicological effects of these ions are usually strongly structure-specific, i.e., they depend on the species (Sigg and Xue, 1994; Szpunar and Lobinski, 1999). The biological efficacy of a single species, i.e., if it acts as an essential (trace) element or as an acute toxin, is critically determined by its concentration in the respective medium and the up-take paths of an organism (Radisky and Kaplan, 1999).

1.9.1. Copper

Copper is an essential trace metal found in the Cu (II) and Cu (I) states in all living organisms. Table 1.1 presents average values for concentrations of copper in water, soil, and different kinds of foodstuffs. For humans and other mammals, the best plant food sources are seeds, including whole grains, nuts, and beans, where (like most trace elements and vitamins) it is concentrated in the germ and bran. The best animal food sources are shellfish and liver. Even with copper piping, drinking water does not normally contribute significantly to intake (Mercer, 2001)

In mammals, virtually all copper is taken in through the diet and absorbed from the gastrointestinal tract, although small amounts can penetrate the skin when applied in specific ointments and even by leaching into the sweat from copper bracelets (Chelly et al., 1993; Mercer et al., 1993). Average intakes of copper by human adults, at least in the United States and Western Europe, are about 1 mg/d, although they vary in the range from 0.6 to 1.6 mg (Andrews, 2001; Vulpe et al., 1993; Bull et al., 1993). Very recently, a US Recommended Daily Allowance (RDA) of 0.9 mg for normal adult women and men (with higher levels for pregnant women) was hammered out by a committee of the National Academy of Sciences (Tanzi et al., 1993), replacing the earlier “safe and adequate intake” range of 1.5–3.0 mg/d. This considerably lower recommended value is based in part on data obtained from copper balance studies in young men maintained for 2.5–6 wk on diets delivering specific levels of copper (from 0.66 to 0.38 and then 2.49 mg/d) (Tanzi et al., 1993; Vulpe et al., 1999). These studies showed that, at least acutely, humans could adapt considerably to changes in copper intake, retaining more and excreting less when intake was low, and vice versa. Even those on the lowest intake (0.38 mg/d) for 6 wk only, lowered their plasma caeruloplasmin–copper concentrations about 10% (still among the most sensitive indices of copper status). At higher intakes, the percentage of copper absorbed was less and body turnover (excretion) was enhanced (Vulpe et al., 1999). Excretion was the main factor controlling homeostasis.

Table 1.1. Copper content of water, soil, foods, and mammalian organs (Range of average values)

Item	Copper Content (µg/mL or g wet weight)
Uncontaminated fresh water	0.0001–0.001(proposed WHO limit 2 µg/mL)
Uncontaminated seawater	
Surface	0.001
1000 m below	0.1
Soils (other than rocks, where most Cu is)	
Inorganic	≥4
Organic	20-30
Vegetables	0.3-3
Fruits	0.4-1.5
Seeds and grains (whole)	3-8
Nuts (whole)	6-37
Potatoes	2.1
Maize	1.4
Yeast	8
Shellfish	12-37
Fish	
Freshwater	0.3-3
Seawater	2-3
Liver and kidney	4-12
Heart	4.5-4.8
Brain	3.1-5.2
Muscle	0.9-1.0
Hair and nails	8-20

Following ingestion, copper transport across the intestinal mucosa is facilitated by cytosolic metallothionein. In blood, copper is initially albumin-bound and transported via the hepatic portal circulation to the liver where it is incorporated into caeruloplasmin. Ninety-eight per cent of copper in the systemic circulation is caeruloplasmin-bound. This renders free copper innocuous with subsequent excretion via a lysosome-to-bile pathway. This process is essential to normal copper homeostasis and provides a protective mechanism in acute copper poisoning. An impaired or overloaded biliary copper excretion system results in hepatic copper accumulation, as occurs in patients with Wilson's disease and in copper poisoning (Massaro, 2002).

1.9.2. Aluminum

Aluminum is a ubiquitous element used extensively in contemporary life. Despite its ubiquity, evolution has not conferred essentiality or utility as far as is known in biological systems. This nonessential metal was long considered virtually innocuous to humans (Sorrenson et al., 1974). The impact of aluminum on biological systems have been the subject of much controversy in the past few decades (Campbell and Bondy, 2000). A wealth of research now suggests that aluminum is toxic to plants, some aquatic animals, and humans (Ganrot, 1986; Chadwick and Whelan, 1992; Yokel, 2000; Nayak and Chatterjee, 2000; Pineros and Kochian, 2001).

Natural aluminum occurs in the soil and makes up about 8 % of the surface of the earth. Higher concentrations may exist in soil surrounding waste sites associated with certain industries such as coal combustion and aluminum mining and smelting (U. S. Public Health Service, 1992, p. 67).

Flux of dust from ores and rock materials are the largest source of particle-borne aluminum (Lee and von Lehmden, 1973; Sorrenson *et al.,* 1974). Both natural processes (weathering of aluminosilicate crystal material) and human activities (mining and agriculture) continually add dust particles to the environment (Eisenrich, 1980; Filipek et al., 1987). In the atmosphere, aluminum is mainly found as aluminosilicates associated with particulate matter and the background levels of aluminum in the atmosphere generally range from 0.005 to 0.18 mg/m^3 (Sorrenson et al., 1974). Aluminum concentrations in natural water normally are small but are found to be higher in the urban areas (Constantini and Giordano, 1991). The increasing amount of aluminum is being leached continuously by acid rain (Harris et al., 1996) and contributes significantly to environmental inputs. Worldwide, it has been estimated that 40 % of arable soils and perhaps as much as 70 % of lands that can be cultivated are acidic enough to have an aluminum toxicity problem (World Food Nutrition Study, 1977).

Many types of foods contain aluminum because they are grown in soil that contains aluminum. When the soil pH is lower than 4.5-5.0, Al is solubilized in the soil water and absorbed by plant roots (Matsumoto, 2000). Apart from this, food additives also contribute substantial amounts of aluminum in the diet. Aluminum is present in many manufactured foods and is added to drinking water for purification purposes (Levesque et al., 2000). The common foods with aluminum-containing food additives include some processed cheese, baking powders, cake mixes, frozen dough, pancake mixes, etc. The average concentration of aluminum in cola drinks was found to be 0.1 mg/g. Dry tea leaves have 555-1009 μg /g aluminum and a typical infusion has 4.5-6.0 µg /ml aluminum. Infusion of coffee has an aluminum concentration 0.04-0.30 µg /ml (Koch *et al*., 1988).

Aluminum absorption seems to be very low, but many factors can enhance it in animals and humans (Deng *et al*., 1998). One of the significant routes of aluminum absorption is through the gut (Ittel, 1993). Aluminum is clearly a powerful neurotoxicant. Considerable evidence exists that aluminum may play a role in the aetiology or pathogenesis of Alzheimer's disease, but whether the link is causal is still open to debate (Flaten, 2001).

1.9.3. Zinc

Zinc (~3 g) is the second most abundant trace element in the body after Fe (4 g) and considerably more abundant than copper. The body does not store Zn and a constant dietary intake is essential. Zn is normally obtained from red meat and other animal proteins, which have a high Zn content and it is also of easy absorption. Zinc deficiency is diffused in aged individuals who tend to have an inappropriate diet due to several factors like difficulty in chewing because of lack of teeth, lack of taste, fatigue and frailty. Changes in appetite, taste, and swallowing can impact the eating habits of the elderly individual, hence micronutrients are not consumed in adequate amount (Martin 2006).

The bulk of body Zn is tightly bound within cellular metalloenzymes and Zn finger proteins. This fixed pool of Zn turns over very slowly and is mainly responsible for housekeeping functions in cellular metabolism and gene expression. The remaining 10–15% of Zn (labile Zn) comprises more dynamic pools that are readily depleted in Zn deficiency. While fixed Zn is distributed uniformly throughout the body, labile Zn is concentrated in certain tissues and in specific regions within tissues (Vasto et al. 2006, 2007).

The brain has the highest zinc content compared to other organs. The average of total brain zinc concentration was estimated to be approximately 150 μmol/L (about ten-fold serum zinc levels). However, free zinc ion concentration estimated in the cytosol from cultured neurons is subnanomolar and it is approximately 500 nM in brain extra cellular fluids. On the contrary, the zinc content in the synaptic vesicles of some neurons in the forebrain was found to be approximately >1 mmol/L (Frederickson and Moncrieff, 1994).

Zn has a regulating function for some postsynaptic receptors and is a contributing element in some neurobiological disorders such as ischemia, epilepsy and Alzheimer's disease (Gee, et al., 2002). But so far, only very little information is known concerning its physiological significance and regulation and its intracellular signaling functions.

1.10. The Purpose of This Study

In this study, the selective and sensitive determination of copper(II), zinc(II) and aluminum(III) were accomplished by the use of the optical sensor. The sensor performance characteristics such as response time, dynamic working range, sensitivity and limit of detection were reported. In addition the influence of a number of common metal ions on the fluorescence intensity of the proposed optical sensors was investigated.

2. CHAPTER TWO - EXPERIMENTAL

2.1. Reagents

The polymer membrane components, polyvinylchloride (PVC) (high molecular weight) was obtained from Fluka. Ethyl cellulose (with an ethoxy content of 48 %) was from Aldrich. The plasticizers, bis-(2-ethylhexyl) phtalate (DOP), bis(2-ethylhexyl)sebecate (DOS), bis-(2-ethylhexyl)adipate (DAO) were obtained from Fluka. The additive potassium tetrakis-(4-chlorophenyl) borate (PTCPB) was selectophore, 98 % from Aldrich.

The sol-gel component tetraethyl ortosilicate (TEOS) was obtained from Merck (98 % purity, for synthesis). The surfactant additive Triton X-100 was obtained from Merck (98 % purity, GR).

All solvents used in this thesis were analytical grade and purchased from Merck, Fluka and Riedel.

The copper sensitive dyes of 4-(1-phenyl-1-methylcyclobutyl-3-yl)-2-(2-hydroxy-1-naphtylidene) thiazole and 4-(1-phenyl-1-methylcyclobutane-3-yl)-2-(2-hydroxy-5-bromobenzylidene) aminothiazole and zinc sensitive dye 2-(2-hydroxy-5-chloro)benzaldehyde-[4-(3-methyl-3-mesitylcyclobutyl)-1,3-thiazol-2yl]hydrazone were supplied by the research group of A. Çukurovalı and I. Yılmaz were synthesized in the laboratories of the University of Fırat.

The standard metal solutions were obtained by dilution of their 0.1 M stock solutions prepared by using metallic Al, and the metal salts of $Cu(NO_3)_2$, $NiCl_2.6H_2O$, $Co(NO_3)_2$, $Pb(NO_3)_2$, NaCl, KCl, $MgCl_2$, $Fe(NO_3)_3$, $CdCl_2$.

Sheets of Mylar-type polyester (Dupont, Switzerland) were used as support. All solutions were prepared with glass-distilled water.

For fluorescence quantum yield determinations, standard reference material (Quinine sulphate) (Φ_{st}=0.54) was obtained from Sigma. Buffer components were analytical grade (Merck and Fluka).

2.2. Instrumentation

UV-Vis absorption spectra were recorded using Varian Cary 100 bio UV-Visible spectrophotometer. All fluorescence measurements were carried out on a Shimadzu RF-5301 PC spectrofluorimeter with a Xenon short arc lamp as the light source.

The cuvette with the sensing element stuck on its side wall was secured in the cell holder. The polymer films were placed in diagonal position in the quartz cell. The solution in the cuvette was changed by using a disposable pipette. The advantage of this kind of placement was to improve the reproducibility of the measurements (Figure 2.1).

Measurement of pH was performed with a pH-meter (WTW Multiline P4) calibrated with Merck pH standards of pH 4.00, 7.00, and 10.00. Magnetic stirrer was obtained from Chiltern. All of the experiments were carried out at room temperatures.

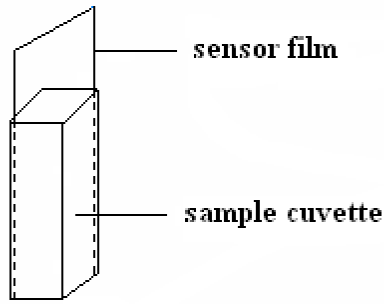

Figure 2.1. The placement of the sensor film in the sample cuvette.

2.3. Construction of the sensing films

The sensing cocktails were prepared according to the analyte type either with PVC, ethyl cellulose or sol-gel matrix.

2.3.1. PVC cocktail preparation

The membranes were prepared to contain the dye, 33 % PVC (high molecular weight), 66 % plasticizer bis-(2-ethylhexyl)phtalate (DOP) by weight and the additive potassium tetrakis-(4-chlorophenyl) borate (PTCPB). The chemical structures of PVC, DOP and PTCPB are shown in Figure 2.2. The mixture was dissolved in tetrahydrofuran (THF) and mixed for approximately one hour by the help of a magnetic stirrer (Seiler and Simon, 1992; Bakker and Simon, 1992; Lerchi et al., 1992).

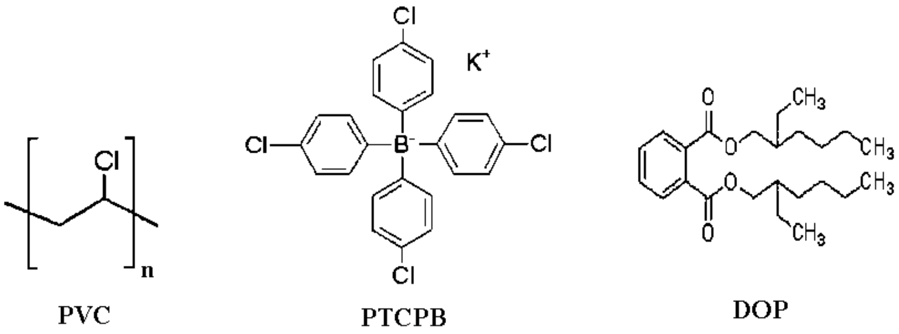

Figure 2.2. Structures of PVC, PTCPB and DOP

The resulting cocktail was spread on a 125 µm polyester support (Mylar TM type) and dried in a desiccator which was saturated with the solvent vapour. The polymer support is optically fully transparent, ion impermeable and exhibits good adhesion to PVC. The most important function of the polyester was to act as a mechanical support because the thin silicon films were impossible to handle. Once dried, the film was insoluble in water and could be cut into pieces of appropriate size. The thickness of dry membrane was estimated to be approximately 5 µm. The films were kept in a desiccator in dark. This way, the photostability of the membrane was ensured and the damage from the ambient air of the laboratory was avoided. For absorbance and fluorescence measurements each sensing film was cut to 1.2 cm width and 2.5 cm length and fixed diagonally into the sample cuvette (Figure 2.1) and the absorption or emission spectra were recorded.

2.3.2. Ethyl cellulose cocktail preparation

The membranes were prepared to contain the dye, 33% ethyl cellulose (48-49.5 % ethoxy content, EC) and 66 % plasticizer (DOP) by weight. The mixture was dissolved in tetrahydrofuran (THF) and stirred for several hours by the help of a magnetic stirrer. The same procedure used with the PVC matrix was employed after. The structure of ethyl cellulose is shown in Figure 2.3.

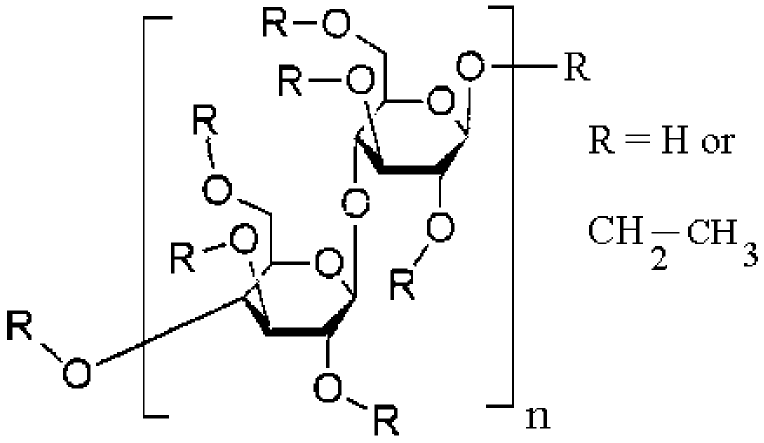

Figure 2.3. Structures of ethyl cellulose

2.3.3. Sol-gel cocktail preparation

The sol-gel components are tetraethyl ortosilicate (tetraethoxysilane, TEOS) and hydrochloric acid or sodium hydroxide whether it is acid catalyzed or base catalyzed sol-gel. Triton X-100 was added in order to improve the homogeneity of the silica sol-gel and to give a crack-free monolith. Dye doped silica gel glasses were prepared by hydrolization and condensation of TEOS with acidic water.

2.4. Quantum Yield Calculations

When a fluorophore absorbs a photon of light, an energetically excited state is formed. The fate of this species is varied, depending upon the exact nature of the fluorophore and its surroundings, but the end result is deactivation (loss of energy) and return to the ground state. The main deactivation processes which occur are fluorescence (loss of energy by emission of a photon), internal conversion and vibrational relaxation (non-radiative loss of energy as heat to the surroundings), and intersystem crossing to the triplet manifold and subsequent non-radiative deactivation.

The fluorescence quantum yield (Φ_F) is the ratio of photons emitted through fluorescence to photon absorbed. In other words the quantum yield gives the probability of the excited state being deactivated by fluorescence rather than by another, non-radiative mechanism.

The most reliable method for recording Φ_F is the comparative method of Williams et al., which involves the use of well characterized standard samples with known ΦF values (Williams et al., 1983). Essentially, solutions of the standard and test samples with identical absorbance at the same excitation wavelength can be assumed to be absorbing the same number of photons. Hence, a simple ratio of the integrated fluorescence intensities of the two solutions (recorded under identical conditions) will yield the ratio of the quantum yield values. Since Φ_F for the standard sample is known, it is trivial to calculate the Φ_F for the test sample.

In practice, the measurement is slightly more complicated than this because it must take into account a number of considerations. For example:

• The presence of concentration effects, *e.g.* self-quenching;

• The use of different solvents for standard and test samples;

• The validity in using the standard sample and its Φ_F value.

These considerations are answered by

• Working within a carefully chosen concentration range and acquiring data at a number of different absorbances (*i.e.* concentrations) and ensuring linearity across the concentration range;

• Including the solvent refractive indices within the ratio calculation;

• Cross-calibrating the standard sample with another, to ensure both are behaving as expected and allowing their Φ_F values to be used with confidence.

The measurement of Φ_F values is challenging if the values are to be trusted. Incorrect quantum yields are all too easy to obtain!

Procedure:

1. Record the UV-vis absorbance spectrum of the solvent background for the chosen sample. Note down the absorbance at the excitation wavelength to be used.

2. Record the fluorescence spectrum of the same solution in the 10 mm fluorescence cuvette. Calculate and note down the integrated fluorescence intensity (that is, the area of the fluorescence spectrum) from the fully corrected fluorescence spectrum.

3. Repeat steps 1. and 2. for five solutions with increasing concentrations of the chosen sample.

(There will be six solutions in all, corresponding to absorbances at the excitation wavelength of ~0/solvent blank, 0.02, 0.04, 0.06, 0.08 and 0.10.)

4. Plot a graph of integrated fluorescence intensity *vs* absorbance. The result should be a straight line with gradient m, and intercept = 0.

5. Repeat steps 1. to 4. for the remaining samples.

The gradients of the graphs obtained in 4. above are proportional to the quantum yield of the different samples. Absolute values are calculated using the standard samples which have a fixed and known fluorescence quantum yield value, according to the following equation:

$$\Phi_X = \Phi_{ST}\left(\frac{Grad_X}{Grad_{ST}}\right)\left(\frac{n_x^2}{n_{ST}^2}\right) \qquad \text{Eq (2.1)}$$

Where the subscripts ST and X denote standard and test respectively, Φ is the fluorescence quantum yield, Grad the gradient from the plot of integrated fluorescence intensity *vs* absorbance, and η the refractive index of the solvent.

The measurement of fluorescence quantum yields can often be difficult and troublesome, and the need for absolute care during every step cannot be over emphasized. However, it is possible to make such measurements routinely, and following these guidelines should make this an achievable goal.

3. CHAPTER THREE

SELECTIVE OPTICAL SENSING OF COPPER(II) IONS BASED ON A NOVEL CYCLOBUTANE-SUBSTITUTED SCHIFF BASE LIGAND EMBEDDED IN POLYMER FILMS

3.1. Introduction

Copper is an essential trace element for humans, plants and other animals. This metal occurs naturally throughout the environment, in soil, water, and air. Copper compounds are generally employed to treat plant diseases, for water treatment and as protectives for wood and leather. Daily ingestion of copper is indispensable for good health. However, high amounts of copper can be harmful, causing irritation of nose and throat, nausea, vomiting, and diarrhea. Very high doses of copper can cause damage to liver and kidneys. Humans are commonly exposed to copper from drinking water, breathing air, eating foods, or having skin contact with copper, particulates attached to copper, or copper-containing compounds. In this manner, the determination of trace amounts of copper in several matrices is fundamental to identify the metal contamination in environment, water or human body (Baird, 1999; Mckenzie and Smythe, 1988).

High number of analytical methods such as flame (FAAS) or graphite furnace atomic absorption spectroscopy (GFAAS), inductively coupled plasma atomic emission or mass spectroscopy (ICP-AES, ICP-MS), and stripping voltammetry have been proposed for the determination of copper ions at low concentration level. These methods need relatively high cost apparatus, large size samples and disability for on-line monitoring. Therefore, a growing interest showed up in different laboratories to develop metal ion monitoring chemical sensors (Oehme and Wolfbeis, 1997). Chemical sensors based on optical signal measurement are those of the advanced techniques in analytical chemistry and they have been accepted as advantageous because they can be miniaturized and can be manufactured at low cost (Moody et al., 1988). In recent years, several fluorescence sensors have been developed for the detection of metal ions such as Li^+ (Chenthamarakshan and Ajayaghosh, 1998; Kurihara et al., 2001), Na^+ (Yang et al., 2000; Benco et al., 2002; Ertekin et al., 2002), K^+ (Ertekin et al., 2002), Ca^{2+} (Capitan-Valley et al., 2000), Ag^+ (Shamsipur et al., 2006a), Cd^{2+} (Saleh et al., 2007), Zn^{2+} (Sali et al., 2006), Hg^{2+} (Chan et al., 2001) and Fe^{3+} (Oter et al., 2007a).

Steinberg et al. have prepared and characterized a plasticized poly(vinyl chloride) (PVC) optical sensor membrane based on the lipophilic form of a non-specific metal indicator dye Pyrocatechol Violet in order to evaluate its potential use for Cu^{2+} sensing (Steinberg et al., 2003).

Jain et al. investigated as copper(II) selective sensors PVC based membranes of three different chelates. The sensor could be put to analytical use both by direct potentiometry as well as potentiometric titration. The sensor shows a linear potential response Cu^{2+} concentration range 2.0×10^{-6} to 1.0×10^{-1} M (Jain et al., 2005).

A selective fiber optic sensor for copper(II) was offered by Oter et al. (Oter et al., 2007b). They doped a newly synthesized fluorescent semicarbazone derivative in plasticized PVC membrane. The sensor can be used at pH 4.0 for quantitative determination of Cu^{2+} in the concentration range of 1.0×10^{-9} to 3.0×10^{-4} M.

Mei et al. proposed a new probe of rhodamine B hydrazide oxalamide (RBHO), which showed highly selective and sensitive response to copper ion at room temperature in acetonitrile (Mei et al., 2007).

Plasticised PVC membranes are believed to be useful for analytical applications because of their good mechanical properties, homogeneity, simplicity of preparation and optical transparency (Kurochkin and Makaroa, 1996). Several publications have demonstrated the feasibility of using PVC membranes in optical heavy metal sensors (Ozturk et al., 2007; Shamsipur et al., 2006b; Zhang et al., 2006).

The development of a new highly sensitive and selective optical sensor procedure for Cu^{2+}, based on fluorescent measurements was described in this chapter. The photophycial and photochemical characteristics of newly synthesized thiazole derivatives 4-(1-phenyl-1-methylcyclobutyl-3-yl)-2-(2-hydroxy-1-naphtylidene)thiazole (LH) in three different solvents and plasticized PVC matrix were determined. The sensor performance characteristics such as response time, dynamic working range, sensitivity and limit of detection were reported. In addition the influence of a number of common metal ions on the fluorescence intensity of the proposed Cu^{2+} optical sensor was investigated.

3.2. Synthesis of the 4-(1-phenyl-1-methylcyclobutyl-3-yl)-2-(2-hydroxy-1-naphtylidene) thiazole

Schematic structure of the employed dye molecule (LH) synthesized in the laboratory at Fırat University (Çukurovalı et al., 2001) is shown in Figure 3.1.

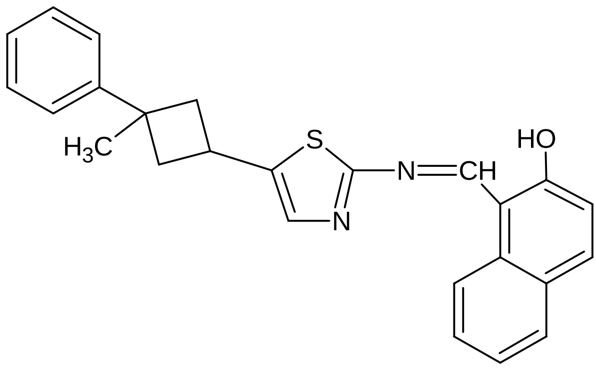

Figure 3.1. Chemical structure of 4-(1-phenyl-1-methylcyclobutyl-3-yl)-2-(2-hydroxy-1-naphtylidene) thiazole (LH) dye

4-(1-phenyl-1-methylcyclobutyl-3-yl)-2-(2-hydroxy-1-naphtylidene) thiazole was synthesized in two steps. In the first step; to a solution of 0.76 g (10 mmole) of thiourea in 50 mL of absolute ethanol, a solution of 2.225 g (10 mmole) of 1-phenyl-1-methyl-3-(2-chloro-1-oxoethyl)cyclobutane in 20 mL of absolute ethanol was added dropwise at 60–70 °C with continuous stirring. By monitoring the IR frequency of the carbonyl group of 1-phenyl-1-methyl-3-(2-chloro-1-oxoethyl)cyclobutane the completion of the reaction was easily seen. The solution was then made alkaline with an aqueous solution of NH_3 (5%) to separate the pale yellow 4-(1-phenyl-1-

methylcyclobutane-3-yl)-2-aminothiazole from the reaction mixture. The precipitate was filtered off, washed with aqueous ammonia solution and water several times, dried in air and recrystallized from aqueous ethanol(1:3). (Yield: 85.21%; mp: 174 °C).

In second step; to a hot (60–70 °C) solution of 2.44 g (10 mmole) of 4-(1-phenyl-1-methylcyclobutane-3-yl)-2-aminothiazole in 30 mL of absolute ethanol, a hot (60–70°C) solution of 1.56 g (10 mmole) of 2-hydroxy-1-napthalaldehyde in 20 mL absolute ethanol was added dropwise with continuous stirring. The mixture was stirred for 1 h and left to stand overnight. The resulting precipitate was filtered, washed several times with cold ethanol and dried at 110 °C to constant weight. (Yield: 75%; mp: 154 °C). The analytical data for the LH dye are shown in Table 3.1.

Table 3.1. The color, formula, formula weights, melting points, yield, and elemental analyses results of the LH dye (Çukurovalı et al., 2001).

Compound	F.W. (g/mole)	Color	m.p. °C	Yield %	Elemental Analyses % Calculated (Found) C	H	N	S
$C_{25}H_{22}N_2OS$	398.53	light brown	154	75	75.35 (75.11)	5.56 (5.48)	7.03 (7.17)	8.05 (8.25)

3.3. Results and Discussion

In this chapter, the optode membranes were prepared to contain 120 mg of PVC, 240 mg of plasticizer (DOP), 1.0 mg of LH dye, equivalent amount of potassium tetrakis (4-chlorophenyl) borate and 1.5 ml of THF (Chapter 2, Section 3.1).

3.3.1. Spectral characterization studies

The UV-Vis spectroscopy related results (absorption maxima; λ_{max} and molar extinction coefficients, ε) obtained were presented in Table 3.2. In all of the solvents used, efficient absorbance and high molar extinction coefficients were observed at around 400 nm. In comparison to the solution phase, the PVC matrix provided high molar extinction coefficient due to the matrix rigidity.

Table 3.2. UV-Vis absorption maxima λ_{max} (nm), and molar extinction coefficients ε (L mol^{-1} cm^{-1}) of the dye (LH) in the different solvents and polymer film

Solvent	ε_1(molar extinction coefficient, L mol^{-1} cm^{-1})	λ_{max}
EtOH	46 000	408
$CHCl_3$	52 000	405
THF	37 000	399
PVC film*	7 284 000	407

* The concentration of LH in the PVC film was 1.0 X 10^{-3} M and the optical path was 5 μm.

The excitation and emission spectra of thiazole derivative dye LH were recorded in the solvents of different polarities and PVC matrix (Figure 3.2). These spectral properties such as visible region excitation (417 nm) and emission wavelength (500 nm), high molar extinction coefficient (7 284 000 L mol^{-1} cm^{-1}), satisfactory quantum yield in immobilized form and intensity-based response to Cu^{2+} ions encouraged us to use the LH dye in optical sensor design for copper sensing.

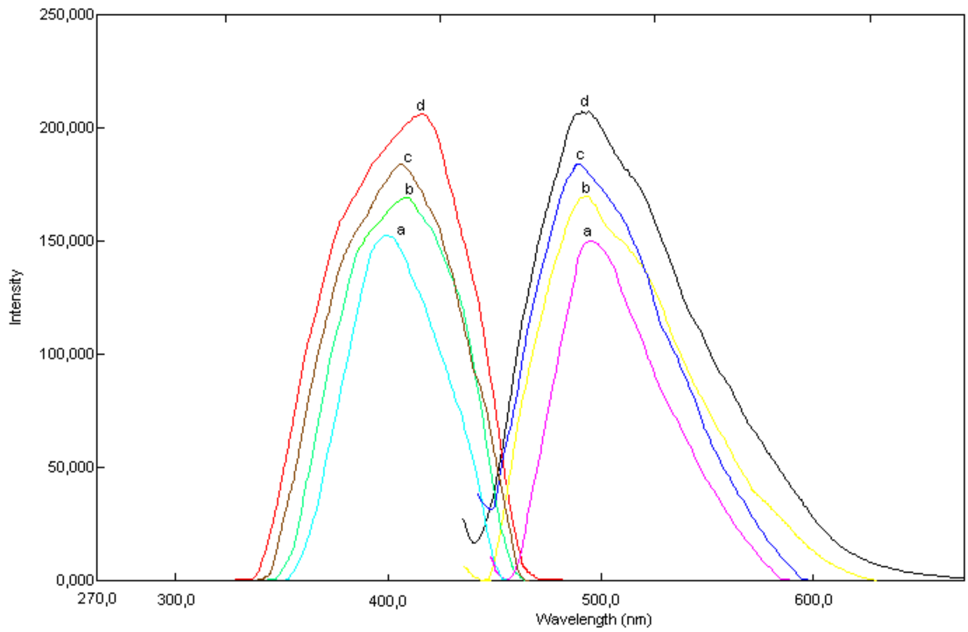

Figure 3.2. Excitation and emission spectra of LH dye in different solvents and PVC.
(a) THF (λ_{ex} = 400 nm, λ_{em} = 502 nm), (b) EtOH (λ_{ex} = 410 nm, λ_{em} = 500 nm),
(c) $CHCl_3$ (λ_{ex} = 408 nm, λ_{em} = 497 nm), (d) PVC (λ_{ex} = 417 nm, λ_{em} = 505 nm).

Table 3.3.

Luminescence characteristics of LH dye (λ_{ex}: excitation wavelength, nm; λ_{em}: emission wavelength, nm; Stokes shift, $\Delta\lambda$ nm)

Solvent	Excitation wavelength λ_{ex}(nm)	Emission wavelength λ_{em}(nm)	Stokes shift $\Delta\lambda_{ST}$
EtOH	410	500	90
$CHCl_3$	408	497	89
THF	400	502	102
PVC film	417	505	88

3.3.2. Quantum yield calculation

The fluorescence quantum yield is the most important characteristic of a fluorophore. Fluorescence quantum yield values (Φ_F) of the employed dye was calculated by using the comparative William's method (Williams et al., 1983). This is a reliable method for recording Φ_F and involves the use of well characterized standard samples with known Φ_F values. The Williams method and the calculation of quantum yield values was explained in detail in Chapter 2. For this purpose, quinine sulphate was used as reference quantum yield standard (λ_{ex} =415 nm, quantum yield = 0.54 in 0.1 M H_2SO_4). The integrated fluorescence intensities were plotted versus absorbance for the reference standard and the dye (Figure 3.3). The gradients of the plots are proportional to the quantity of the quantum yield of the studied molecules.

The equations of the plots are y= 1780970 x; R^2= 0.9984 for reference standard, y= 73197 x; R^2= 0.9921 for LH dye in PVC, and y= 35942 x; R^2= 0.9977 for LH dye in EtOH. The data and quantum yield (Φ_F) values calculated according to Eq. (2.1) are shown in Table 3.4.

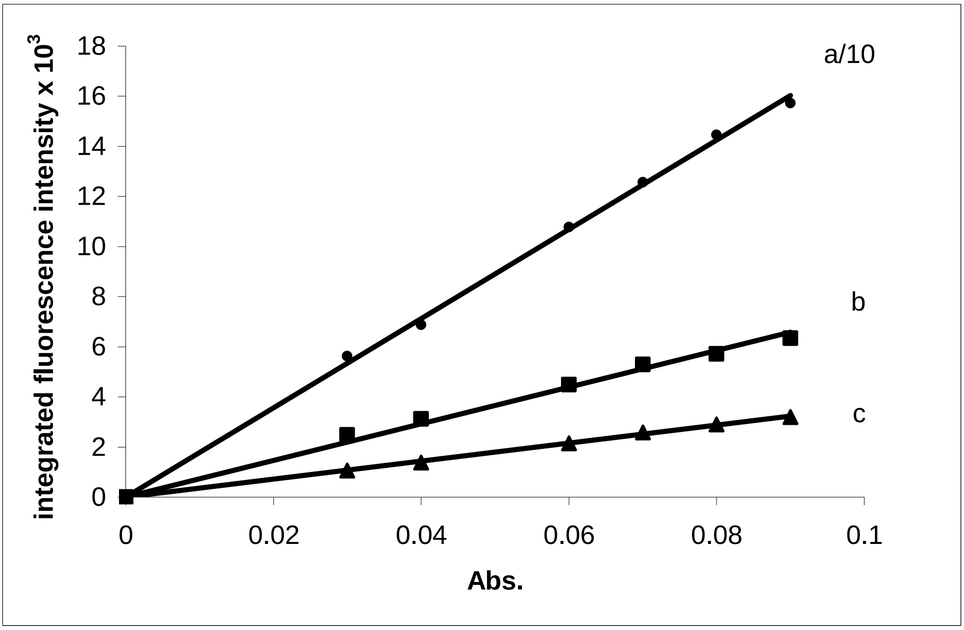

Figure 3.3. The integrated fluorescence intensities vs. absorbance (λ_{ex} =415 nm)

a) for the reference standard (quinine sulphate in 0.1 M H_2SO_4)

b) the LH dye in PVC matrix

c) LH dye in EtOH

Table 3.4. Quantum yield related data for LH in EtOH and PVC matrices.

Dye	LH (in EtOH)	LH (in PVC)	QS (in 0.1MH_2SO_4)
Refractive index,n	1.3590	1.5200	1.3328
Equations of plots	y= 35942 x	y= 73197 x	y=1780970x
Quantum yields	0.0099 (calculated)	0.0288 (calculated)	0.54

3.3.3. Effect of pH on sensor response

The influence of pH of the test solution on the fluorescence response of the proposed Cu^{2+} sensor was studied and the results are illustrated in Figure 3.4. The fluorescence intensity measurements were made in the presence of 5.0 x 10^{-7} M Cu^{2+} solution of different pH values. The pH of solution was adjusted by buffers of $CH_3COOH/NaCH_3COO^-$ (pH 4-6), NaH_2PO_4/Na_2HPO_4 (pH 7-8) and NH_4Cl/NH_3 (pH 9-10). As it is seen in Figure 3.4, in the range of lower pH values, the fluorescence intensity of the sensor membrane decreased with decreasing pH value. On the other hand, the reduced optical response of the sensor at pH > 8.0 could be due to a possible slight swelling of the polymeric film under alkaline conditions. It can be seen that, in a range of pH from 5.0 to 8.0, pH does not affect the determination of Cu^{2+} with the proposed sensor membrane. This result simplifies the practical application of the sensor in the determination of Cu^{2+} concentration in real samples. In subsequent experiments, a pH 6.0 $CH_3COOH/NaCH_3COO^-$ buffer solution was selected for further studies.

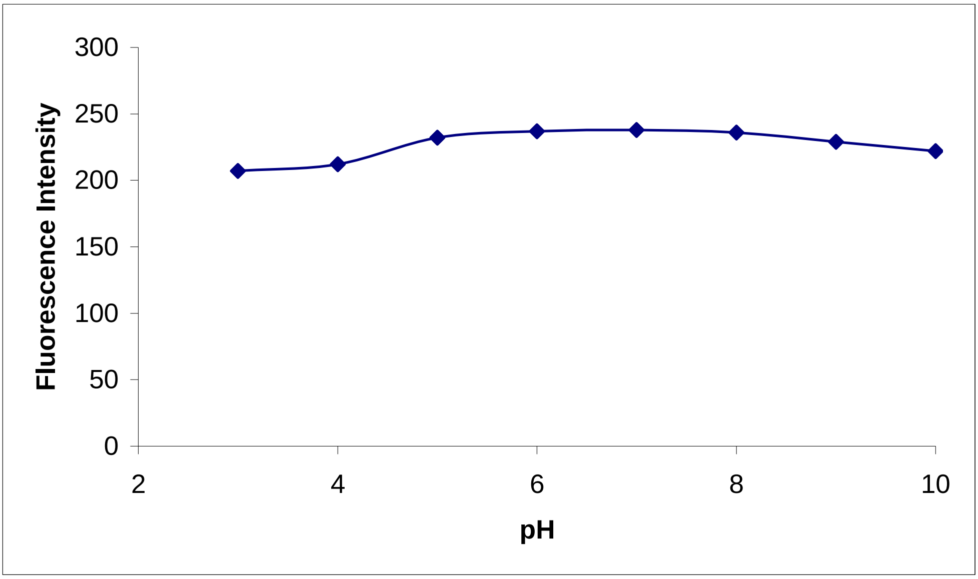

Figure 3.4. Effect of pH on the response of the copper sensor 5.0 x 10^{-7} M Cu^{2+}

3.3.4. Response to Cu^{2+} ions

Cu^{2+} form a complex with LH corresponding to the $M(L)_2$ with a suggested tetrahedral geometry (Figure 3.5). Cu^{2+} bonding takes place with nitrogen of imine groups and by proton exchange with hydroxide groups (Çukurovalı et al., 2001).

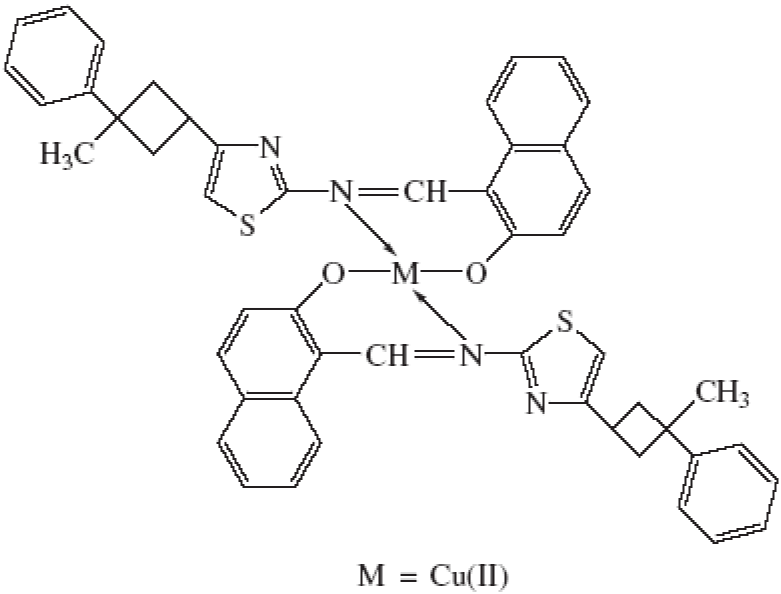

Figure 3.5. Suggested structure of the tetrahedral and square-planar complex of the ligand LH (Çukurovalı et al., 2001).

The dye-doped PVC membrane exhibited remarkable fluorescence intensity quenching upon exposure to Cu^{2+} ions at pH 6.0. Figure 3.5 shows the fluorescence spectra of the LH membrane exposed to a solution containing different concentrations of Cu^{2+}, which are recorded at λ_{ex}: 405 nm. The fluorescence intensities of the sensor membrane decrease with increasing concentration of Cu^{2+}, which constitutes the basis for the determination of Cu^{2+} with the fluorescent sensor proposed in this study. Upon exposure to copper concentrations from 5.0×10^{-8} to 1.0×10^{-5} M, the membrane exhibits a 84.8% relative signal change in direction of decrease in fluorescence intensity (Figure 3.6).

In the concentration range of 5.0 x 10^{-8} to 1.0 x 10^{-4} M at pH 6.0, a linear correlation was obtained with R^2 value of 0.9868 for Cu^{2+} (Figure 3. 7).

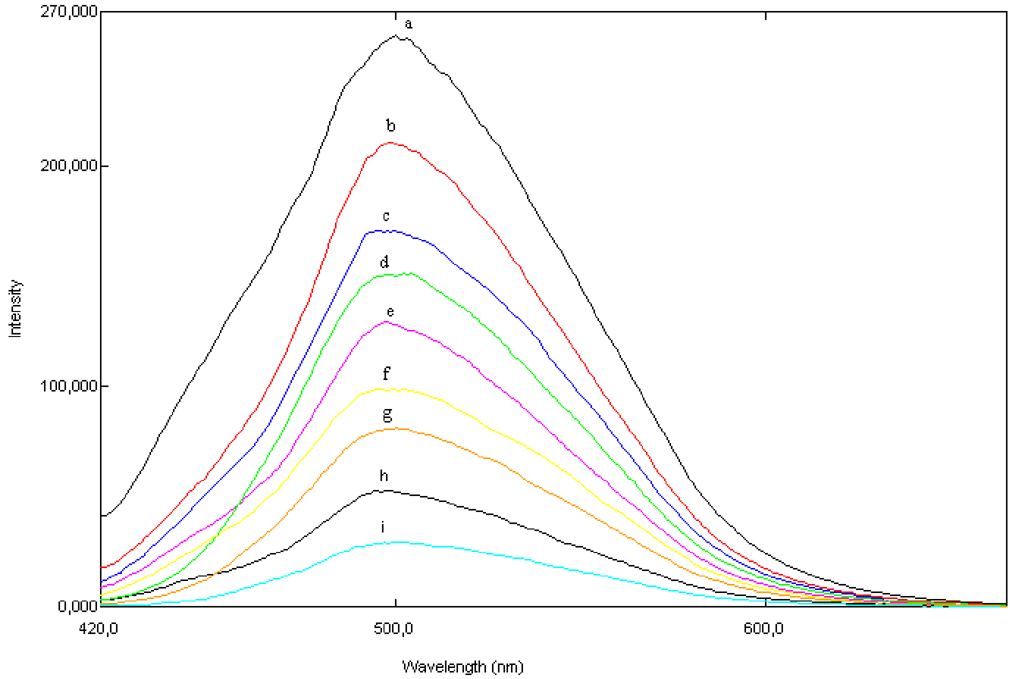

Figure 3.6. Fluorescence emission spectra of the LH sensing membrane after exposure to different concentration of Cu^{2+} at pH 6.0: (a) blank solution; (b) 5.0 x 10^{-8}, (c) 1.0 x 10^{-7}, (d) 5.0 x 10^{-7}, (e) 1.0 x 10^{-6}, (f) 5.0 x 10^{-6}, (g) 1.0 x 10^{-5} , (h) 5.0 x 10^{-5} , (ı) 1.0 x 10^{-4} M Cu^{2+} (λ_{ex} =415 nm)

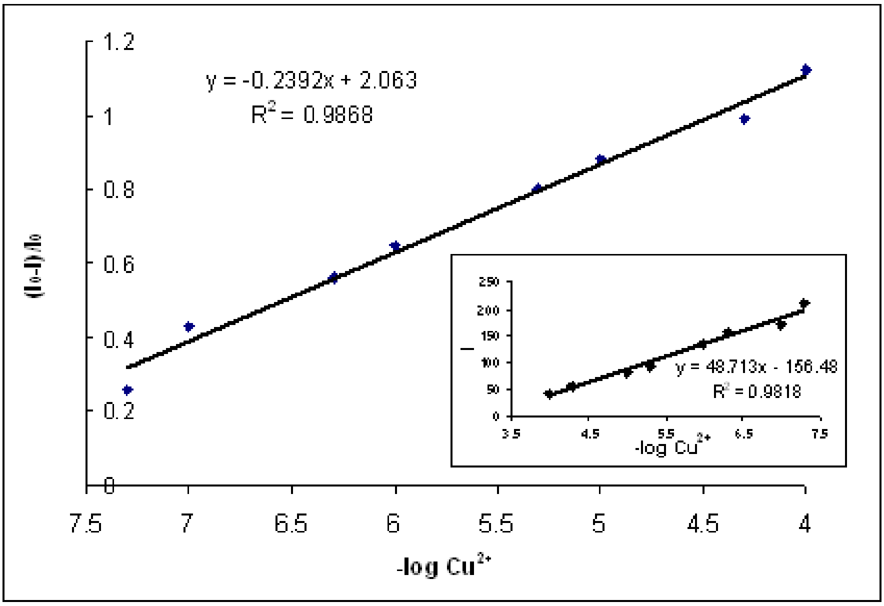

Figure 3.7. Calibration plot of the sensor in the concentration range of 5.0 x 10^{-8} to 1.0 x 10^{-4} M Cu^{2+} at pH 6.0 (λ_{ex} =415 nm)

Upon exposure to copper concentrations from 5.0 x 10^{-8} to 1.0 x 10^{-5} M at pH 3.0, a linear correlation was obtained with R^2 value of 0.9711 for Cu^{2+} (Figure 3. 8 and Figure 3.9).

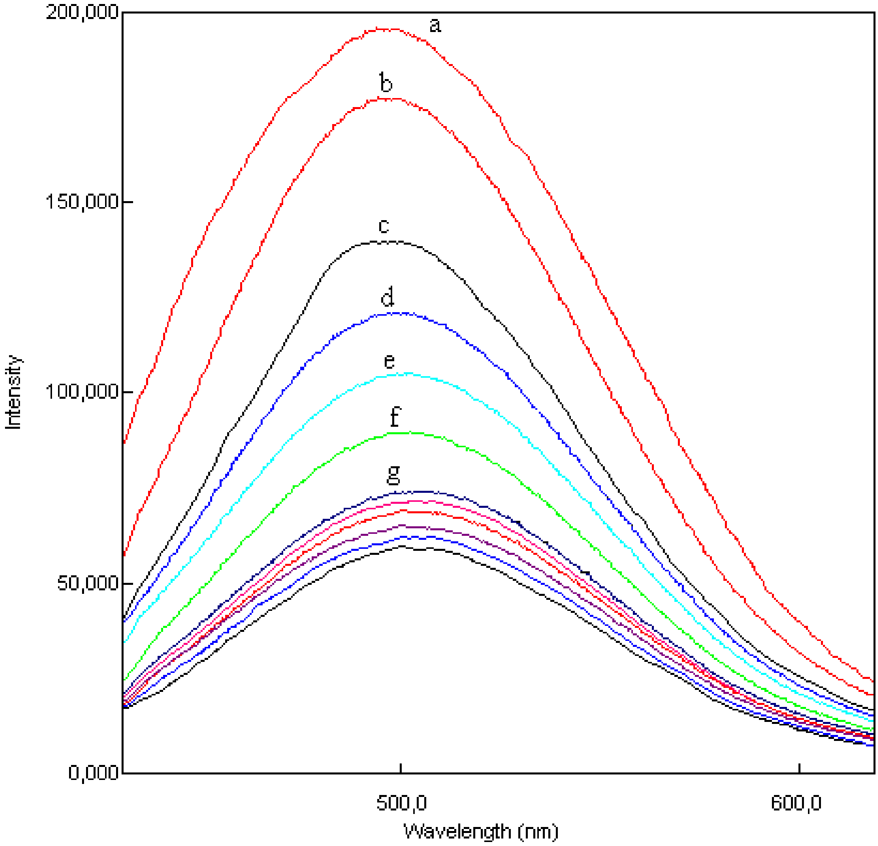

Figure 3.8. Fluorescence emission spectra of the LH sensing membrane after exposure to different concentration of Cu^{2+} at pH 3.0: (a) blank solution; (b) 1.0 x 10^{-7}, (c) 5.0 x 10^{-7}, (d) 1.0 x 10^{-6}, (e) 5.0 x 10^{-6}, (f) 1.0 x 10^{-5} , (g) 5.0 x 10^{-5} M Cu^{2+} (λ_{ex} =415 nm)

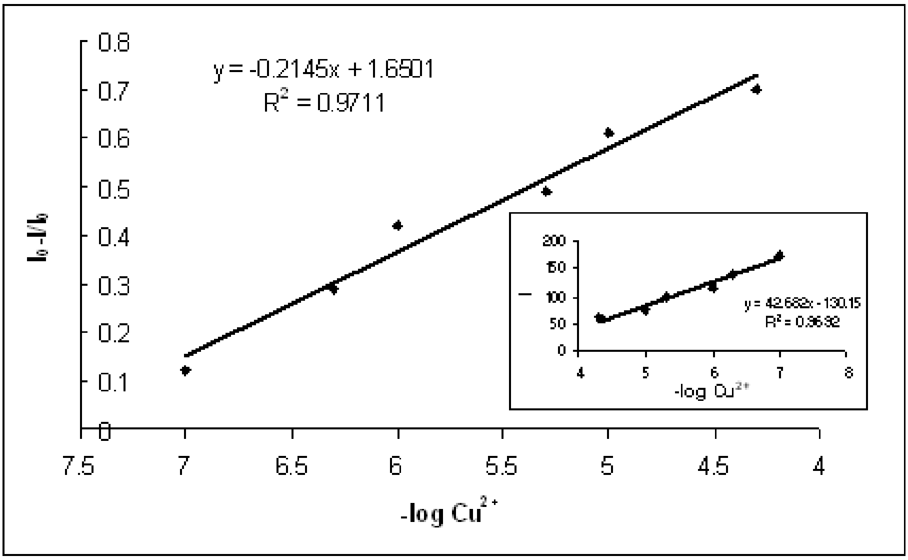

Figure 3.9. Calibration plot of the sensor in the concentration range of 1.0 x 10^{-7} to 5.0 x 10^{-5} M Cu^{2+} at pH 3.0 (λ_{ex} =415 nm)

The linear range of the calibration plot at pH 6.0 was wider than that obtained at pH 3.0. The sensor was found to be more sensitive at pH 6.0 with a better R^2 value.

3.3.5. Response and reproducibility

The approximate response time τ_{90} was measured as 2.5 min. The short-time stability of the optode membrane was tested by recording the fluorescence intensity of 5.0 x 10^{-7} M Cu^{2+} over a period of 20 min for eight measurements. The sensor was fully reversible and can be regenerated with

HCl solution with 100% efficiency (Figure 3.10). The membrane should be washed first with 0.01 M HCl solution and then with blank buffer solution (pH 6.0 CH_3COOH / $NaCH_3COO^-$) after each measurement. Between the 1st and 5th cycles, the level of reproducibility of the upper signal level achieved was quite good with a low standard deviation, 260.98 ± 1.57.

The limit of detection (LOD) based on three standard deviations of the blank signal was found to be 2.6 x 10^{-8} M (1.65 ng mL^{-1}) for Cu^{2+}.

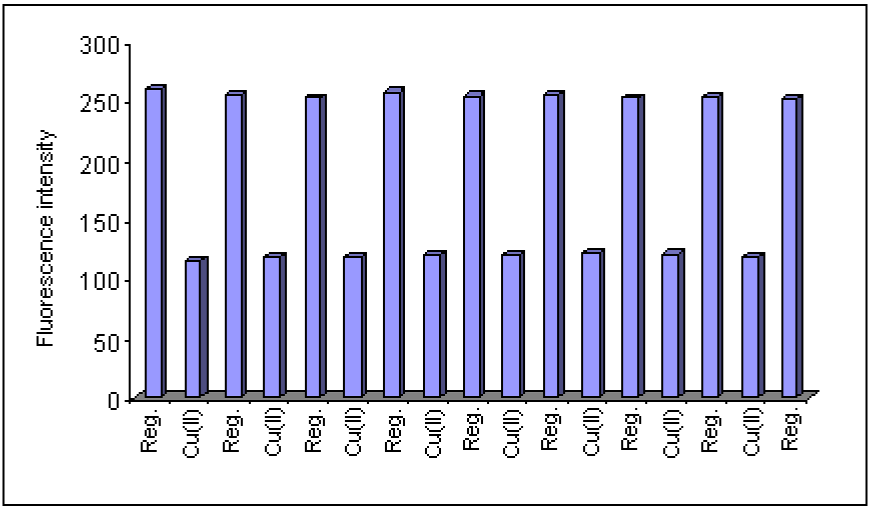

Figure 3.10. Successive responses of the LH membrane to 5.0 x 10^{-7}M Cu^{2+} at pH=6.0.

3.3.6. Selectivity studies

Perhaps the most important characteristic of an ion-selective membrane is its selectivity. Therefore, the influence of a number of common metal ions on the fluorescence intensity of the proposed Cu^{2+} - optical sensor was investigated. The experiments were carried out by fixing the concentration of Cu^{2+} at 1.0 x 10^{-6} M and then recording the change in the fluorescence intensity before (F_0) and after adding the interfering ion at a 1.0 x 10^{-2} M level (F) into the copper ion solution buffered at pH 6.0. The resulting relative error (RE) is defined as relative signal change, RE(%) = $[(F_0-F) / F_0]$ x 100. The results of selectivity studies are summarized in Figure 3.11.

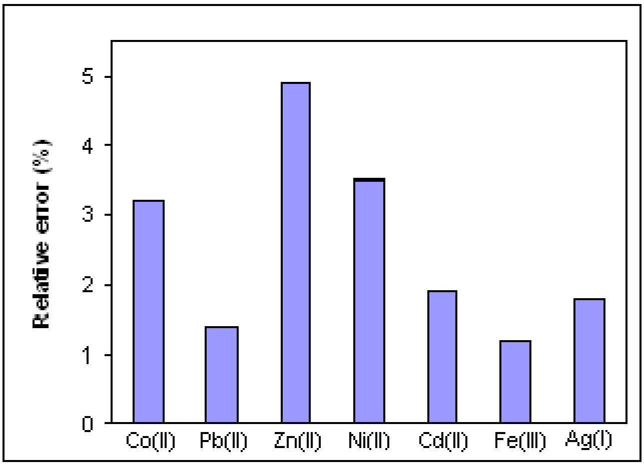

Fig. 3.11. Interferences of different metal ions (1.0 x 10^{-2} M) on the fluorescence determination of Cu^{2+} ion (1.0 x 10^{-6} M) with the proposed membrane sensor at pH 6.0.

The data shown in Figure 3.11 clearly indicate that, in the presence of all the interfering ions studied, the relative error is less than 5.0%, which is recognized as tolerable.

3.4. Conclusion

Highly sensitive and selective determination of Cu^{2+} was accomplished by making the use of the new cyclobutane-substituted schiff base ligand embedded in PVC films. No effect of interferents was observed at the working wavelength. The membrane responds to Cu^{2+} by changing fluorescence intensity reversibly at 505 nm when excited at 415 nm, and is sensitive to Cu^{2+} in the 5.0×10^{-8} - 1.0×10^{-4} M range for an average exposure time of 2.5 min. It has a reproducible response and provides an inexpensive and quick method for the determination of Cu^{2+}. It has also been shown that the response of this sensor does not vary significantly in the pH range 5.0 – 8.0.

4. CHAPTER FOUR

CHARACTERIZATION OF A NEWLY SYNTHESIZED CYCLOBUTANE-SUBSTITUTED SCHIFF BASE LIGAND AND ITS USAGE IN THE CONSTRUCTION OF A SELECTIVE SENSOR FOR COPPER(II)

4.1. Introduction

The determination of traces of metal ions has long been an important subject in environmental analysis and in many types of industrial processes and chemical reactions. Traditional optical techniques for metal ion assay in solution include inductively coupled mass spectroscopy and atomic/molecular absorption spectroscopy. Although these techniques are extremely sensitive down to the subnanomolar level, they are all usually laboratory-based, difficult to use in the field and not amenable to in situ analysis. Additionally, if we consider that, in practice, there exists a large number of samples not contaminated by transition metals which are analyzed in routine analysis, the use of simple and cheap screening systems for the selection of samples is interesting (Cano-Raya et al., 2006).

Optical sensors have attracted a remarkable interest in recent years and an increasing number of studies devoted to the design of devices for the sensing of different species has appeared (Wolfbeis, 2005). Among the different optical properties that can be employed to generate the signal, fluorescence has received the greatest attention, as it is very sensitive, it has several parameters that can be used to obtain analytical information and it uses simple and low-cost instrumentation. Generally, such optical sensors consist of an indicator dye immobilized in or on a solid support: the material so generated responds to the presence of the analyte with a change of its emission properties (Silva and Tecilla, 2005; Ertekin et al., 2000).

In the present work, we studied the photocharacterization of a newly synthesized cyclobutane substituted schiff base ligand and its usage as a selective and sensitive optic sensor for copper ions. The fluorescent 4-(1-phenyl-1-methylcyclobutane-3-yl)-2-(2-hydroxy-5-bromobenzylidene) aminothiazole dye (PCT) has been used for the first time as sensing agent in optical sensor design.

4.2. Synthesis of the 4-(1-phenyl-1-methylcyclobutane-3-yl)-2-(2-hydroxy-5-bromo benzylidene) Aminothiazole

The indicator molecule was synthesized in the laboratories of Fırat University (Çukurovalı et al., 2000). Schematic structure of the employed dye molecule is shown in Figure 4.1.

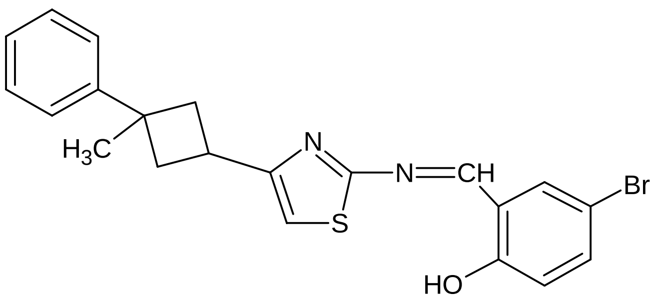

Figure 4.1. Chemical structure of 4-(1-phenyl-1-methylcyclobutane-3-yl)-2-(2-hydroxy-5-bromobenzylidene) aminothiazole (PCT) dye

4-(1-phenyl-1-methylcyclobutane-3-yl)-2-(2-hydroxy-5-bromo benzylidene) aminothiazole (PCT) dye which is a Schiff base was prepared from the reaction of 2-aminothiazole and 5-bromosalicylaldehyde by the literature method (Çukurovalı et al., 2000) in a two steps procedure.

In the first step, to a solution of 0.76 g (10 mmole) of thiourea in 50 mL of absolute ethanol, a solution of 2.225 g (10 mmole) of 1-phenyl-1-methyl-3-(2-chloro-1-oxoethyl)cyclobutane in 20 mL of absolute ethanol was added dropwise at 60–70 °C with continuous stirring. By monitoring the IR frequency of the carbonyl group of 1-phenyl-1-methyl-3-(2-chloro-1-oxoethyl)cyclobutane the completion of the reaction was easily seen. The solution was then made alkaline with an aqueous solution of NH_3 (5%) to separate the pale yellow 4-(1-phenyl-1-methylcyclobutane-3-yl)-2-aminothiazole from the reaction mixture. The precipitate was filtered off, washed with aqueous ammonia solution and water several times, dried in air and recrystallized from aqueous ethanol (1:3). (Yield: 85.21%; mp: 174 °C).

In second step, to a hot (60–70 °C) solution of 2.44 g (10 mmole) of 4-(1-phenyl-1-methylcyclobutane-3-yl)-2-aminothiazole in 30 mL of absolute ethanol, a hot (60–70°C) solution of 2,01 g (10 mmole) of 5-bromosalicylaldehyde in 20 mL absolute ethanol was added dropwise with continuous stirring. The mixture was stirred for 1 h and left to stand overnight. The resulting precipitate was filtered, washed several times with cold ethanol and dried at 110°C to constant weight. Yield: 85%; mp: 180 °C. Characteristic IR bands (KBr, cm^{-1}): 3464 cm^{-1} (OH), 1625 cm^{-1} (C=N, azometine), 1600 cm^{-1} (C=N, in thiazole ring), 1357 cm^{-1} (C-O), 685 cm^{-1} (C-S-C). Characteristic ^{1}HNMR peaks ($CHCl_3$, TMS, δ ppm): 1.57 (s, 3H,CH_3), 2.51–2.62 (m, 4H, –CH_2–in cyclobutane ring), 3.67 (quint, *j*=8.9 Hz, 1H, >CH– in cyclobutane ring), 6.83 (s, 1H, =CH–S in thiazole ring), 7.24–7.54 (m, 8H, aromatics), 9.0 (s, 1H azometine), 12.20 (s, 1H, OH in salicylaldehyde ring). Characteristic ^{13}C NMR peaks ($CDCl_3$, TMS, δ ppm): 128.30 (C1), 129.19 (C2), 120.17 (C3), 124.80 (C4), 135.31 (C5), 119.70 (C6), 137.28 (C7), 163.13 (C8), 101.50 (C9), 149.30 (C10), 31.43 (C11), 31.84 (C12), 41.09 (C13), 30.21 (C14), 135.51 (C15), 124.90 (C16), 126.48 (C17), 125.10 (C18).

The analytical data for the PCT dye are shown in Table 4.1.

Table 4.1. The color, formula, formula weights, melting points, yield, and elemental analyses results of the PCT dye.

Compound	F.W. (g/mole)	Color	m.p. °C	Yield %	Elemental Analyses % Calculated (Found) C	H	N	S
$C_{21}H_{19}N_2OSBr$	427.37	yellow	180	85	59.02 (57.98)	4.48 (4.08)	6.56 (6.21)	7.50 (8.36)

4.3. Results and Discussion

4.3.1. Spectral characterization studies in solution phase

In order to perform the spectral characterization of the PCT dye, absorption, excitation, and emission spectra were recorded in separate solutions of EtOH, THF, and $CHCl_3$. In the employed solvents (EtOH, THF, and $CHCl_3$) the PCT was excited at 443, 440, 438 nm, respectively and the emission spectra were recorded. In order to obtain the excitation spectra, the emission were measured at 520, 526 and 529 nm, respectively while changing the excitation wavelength in the range of 500-330 nm (Figure 4.2). The Stokes shift values, $\Delta\lambda_{ST}$ (the difference between excitation and emission maximum) and quantum yields were extracted from spectral data which are given in Table 4.2.

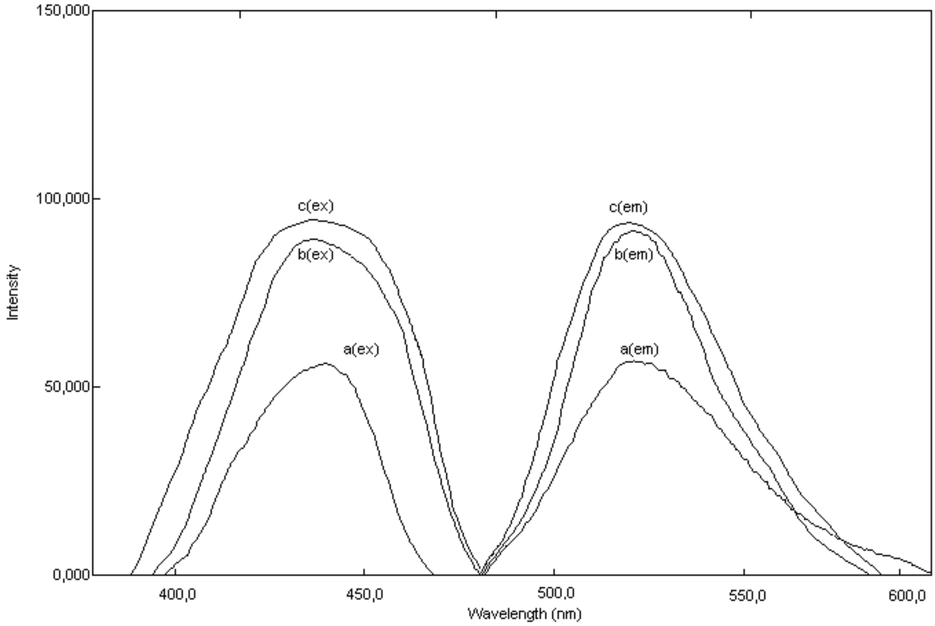

Figure 4.2. Excitation and emission spectra of PCT dye in different solvents
(a) EtOH (λ_{ex} = 443 nm, λ_{em} = 520 nm), (b) THF (λ_{ex} = 440 nm, λ_{em} = 526 nm), (c) $CHCl_3$ (λ_{ex} = 438 nm, λ_{em} = 529 nm)

4.3.2. Spectral characterization studies in solid phase

A comparative study on the effect of different matrix materials on the performance of the sensor was investigated. The PVC and EC doped PCT, excitation and emission spectra of the films were recorded. PCT was excited at 444 and 452 nm in PVC and EC, respectively (see Figure 4.3).

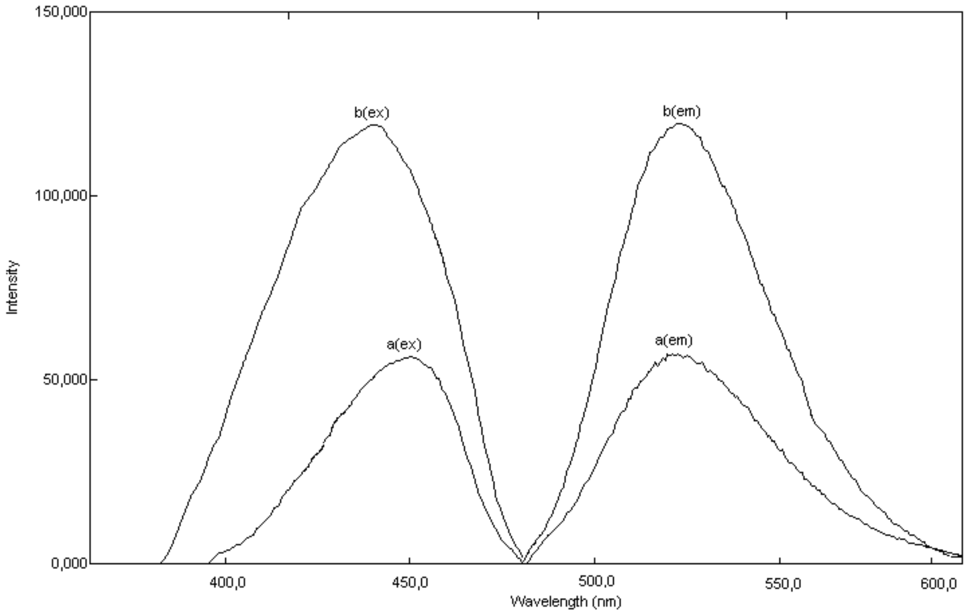

Figure 4.3. Excitation and emission spectra of PCT dye in solid polymer matrix
(a) EC (λ_{ex} = 452 nm, λ_{em} = 523 nm), (b) PVC (λ_{ex} = 444 nm, λ_{em} = 527 nm).

4.3.3. Quantum yield calculations

Fluorescence quantum yield values (Φ_F) of the employed dye was calculated by using the comparative William's method (Williams et al., 1983). For this purpose, the UV-vis absorbance and corrected emission spectra of different concentrations of reference standard (quinine sulphate) and PCT were recorded. The integrated fluorescence intensities were plotted versus absorbance for the reference standard and the Schiff base, PCT, in the PVC, EC matrices and EtOH (Figure 4.4). The gradients of the plots were proportional to the quantity of the quantum yield of the studied molecule.

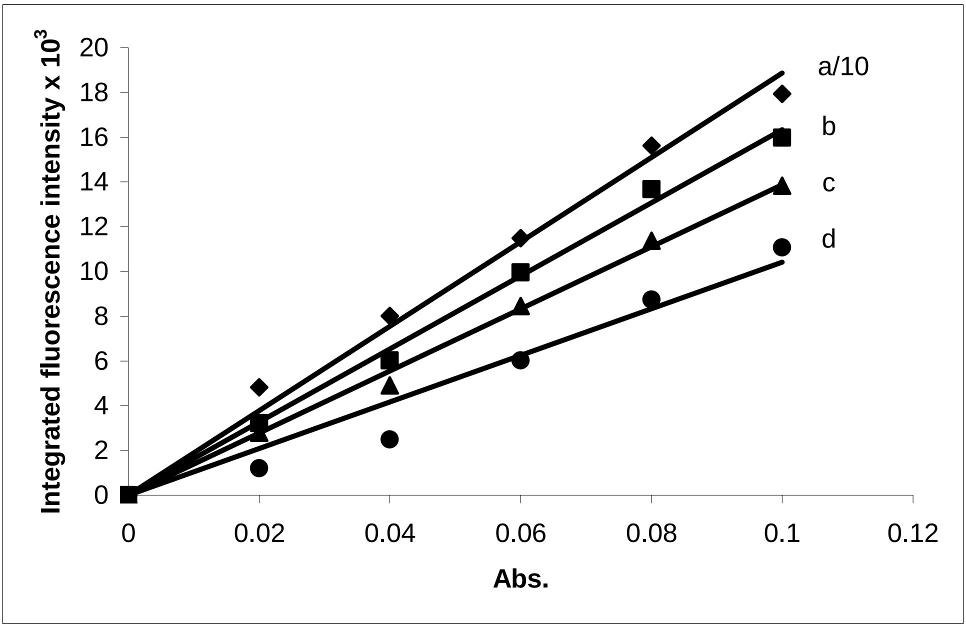

Figure 4.4. The integrated fluorescence intensities vs. absorbance (λ_{ex} =444 nm)

a) for the reference standard (quinine sulphate in 0.1 M H_2SO_4)

b) the PCT dye in PVC matrix

c) PCT dye in EC matrix

d) PCT in EtOH

The equations of the plots are y= 1886550 x; R^2= 0.989 for reference standard, y= 163397 x; R^2= 0.9959 for PCT dye in PVC matrix, and y= 138747 x; R^2= 0.9964 for PCT dye in EC matrix, and y= 104169 x; R^2= 0.9566 for PCT dye in EtOH. Quantum yield (Φ_F) values calculated according to Eq. (2.1) are shown in Table 4.2. According to the data, the PCT dye exhibited quite high quantum yield in plasticized PVC. Therefore, the PVC matrix was chosen as cocktail material for further studies.

Table 4.2.
Emission and excitation spectra related data of dye (λ_{ex}: excitation wavelength, nm; λ_{em}: emission wavelength, nm; Stokes shift, $\Delta\lambda$ nm; Φ_F: quantum yield)

Solvent	Excitation wavelength λ_{ex}(nm)	Emission wavelength λ_{em}(nm)	Stokes shift $\Delta\lambda_{ST}$	Refractive index n	Quantum yield Φ_F
EtOH	443	520	77	1.3590	0.031
$CHCl_3$	440	526	86	1.4458	
THF	438	529	91	1.4070	
PVC	444	527	83	1.5200	0.061
EC	452	523	71	1.4770	0.048

4.3.4. Effect of pH on sensor response

To study the effect of pH on the optode membrane response to copper, the fluorescence intensity versus pH plot for the PCT optode was obtained by changing the solution pH with different buffer solutions and fixing the Cu^{2+} concentration at 1.2 x 10^{-6} M (Figure 4.5). The pH of solution was adjusted by buffers of $CH_3COOH/NaCH_3COO^-$ (pH 4-6), NaH_2PO_4/Na_2HPO_4 (pH 7-8) and NH_4Cl/NH_3 (pH 9-10).

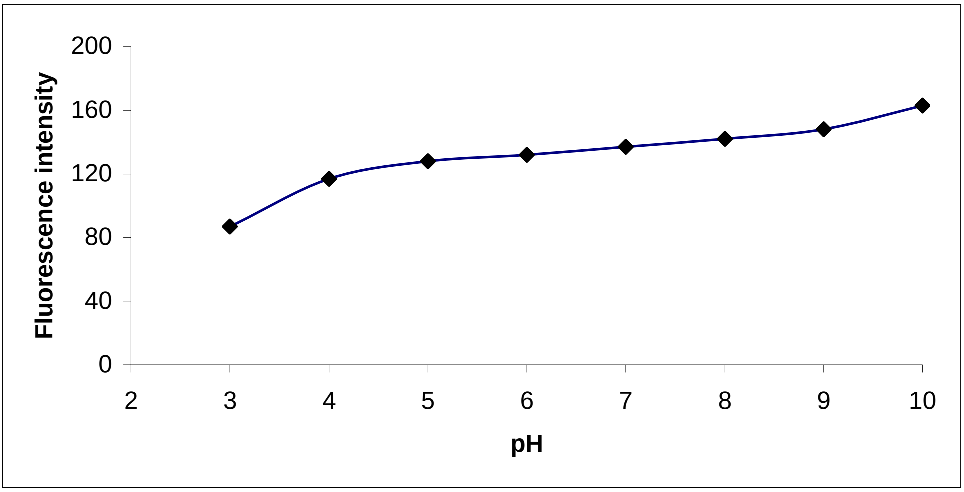

Figure 4.5. Effect of pH on the response of the copper sensor 1.2 x 10^{-6} M Cu^{2+} (λ_{ex} =444 nm).

As it is seen from Figure 4.5, in the pH range below 4.5, the fluorescence intensity of the sensor membrane decreased with decreasing pH value. On the other hand, at pH higher than 9.0 possibly due to a possible slight swelling of the polymeric film under alkaline conditions sensor response increases with pH increase. Moreover, the partial precipitation of $Cu(OH)_2$ under strong basic condition might decrease the actual concentration of Cu^{2+} in the sample solution, which might also cause the increase of fluorescence intensity of the sensor under basic condition. From Figure 4.5 we can see that, in a range of pH from 4.5 to 8.5, acidity does not affect significantly the determination of Cu^{2+} with the proposed sensor membrane. In subsequent experiments, a pH 6.0 $CH_3COOH/NaCH_3COO^-$ buffer solution was selected for further studies.

4.3.5. Fluorescence quenching of sensor membrane by Cu^{2+}

Cu^{2+} form a complex with PCT corresponding to the $M(L)_2$ with a suggested tetrahedral geometry (Figure 4.6). Cu^{2+} bonding takes place with nitrogen of imine groups and by proton exchange with hydroxide groups (Çukurovalı et al., 2000).

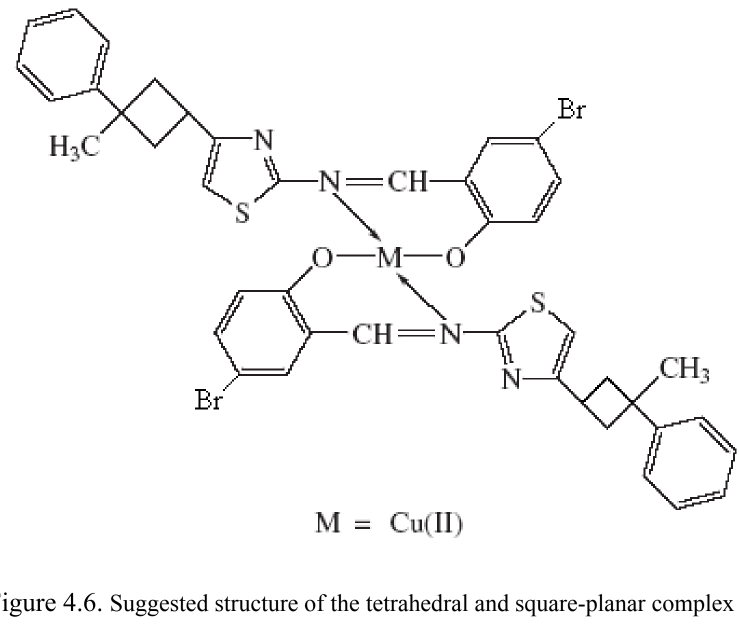

Figure 4.6. Suggested structure of the tetrahedral and square-planar complex of the ligand PCT (Çukurovalı et al., 2000).

Figure 4.7 shows the fluorescence spectra of the PCT optode membrane exposed to a solution containing different concentrations of Cu^{2+}, which are recorded at λ_{ex} =444 nm, λ_{em}=400-650nm.

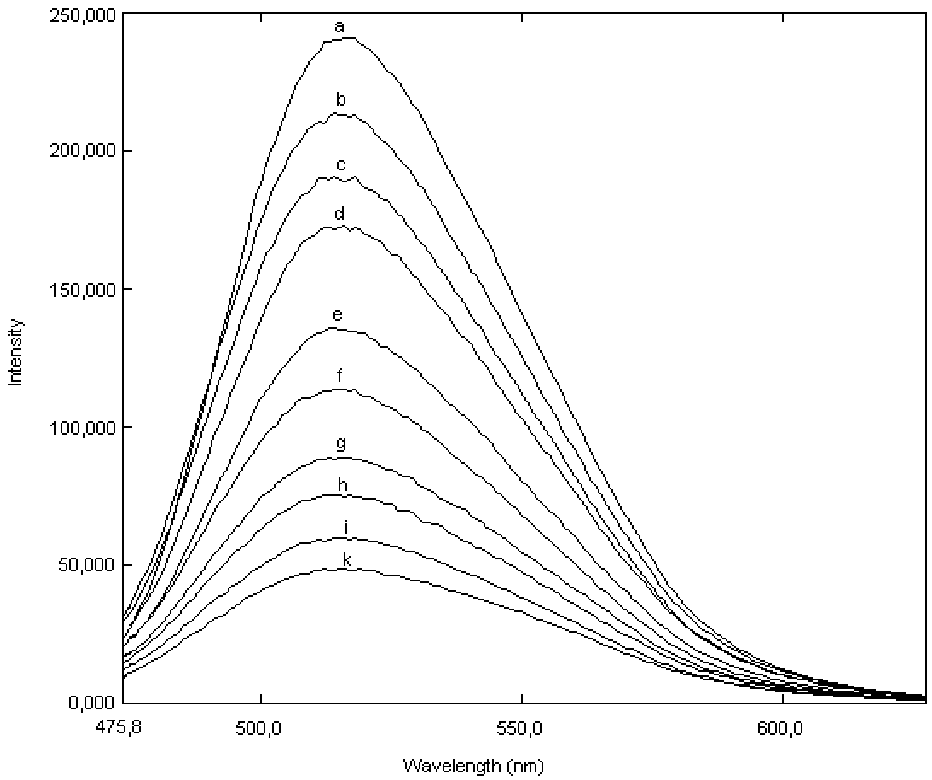

Figure 4.7. Fluorescence emission spectra of the PCT sensing membrane after exposure to different concentration of Cu^{2+}: (a) blank solution; (b) 1.0 x 10^{-8}, (c) 4.0 x 10^{-8}, (d) 1.6 x 10^{-7}, (e) 1.2 x 10^{-6}, (f) 4.8 x 10^{-6}, (g) 2.1 x 10^{-5} , (h) 6.3 x 10^{-5} , (ı) 1.9 x 10^{-4} , (k) 5.7 x 10^{-4} M Cu^{2+} (λ_{ex} =444nm)

Characteristic calibration curve obtained for different concentrations of Cu^{2+} is shown in Figure 4.8. In the concentration range of 1.0 x 10^{-8} to 5.7 x 10^{-4} M a quite good linear correlation was obtained with R^2 value of 0.9946 for Cu^{2+}.

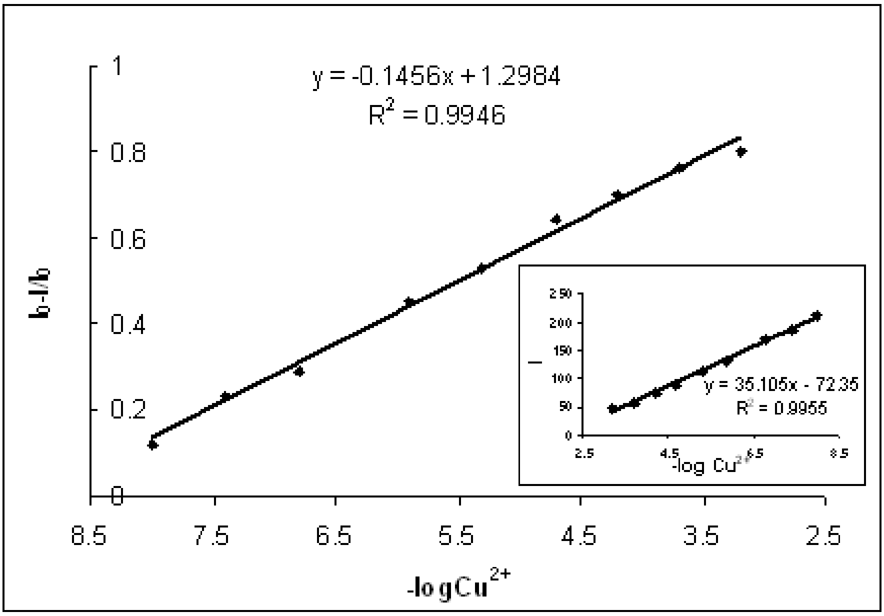

Figure 4.8. Calibration plot of the sensor in the concentration range of 1.0 x 10^{-8} to 5.7 x 10^{-4} M Cu^{2+} (λ_{ex} =444nm)

The photostability of aminothiazole dye in PVC matrix was monitored and recorded with a spectrofluorimeter in the mode of time based measurements. The PCT dye was excited at its excitation wavelength; 444 nm and the data were acquired at maximum emission wavelength of 527 nm during 1 h of monitoring. The acquired data is shown in Figure 4.9. The experimental results reveal that PCT exhibits excellent photostability in PVC matrix.

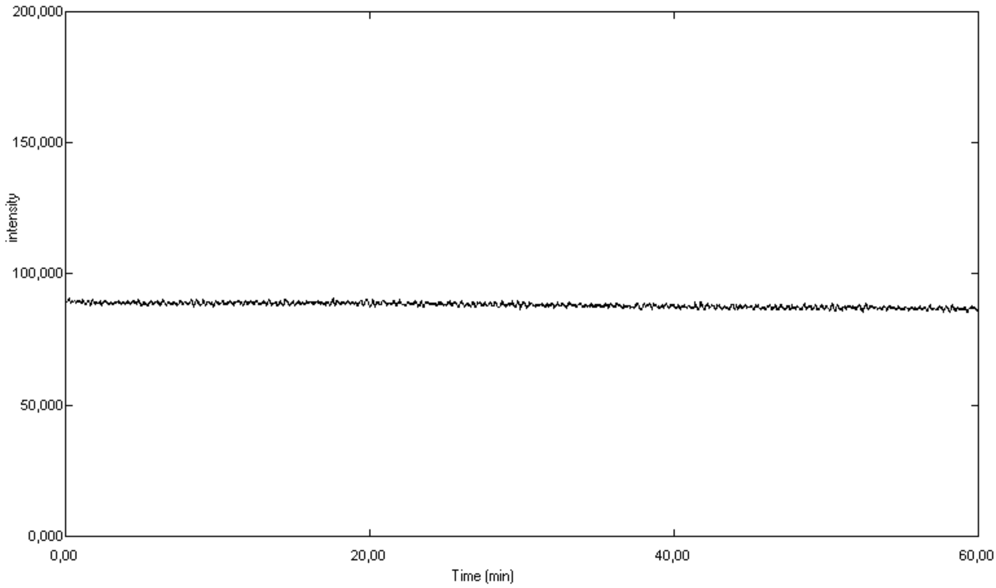

Figure 4.9. Photostability test results of PCT in PVC matrix during 1 h of monitoring.

4.3.6. Response and reproducibility

The approximate response time τ_{90} was measured as 2 min. The short-time stability of the optode membrane was tested by recording the fluorescence intensity of 1.2 x 10^{-6}M Cu^{2+} over a period of 16 min for eight measurements. The sensor was fully reversible and can be regenerated with HCl solution with 100% efficiency (Figure 4.10). The membrane should be washed first with 0.01 M HCl solution and then with blank buffer solution (pH 6.0 CH_3COOH / $NaCH_3COO^-$) after each measurement. The membrane can be easily regenerated by washing once with 0.01 M HCl solution followed by blank buffer solution at the concentration level 1.0 x 10^{-8} M- 5.7 x 10^{-4} M Cu^{2+}. Between the 1st and 5th cycles, the level of reproducibility of the upper signal level achieved was quite good with a low standard deviation, 240.18 ± 1.84.

The limit of detection (LOD) based on three standard deviations of the blank signal was found to be 8.8 x 10^{-9} M (0.56 ng mL^{-1}) for Cu^{2+}.

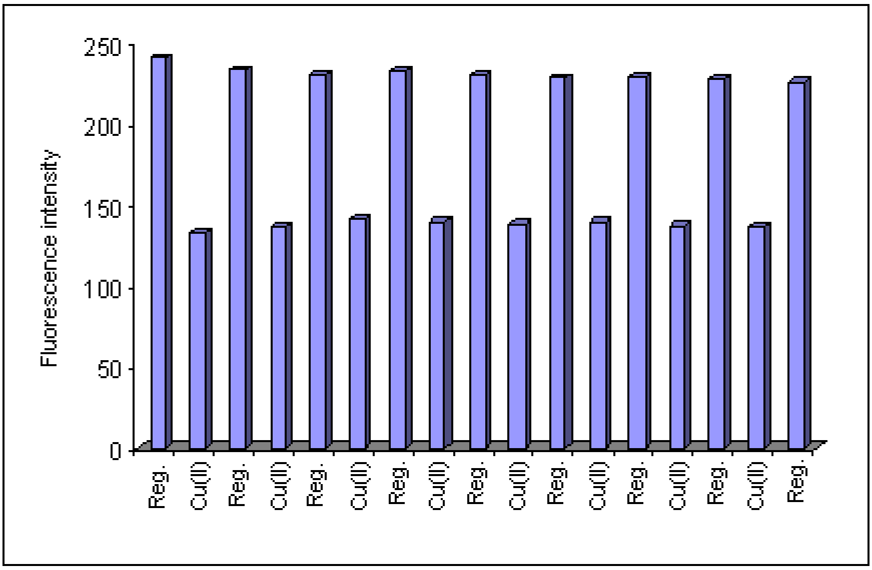

Figure 4.10. Successive responses of the PCT membrane to 1.2 x 10^{-6}M Cu^{2+} at pH=6.0.

4.3.7. Selectivity studies

The effects of various ions on the determination of Cu^{2+} were investigated by analyzing sample solutions containing 1.2 x 10^{-6}M Cu^{2+}. Concentrated solutions of the interfering cations (1.0 x 10^{-2} M) were added into the sample solution, and sensor slides were tested to evaluate the selectivity. The experimental results for common metal cations presented in Table 4.3 reveal that most alkali, and alkaline earth metal cations, and many transition metal cations such as Cd^{2+} and Al^{3+} existing in a concentration of 1.0 x 10^{-2} M do not show significant interfering effect on the Cu^{2+} assay, the relative error being less than ±5%. Ni^{2+} and Co^{2+} in a concentration less than 1.0 x 10^{-3} M do not show appreciable interfering effect on the Cu^{2+} assay.

Table 4.3.

Effects of interferent cations on the fluorescence signal of the optical sensor

Interferent	Concentration (M)[a]	Relative error % ($\Delta F/F_0$ x 100)[b]
Na^{+}	1.0 x 10^{-2}	1.6
K^{+}	1.0 x 10^{-2}	-0.88
Ca^{2+}	1.0 x 10^{-2}	2.2
Mg^{2+}	1.0 x 10^{-2}	3.1
Ag^{+}	1.0 x 10^{-2}	-2.1
Al^{3+}	1.0 x 10^{-2}	3.9
Co^{2+}	1.0 x 10^{-2}	7.1
Co^{2+}	1.0 x 10^{-3}	0.81
Ni^{2+}	1.0 x 10^{-2}	8.8
Ni^{2+}	1.0 x 10^{-3}	0.96
Zn^{2+}	1.0 x 10^{-2}	2.7
Cd^{2+}	1.0 x 10^{-2}	2.4
Pb^{2+}	1.0 x 10^{-2}	1.3
Fe^{3+}	1.0 x 10^{-2}	3.3

[a] The concentration of Cu^{2+} is fixed at 1.2 x 10^{-6} M (pH 6.0).

[b] ΔF is the difference of fluorescence intensities before and after exposure to interferent cations

4.4. Conclusion

The optode described in this part of the study proved that the immobilized PMC dye can be used for copper (II) sensing in the concentration range of 1.0 x 10^{-8} M - 5.7 x 10^{-4} M. It has a reproducible response and provides an inexpensive and quick method for the determination of copper(II). It has been shown that the response of this sensor does not vary significantly in the pH range 4.5 – 8.5. The approximate response time was measured as 2 min. The sensor can easily be regenerated by treatment with 0.01 M HCl. A very low LOD 0.56 µg L^{-1} was reached.

5. CHAPTER FIVE

ZINC(II) SELECTIVE FLUORIMETRIC OPTODE MEMBRANE BASED ON A NEWLY SYNTHESIZED SCHIFF BASE LIGAND EMBEDDED IN POLYMER FILM

5.1. Introduction

Zinc ion is the second most abundant heavy metal ion and well known to play an important role in cellular events including structural co-factors, regulator of enzymes, DNA binding, catalytic centers, and neuronal signal transmission (Berg and Shi, 1996). However, zinc is a metal pollutant of the environment. Too much zinc may reduce the soil microbial activity causing phytotoxic effects (Voegelin et al., 2005) and it is a common contaminant in agricultural and food wastes (Callender, 2004). Therefore, the detection of trace amounts of Zn^{2+} is a significant issue in environmental and biological analysis.

Recent years have seen increasing interest in the development of optical chemical sensors for Zn(II) (Mashraqui et al., 2007; Bereau, 2004). Most of these optodes are based on absorbance or fluorescence measurements of immobilized colorimetric reagent in various matrices. Gupta et al. developed zinc(II)-selective sensor based on dibenzo-24-crown-8 in PVC matrix (Gupta et al., 2005). The practical utility of the sensor has been demonstrated by using it successfully as an indicator electrode in potentiometric titration of Zn^{2+} with EDTA. This sensor can be used in the concentration range 9.2 x 10^{-5} to 1.0 x 10^{-1} M Zn^{2+}.

The immobilization of 4-(2-pyridylazo)resorcinol (PAR) using a base-catalyzed sol-gel process in the presence of amino-groups proved a Zn (II) optical sensor with high sensitivity (Jeronimo et al., 2004). The linear response was obtained for Zn (II) concentration range of 5.0 – 25.0 µg L^{-1}.

Very recently an optical sensor has been designed for the determination of zinc based on zincon as sensing agent (Rastegarzadeh and Rezaei, 2008). The optode can be used for the determination of zinc in the range of 0.76 x 10^{-6} – 30.60 x 10^{-6} M.

In this chapter, we have studied the photocharacterization of a newly synthesized thiazolyl hydrazone derivative schiff base ligand and its usage as a selective and sensitive optical sensor for zinc ions.

5.2. Synthesis of the 2-(2-hydroxy-5-chloro)benzaldehyde-[4-(3-methyl-3-mesitylcyclobutyl)-1,3-thiazol-2yl]hydrazone

Schematic structure of the employed dye molecule (HCB) synthesized in the laboratories at Fırat University (Yılmaz and Çukurovalı, 2003) is shown in Figure 5.1.

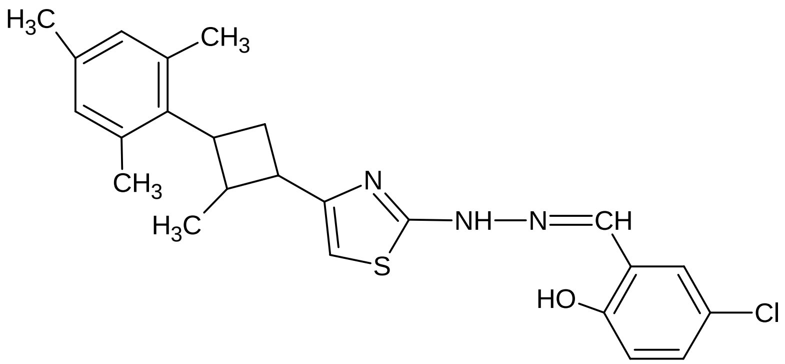

Figure 5.1. Chemical structure of 2-(2-hydroxy-5-chloro)benzaldehyde-[4-(3-methyl-3-mesitylcyclobutyl)-1,3-thiazol-2yl]hydrazone

The compound 2-(2-hydroxy-5-chloro)benzaldehyde-[4-(3-methyl-3-mesitylcyclobutyl)-1,3-thiazol-2yl]hydrazone (HCB) which is a Schiff base was prepared from the reaction of 1-(2-Hydroxy-5-chlorobenzylidene)thiosemicarbazide and 1-Methyl-1-mesityl-3-(2-chloro-1-oxoethyl)cyclobutane by the literature method (Yılmaz and Çukurovalı, 2003) in a two steps procedure as follows. In the first step; to a solution of thiosemicarbazide (0.91 g, 10 mmol) in 50 ml absolute EtOH, a solution of 5-chlorosalicylaldehyde (1.57 g, 10 mmol) in 20 ml absolute EtOH was added dropwise at 60–70°C with continuous stirring. The reaction was monitored by IR spectroscopy. After completing the reaction, the mixture was left overnight. The solid product was filtered off, washed with H_2O several times, dried in air, and crystallized from aqueous EtOH (1:3). (Yield: 94%; mp: 290 °C).

In the second step; to a suspension of 10 mmol 1-(2-hydroxy-5-chlorobenzylidene)thiosemicarbazide (1.95 g) in 30 ml absolute EtOH, a solution of 2.645 g (10 mmol) of 1-mesityl-1-methyl-3-(2-chloro-1-oxoethyl) cyclobutane in 20 ml absolute EtOH was added dropwise at 30–40°C with continuous stirring. After completing the addition, the temperature was raised to 50–55°C. Monitoring the carbonyl group with IR it was easy to determine when the reaction is complete. The solution was then made alkaline with an aqueous solution of NH_3 (5%) and pale yellow solids separated. The precipitates were filtered off, washed with aqueous NH_3 solution several times, dried in air, and crystallized from EtOH. (Yield: 83%; mp: 240 °C) (Figure 5.2)

Step one:

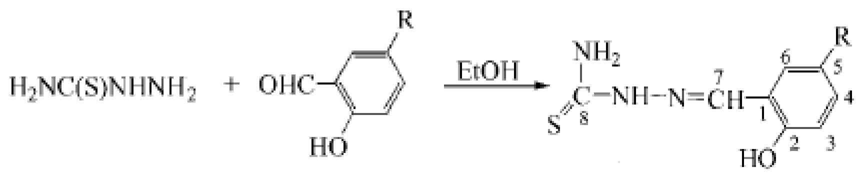

Step two

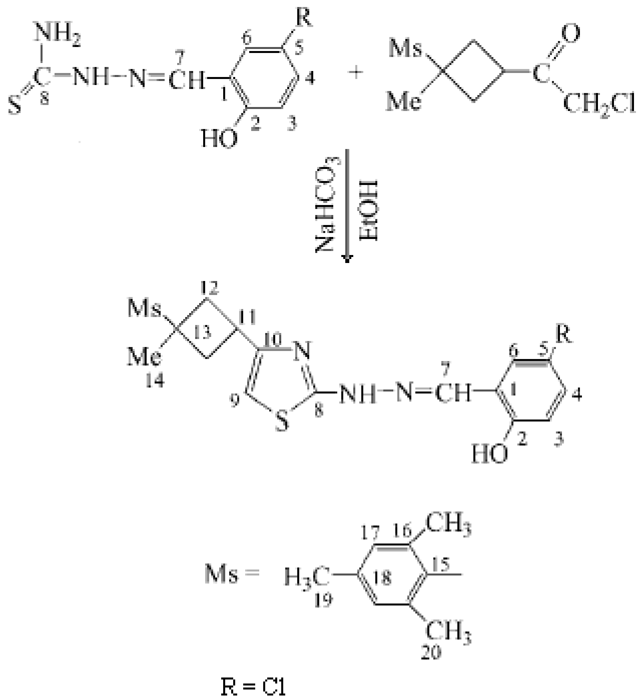

Figure 5.2. Reaction steps for the synthesis of HCB dye.

The analytical data for the HCB dye are shown in Table 5.1.

Table 5.1. The color, formula, formula weights, melting points, yield, and elemental analyses results of the HCB dye (Yılmaz and Çukurovalı, 2003).

Compound	F.W. (g/mole)	Color	m.p. °C	Yield %	Elemental Analyses % Calculated (Found) C	H	N	S
$C_{24}H_{22}ClN_3OS$	440.00	yellow	240	83	65.5 (65.6)	6.0 (6.1)	9.6 (9.5)	7.3 (7.3)

5.3. Results and Discussion

5.3.1. Spectral characterization studies

The emission and related excitation spectra of thiazolyl hydrazone derivative dye, HCB, in the solvents of different polarities and PVC matrix, are presented in Figure 5.3. In all the employed solvents and PVC the Stokes shift values, $\Delta\lambda_{ST}$ (the difference between excitation and emission maximum), calculated from the spectral data were quite high and was found to spread in the wavelength range of 107-125 nm (Table 5.2).

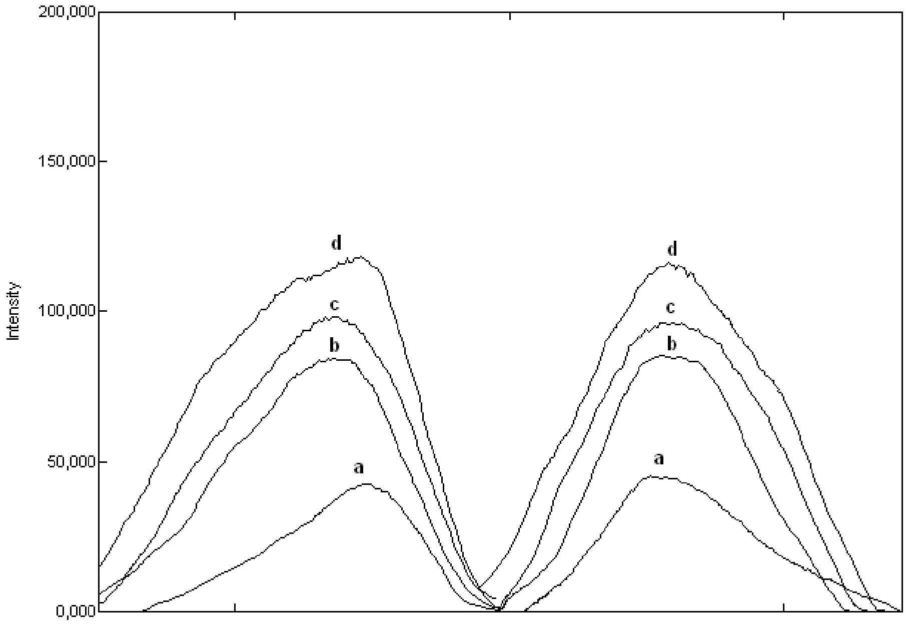

Figure 5.3. Excitation and emission spectra of HCB dye in different solvents and PVC. (a) THF (λ_{ex} = 348 nm, λ_{em} = 455 nm), (b) EtOH (λ_{ex} = 335 nm, λ_{em} = 460 nm), (c) PVC (λ_{ex} = 337 nm, λ_{em} = 462 nm), (d) $CHCl_3$ (λ_{ex} = 340 nm, λ_{em} = 464 nm).

Table 5.2.
Excitation and emission spectra related data of HCB dye (λ_{ex}: excitation wavelength, nm; λ_{em}: emission wavelength, nm; Stokes shift, $\Delta\lambda$ nm)

Solvent	Excitation wavelength λ_{ex}(nm)	Emission wavelength λ_{em}(nm)	Stokes shift $\Delta\lambda_{ST}$
EtOH	335	460	125
$CHCl_3$	340	464	124
THF	348	455	107
PVC film	337	462	125

5.3.2. Quantum yield calculation

Fluorescence quantum yield values (Φ_F) of the HCB compound was calculated employing the comparative William's method which involves the use of well-characterized standards with known (Φ_F) values (Williams et al., 1983). For this purpose, the UV-vis absorbance and emission spectra of six different concentrations of reference standard (quinine sulphate in 0.1 M H_2SO_4) and PCT were recorded. The integrated fluorescence intensities were plotted versus absorbance for the reference standard and the dye (Figure 5.4). The gradients of the plots are proportional to the quantity of the quantum yield of the studied molecules. The equations of the plots are y= 1723680 x; R^2= 0.9991 for reference standard, y= 67375 x; R^2= 0.9919 for HCB dye in

PVC, and y= 30619 x; R^2= 0.9731 for HCB dye in EtOH. The data and quantum yield (Φ_F) values calculated according to Eq. (2.1) are shown in Table 5.2.

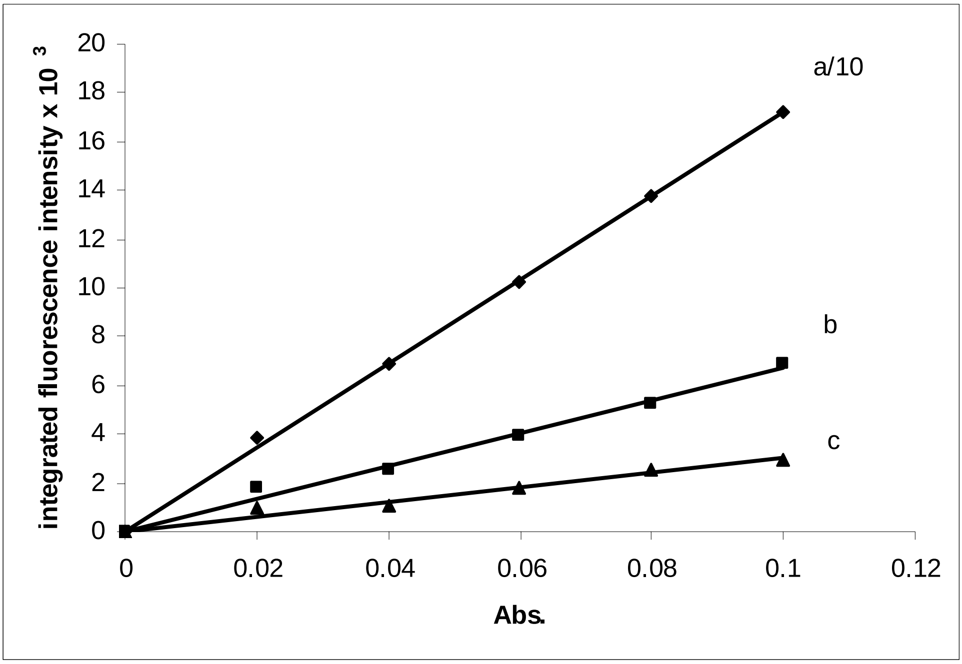

Figure 5.4. The integrated fluorescence intensities vs. absorbance (λ_{ex} =336 nm)

a) for the reference standard (quinine sulphate in 0.1 M H_2SO_4)

b) the HCB dye in PVC matrix

c) HCB dye in EtOH

Table 5.3. Quantum yield related data for HCB in EtOH and PVC matrices.

Dye	HCB (in EtOH)	HCB (in PVC)	QS (in 0.1MH_2SO_4)
Refractive index,n	1.3590	1.5200	1.3328
Equations of plots	y= 30619 x	y= 67375 x	y = 1723680 x
Quantum yields	0.0099 (calculated)	0.0275 (calculated)	0.54

5.3.3. Effect of pH on sensor response

In Figure 5.5 is illustrated the influence of pH of test solution on the fluorescence response of the proposed optical sensor. The fluorescence intensity measurements were made in the presence 2.0 x 10^{-6} M Zn^{2+} solution of different pH values. Maximum signal was obtained between the pH 6.0 and 7.0, and response was slightly decreased above and below this range.

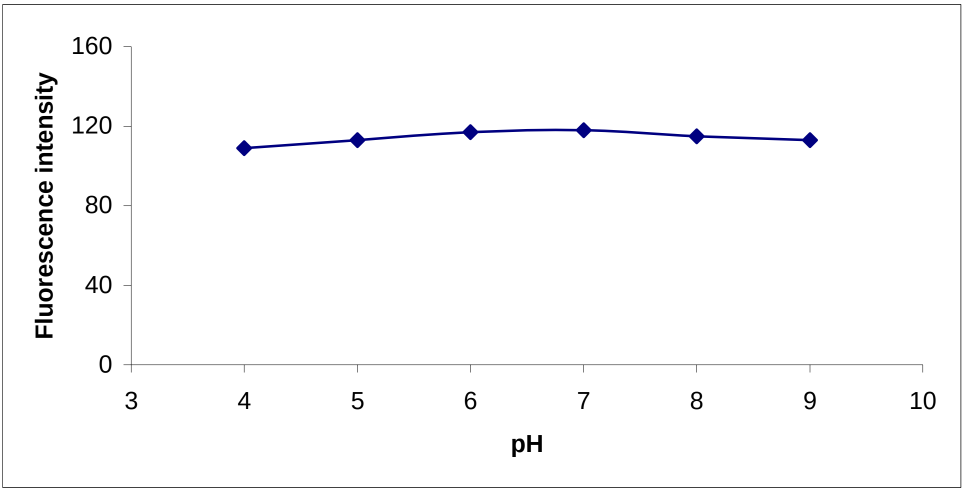

Figure 5.5. Effect of pH on the response of the zinc sensor 2.0 x 10^{-6} M Zn^{2+}

5.3.4. Effect of plasticizers on the performance of sensor

A comparative study on the effect of different plasticizers on the performance of the sensor has been made. The results given in Table 5.4. The optode with DOP as the plasticizer gave the best response for Zn^{2+}, probably due to its highest lipophilicity and suitable polarity, hence selected for all further studies.

Table 5.4. The effect of plasticizers on the response behavior of optodes

Optode	Plasticizer	Working concentration range (M)
1	DOP	5.0×10^{-7} to 9.6×10^{-5}
2	DOS	1.0×10^{-6} to 5.0×10^{-5}
3	DOA	2.0×10^{-6} to 5.0×10^{-5}

5.3.5. Response to Zn^{2+} ions

Zn^{2+} form a complex with HCB corresponding to the $M(L)_2$ with a suggested tetrahedral geometry (Figure 5.6).

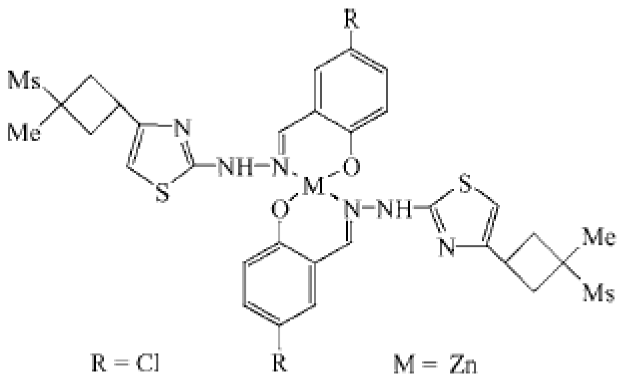

Figure 5.6. Suggested structure of the complex (Yılmaz and Çukurovalı, 2003).

The optical responses of the proposed Zn^{2+} selective fluorescence sensor at different zinc ion concentrations, under the experimental conditions, are shown in Figure 5.7.

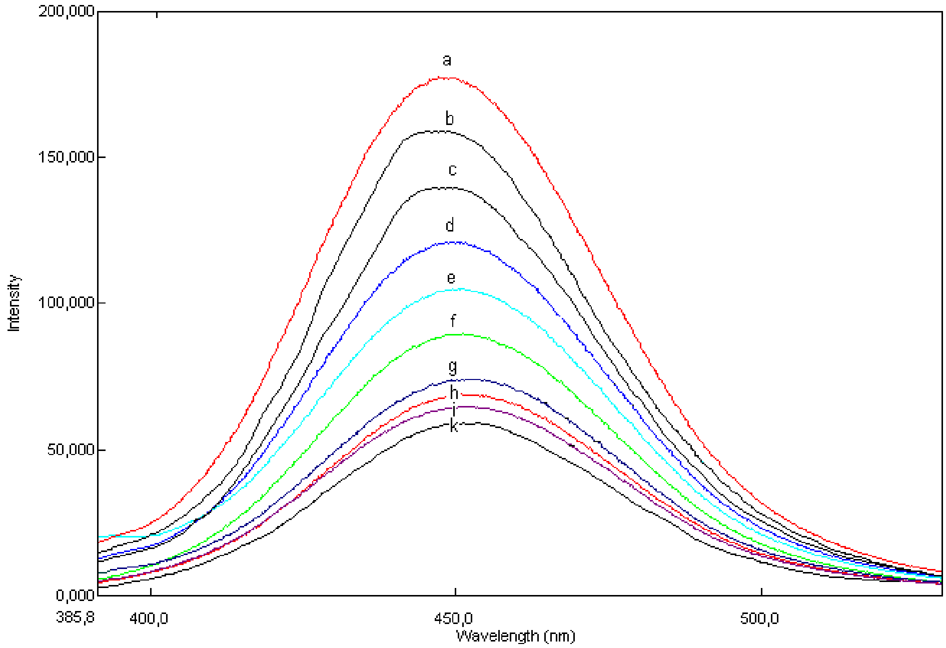

Figure 5.7. Fluorescence emission spectra of the HCB sensing membrane after exposure to different concentration of Zn^{2+}: (a) blank solution; (b) 5.0 x 10^{-7}, (c) 1.0 x 10^{-6}, (d) 2.0 x 10^{-6}, (e) 4.0 x 10^{-6}, (f) 6.0 x 10^{-6}, (g) 1.2 x 10^{-5} , (h) 2.4 x 10^{-5} , (ı) 4.8 x 10^{-5} , (k) 9.6 x 10^{-5} M Zn^{2+} (λ_{ex} =336 nm)

Characteristic calibration curve obtained for different concentrations of Zn^{2+} is shown in Figure 5.8. In the concentration range of 5.0 x 10^{-7} to 9.6 x 10^{-5} M and 5.0 x 10^{-7} to 6.0 x 10^{-5} M Zn^{2+}, linear correlations were obtained with R^2 values of 0.9639 and 0.9941, respectively.

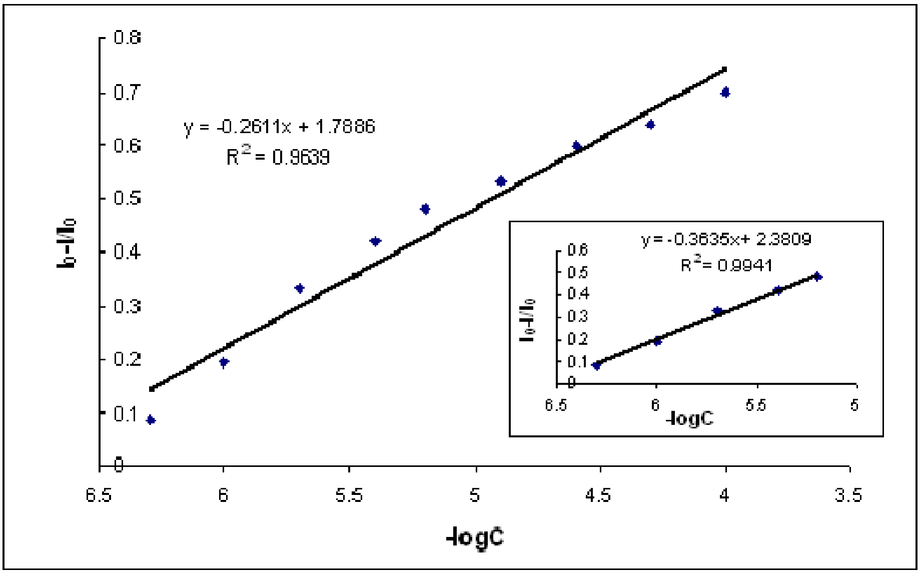

Figure 5.8. Calibration plots of the sensor in the concentration range of 5.0 x 10^{-7} to 9.6 x 10^{-5} M and 5.0 x 10^{-7} to 6.0 x 10^{-5} M Zn^{2+} (λ_{ex} =336 nm)

5.3.6. Response and reproducibility

The sensor was fully reversible within the dynamic working range and the approximate response time τ_{90} was 3 min. Regeneration experiments were carried out in 0.1 M EDTA (Figure 5.9). The limit of detection (LOD) for Zn^{2+} was found to be 2.2 x 10^{-7} M (14.4 ppb). The relative standard deviation for six replicates 2.0 x 10^{-6} M Zn^{2+} was 2.78 %.

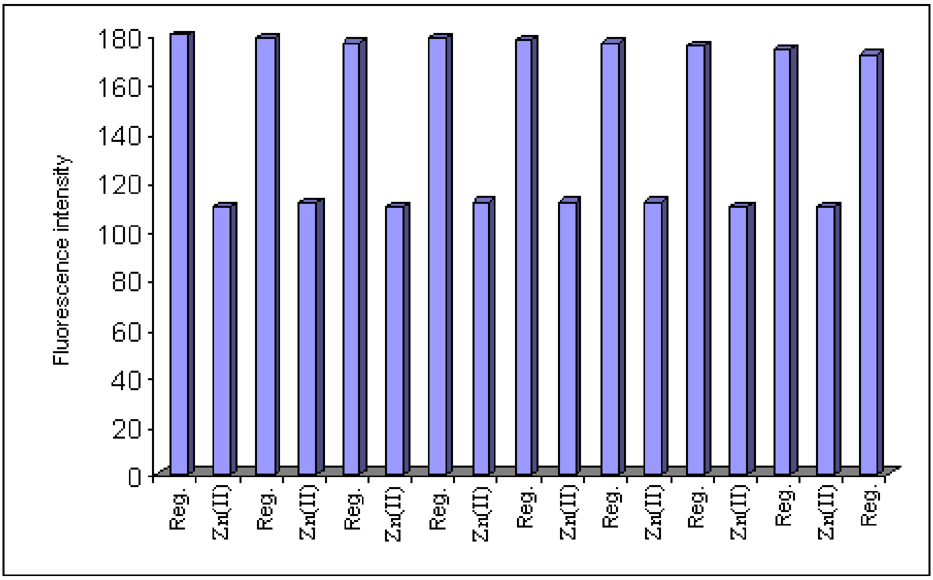

Figure 5.9. Response and reproducibility of the HCB membrane to 4.0 x 10^{-6} M Zn^{2+}

5.3.7. Selectivity studies

The selectivity of the optode was studied for 2.0 x 10^{-6} M Zn^{2+} solution in the presence of different amount of foreign ions using the proposed method. For this purpose, recording the change in the fluorescence intensity before (F_0) and after adding the interfering ion at a 1.0 x 10^{-2} M or 1.0 x 10^{-3} M level (F) into the zinc ion solution. The resulting relative error (RE) is defined as relative signal change, RE(%) = $[(F_0-F) / F_0]$ x 100. The results of selectivity studies are summarized in Table 5.5.

Table 5.5.

Effects of interferent ions on the determination of 2.0 x 10^{-6} M Zn^{2+}

Interferent	Concentration (M)	Relative error % ($\Delta F/F_0$ x 100)[a]
Na^{+}	1.0 x 10^{-2}	2.9
K^{+}	1.0 x 10^{-2}	1.4
Ca^{2+}	1.0 x 10^{-2}	3.3
Mg^{2+}	1.0 x 10^{-2}	3.7
Ag^{+}	1.0 x 10^{-2}	1.6
Al^{3+}	1.0 x 10^{-2}	2.1
Co^{2+}	1.0 x 10^{-2}	7.1
Co^{2+}	1.0 x 10^{-3}	1.8
Ni^{2+}	1.0 x 10^{-2}	7.3
Ni^{2+}	1.0 x 10^{-3}	1.9
Cu^{2+}	1.0 x 10^{-2}	9.2
Cu^{2+}	1.0 x 10^{-3}	2.8
Cd^{2+}	1.0 x 10^{-2}	2.3
Pb^{2+}	1.0 x 10^{-2}	1.4
Fe^{3+}	1.0 x 10^{-2}	2.1

[a] ΔF is the difference of fluorescence intensities before and after exposure to interferent cations

5.4. Conclusion

A new optical sensor has been developed for the selective determination of Zn^{2+} ions. The reversible sensing system was prepared by embedding 2-(2-hydroxy-5-chloro)benzaldehyde-[4-(3-methyl-3-mesitylcyclobutyl)-1,3-thiazol-2yl]hydrazone (HCB) in plasticized PVC membrane. The response of the sensor is based on the fluorescence quenching of HCB by Zn^{2+} ions. The proposed sensor displays a calibration response for Zn^{2+} over a wide concentration range of 5.0×10^{-7} to 9.6×10^{-5} M with a detection limit of 2.2×10^{-7} M (14.4 μg L^{-1}). The sensor can readily be regenerated with EDTA solution.

6. CHAPTER SIX

DEVELOPMENT OF AN OPTICAL SENSOR FOR THE DETERMINATION OF ALUMINUM USING MORIN IMMOBILIZED IN ETHYL CELLULOSE AND SOL-GEL MATRIX

It has been suspected that aluminum may be an important cause of Alzheimer's disease, bone softening and severe toxic effect to patients with chronic renal failure (Flaten, 2001). Much of the aluminum intake is caused either by drinking water and food. For renal failure patients, presence of aluminum in water used for the preparation of dialysis fluid has adverse effects to kidney. Therefore, there is a strong need for development of a sensitive and selective aluminum sensor.

A particularly sensitive fluorometric reagent for the determination of trace aluminum is morin (3,5,7,2',4'-pentahydroxyflavone). Morin can selectively form a highly fluorescent complex with aluminum and has been used widely as a reagent for both fluorometric and spectrophotometric determinations. Various investigations have been undertaken to improve both the extraction efficiency of the fluorescent complex into isobutyl methyl ketone (IBMK) (Hernandez, and Escriche, 1984), and the sensitivity via the addition of non-ionic surfactants (Escriche, 1983).

A recent paper by Lian et al. describes a reversed-phase high-performance liquid chromatographic method, with pre-column complexation of morin and aluminum and fluorometric detection (Lian et al., 2003). A detection limit of 2.0 nmol L^{-1} in a distilled water matrix and precision of 1.8 % at the 1.0 µmol L^{-1} level was achieved and a wide linear range for detection was possible due to the unreacted morin being separated from the fluorescent Al-morin complex.

Gupta et al. proposed Al^{3+} selective potentiometric sensor based on morin in PVC matrix (Gupta et al., 2007). This method worked over a activity range of 5.0 x 10^{-7} to 1.0 x 10^{-1} M of Al^{3+}.

The aim of this study was to develop an optical sensor for the determination of aluminum. These sensors developed were based on the immobilization of morin in ethyl cellulose matrix and sol-gel matrix.

6.1. Effect of pH on Sensor Response

Morin is only weakly fluorescent by itself but forms highly fluorescent complexes with aluminum(III). The fluorescence intensity depends on pH because Al^{3+} displaces hydrogen ion when binding to morin as shown Figure 6.1.

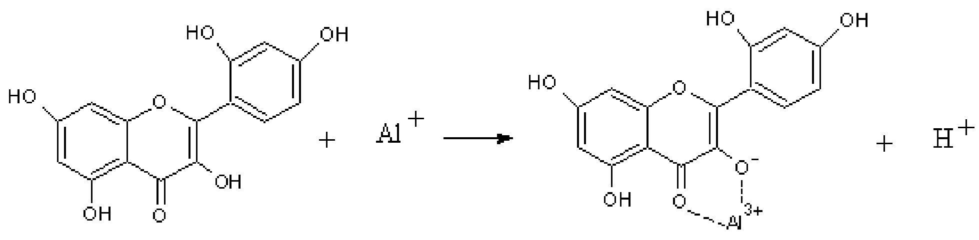

Figure 6.1. Suggested structure of the complexes

As it is seen from Figure 6.2, at low pH the aluminum complex formation decreases because protons tend to displace Al^{3+}. At high pH the fluorescence decreases because more of the aluminum is in the form of hydroxide complexes. Thus, in subsequent experiments, a solution of pH 4.8, adjusted by an acetate buffer, was conducted.

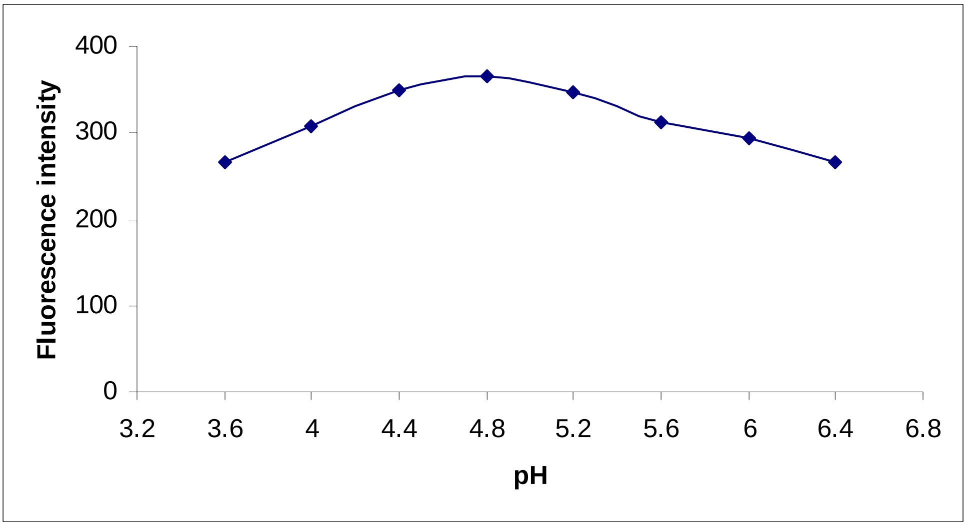

Figure 6.2. Effect of pH on the response of the proposed Al^{3+} sensor in ethyl cellulose matrix ($Al^{3+} = 1.0 \times 10^{-5}$ M)

6.2 Fluorescence Enhancement of the Sensor Membrane by Al^{3+} in Ethyl Cellulose (EC) Matrix

Figure 6.3 shows the change in the fluorescence of the optode with Al^{3+} concentration. The fluorescence intensities of the sensor membrane increase with increasing concentration of Al^{3+}.

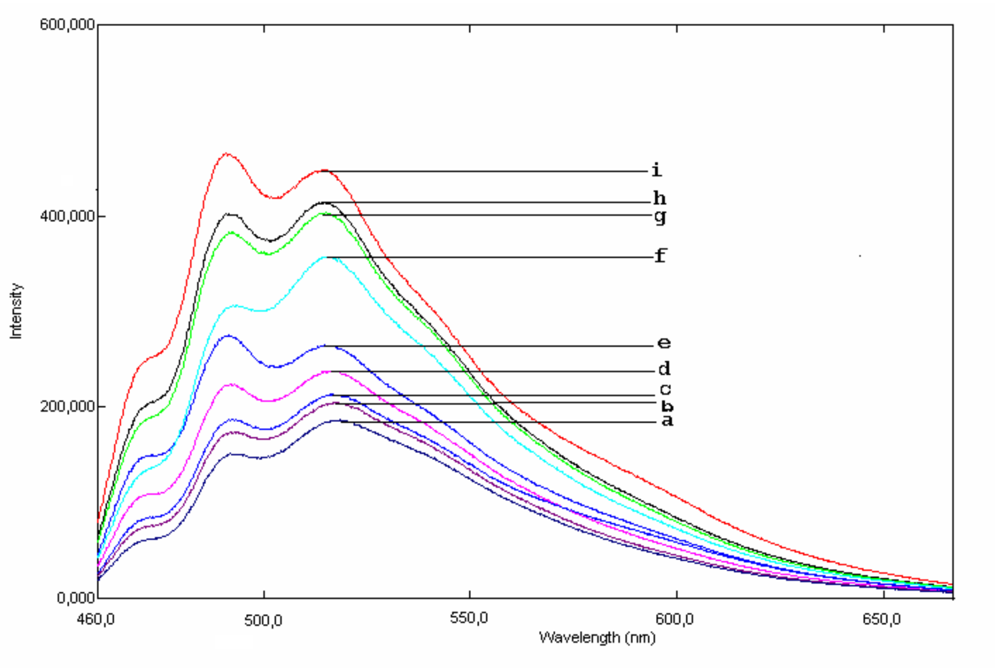

Figure 6.3. Emission spectra of aluminum-selective composition after exposure to different Al^{3+} concentrations (Ethyl cellulose matrix) (a) [Al^{3+}]= 0 M; (b) 1.0 x 10^{-7} M; (c) 5.0 x 10^{-7} M; (d) 1.0 x 10^{-6} M; (e) 5.0 x 10^{-6} M (f) 1.0 x 10^{-5} M; (g) 5.0 x 10^{-5} M; (h) 1.0 x 10^{-4} M; (İ) 5.0 x 10^{-4} M (λ_{ex} = 448 nm)

The linearized calibration plot of sensor can be described by y = -0.3711 x + 3.6113 and the correlation coefficient is 0.9727 (Figure 6.4).

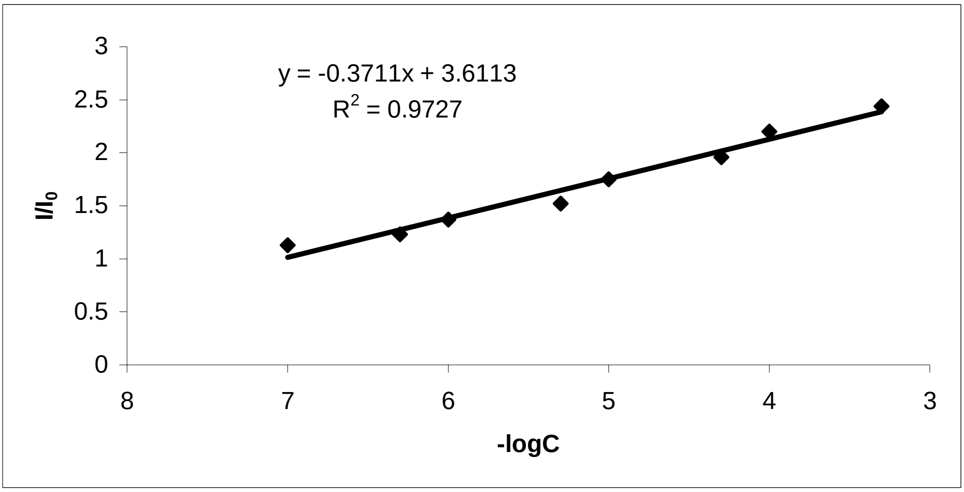

Figure 6.4. Linearized calibration curve of morin immobilized membrane after exposure to Al^{3+} (Ethyl cellulose matrix)

6.2.1. Response and reproducibility in ethyl cellulose matrix

❖ The dynamic working range of the sensor membrane has been found between 1.0×10^{-7} and 5.0×10^{-4} M Al^{3+}.

❖ The sensor is fully reversible within the dynamic range.

❖ The approximate response time (τ_{90}) is found to be 2 min.

❖ Regeneration was accomplished in 0.01 M sodium citrate solution (Figure 6.5)

❖ Relative standard deviation for 1.0×10^{-6}M Al^{3+} (n=6) is 2.5%.

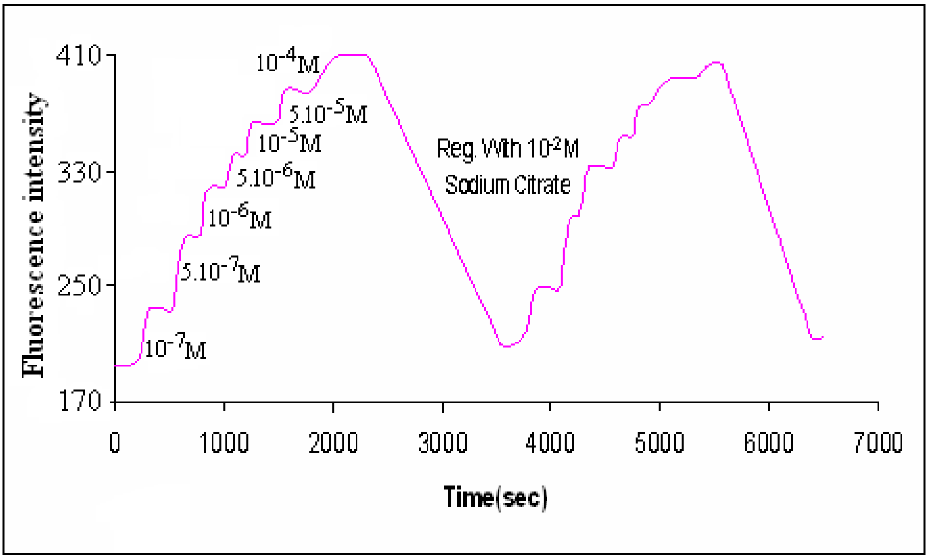

Figure 6.5. The intensity based response curve of membrane (ethyl cellulose matrix) for the determination of aluminum in the concentration range from 10^{-7} to 10^{-4} M (Regeneration with 10^{-2}M sodium citrate solution)

6.3. Fluorescence Enhancement of Sensor Membrane by Al^{3+} in Sol-gel Matrix

The morin embedded optode membrane exhibited remarkable fluorescence intensity enhancement upon exposure to Al^{3+} ions. Figure 6.6 shows the fluorescence spectra of the optode exposed to a solution containing different concentrations of Al^{3+}, which are recorded at λ_{ex}: 460 nm. The fluorescence intensities of the sensor membrane increase with increasing concentration of Al^{3+}, which constitutes the basis for the determination of Al^{3+} with the fluorescent sensor proposed in this part of the study.

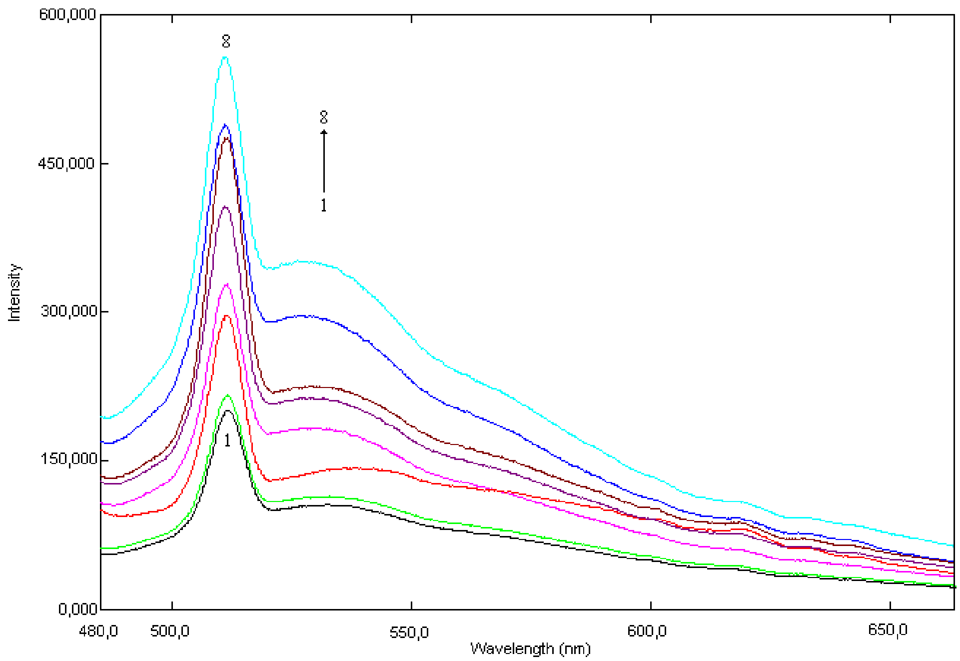

Figure 6.6. Emission spectra of aluminum-selective composition after exposure to different Al^{3+} concentrations (Sol-gel matrix) (1) $[Al^{3+}]$= 0 M; (2) 2.0 x 10^{-6} M; (3) 1.0 x 10^{-5} M; (4) 2.0 x 10^{-5} M; (5) 1.0 x 10^{-4} M (6) 2.0 x 10^{-4} M; (7) 1.0 x 10^{-3} M; (8) 2.0 x 10^{-3} M (λ_{ex} = 460 nm)

In the concentration range of 2.0 x 10^{-6} to 2.0 x 10^{-3} M a linear correlation was obtained with R^2 value of 0.9772 for Al^{3+} (Figure 6. 7).

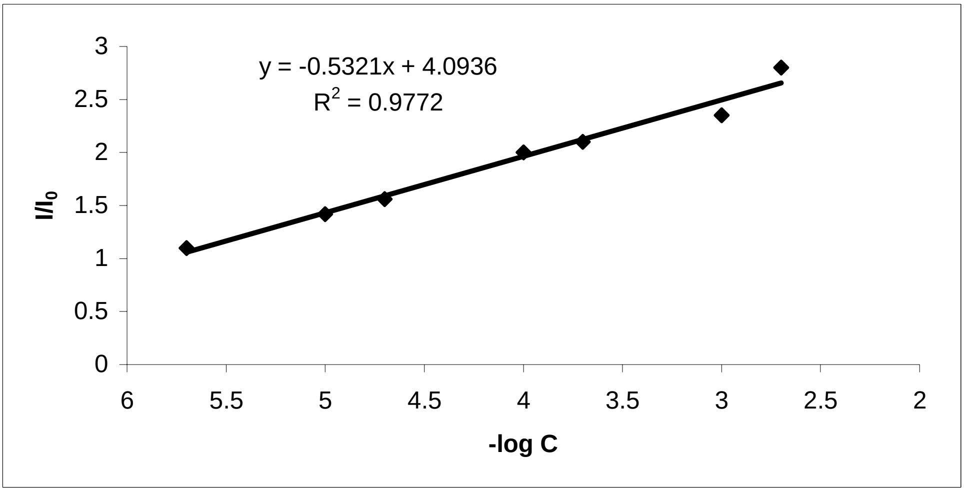

Figure 6.7. Linearized calibration curve of morin immobilized membrane after exposure to Al^{3+} (Sol-gel matrix)

6.3.1. Response and reproducibility in sol-gel matrix

❖ The dynamic working range of the sensor membrane has been found between 2.0 x 10^{-6} to 2.0 x 10^{-3} M Al^{3+}.

❖ The sensor is fully reversible within the dynamic range.

❖ The approximate response time (τ_{90}) is found to be 2.3 min.

❖ Regeneration was accomplished in 0.01 M sodium citrate solution.

❖ Relative standard deviation for 1.0 x 10^{-6} M Al^{3+} (n=6) is 3.1 %.

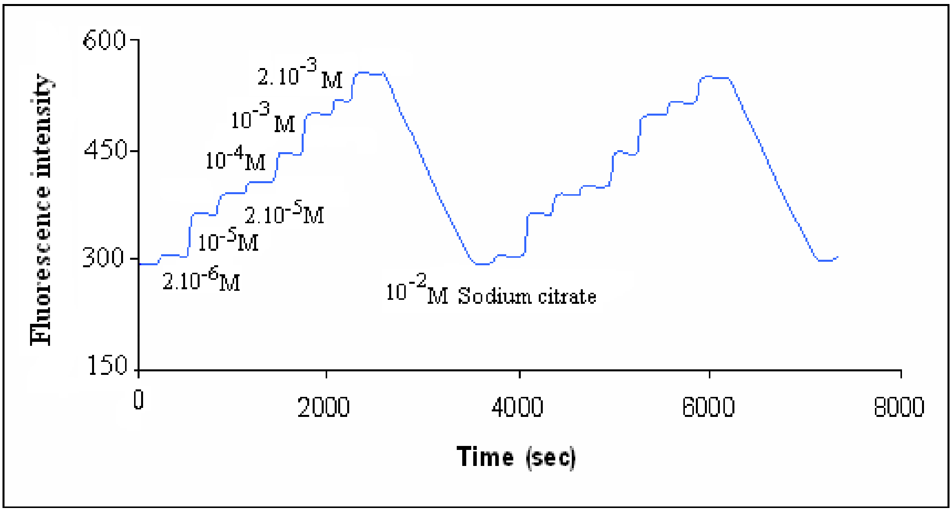

Figure 6.8. The intensity based response curve of membrane (sol-gel matrix) for the determination of aluminum in the concentration range from 2.0 x 10^{-6} to 2.0 x 10^{-3} M (Regeneration with 10^{-2}M sodium citrate solution)

6.4. Selectivity Studies

It is well known that some metals form complexes with morin, so the determination of 1.0 x 10^{-6} M Al^{3+} was tested in presence of these metals. The results are summarized in Table 6.1. Only Pb^{2+} and Fe^{3+} were found to interfere significantly.

Table 6.1.

Effects of interferent ions on the determination of 1.0 x 10^{-6} M Al^{3+}

Interferent	Concentration (M)	Relative error % (ethyl cellulose matrix)	Relative error % (Sol-gel matrix)
Ca^{2+}	1.0 x 10^{-4}	+3.5	+2.9
Mg^{2+}	1.0 x 10^{-4}	+5.3	+4.3
Cu^{2+}	1.0 x 10^{-4}	-6.7	-2.3
Zn^{2+}	1.0 x 10^{-4}	-5.9	-3.5
Cd^{2+}	1.0 x 10^{-4}	-5.6	-5.9
Pb^{2+}	1.0 x 10^{-4}	-8.2	-7.2
Ag^{+}	1.0 x 10^{-4}	-6.8	-4.1
Fe^{3+}	1.0 x 10^{-4}	-9.1	-6.3

6.5. Conclusion

In this part of the study, an optical sensor has been proposed for the determination of aluminum. These sensors developed were based on the immobilization of morin in ethyl cellulose matrix and sol-gel matrix. The response to the concentration of Al(III) at pH 4.8 is linear in ethyl cellulose and sol-gel matrix in the range of 1.0 x 10^{-7}-5.0 x 10^{-4} M, and 2.0 x 10^{-6} to 2.0 x 10^{-3} M, respectively. The sensor is fully reversible within the dynamic range. Regeneration was accomplished in 0.01 M sodium citrate solution.

References

Aelion, R., Loebel, A., and Eirich, F. J., 1950, Hydrolysis of ethyl silicate, *Am. Chem. Soc.,* 72, 5705-5712.

Andrew, K. N., and Worsfold, P. J., 1994, Comparison of multivariate calibration techniques for the quantification of model process streams using diode-array, *Analytes,* 119, 1541-1569.

Andrews, N. C., 2001, Mining copper transport genes. *Proc. Natl. Acad. Sci. USA* 98, 6543–6545.

Assink, R. A., and Kay, B. D. J., 1998, Sol-gel kinetics I, Function group kinetics, *Non-Crystalline Solids.,* 99, 359-370.

Bacci, M., Baldini, F., Scheggi, A. M., 1988, Spectrophotometric investigations on immobilized acid-base indicators, *Anal. Chim. Acta,* 207, 308.

Baird, **C.,** 1999. Enviromental Chemistry, second ed., Freeman and Longman, UK.

Bakker, E. and Simon, W., 1992, Selectivity of ion-sensitive bulk optodes, *Anal. Chem.,* 64 (17) 1805-1812.

Beeler, T. J., Farmen, R. H., Martonosi, A. N., 1981, The mechanism of voltage-sensitive dye responses on sarcoplasmic reticulum, *J. Membr. Biol.,* 62, 113.

Benco, J. S., Nienaber, H.A., McGimpsey, W. G., 2002, A sodium ion sensor based on a covalently-linked aminorhodamine B-calix[4]arene chromoionophore, *Sensors and Actuators B,* 85, 126-130.

Bereau, V., 2004, Coordination studies of a fluorescent sensor for Zn^{2+} detection: characterization in solution and solid state, *Inor. Chem. Commun.,* 7, 829-833.

Berg, J. M., and Shi, Y., 1996, The galvanization of biology: a growing appreciation for the rols of zinc, *Science,* 271, 1081-1085.

Bishop, E., Ed., 1972, Indicators, Pergamon Press, Oxford.

Brinker, C. J., and Scherer, G. W., 1990, Sol-gel science: The physics and chemistry of sol-gel processing, Academic Press, New York.

Bull, P. C., Thomas, G. R., Rommens, J. M., Forbes, J. R., and Cox, D. W., 1993, The Wilson disease gene is a putative copper transporting P-type ATPase similar to the Menkes gene. *Nature Genet.* 5, 327–337.

Callender, E., 2004, Heavy metals in the environment-historical trends, *Tre. On Geochem.,* 9, 67-105.

Campbell, A., and Bondy, S. C., 2000, Aluminum induced oxidative events and its relation to in8ammation: A role for the metal in Alzheimer's disease. *Cell Mol. Biol.* 46, 721}730.

Cano-Raya, C., Fernandez-Ramos, M. D., Capitan-Valey, L. F., 2006, Fluorescence resonance transfer disposable sensor for copper(II), *Anal. Chim. Acta* 555 (2006) 299-307.

Cao, N. W., Shakin, C. M. & Sun, W. D., 1992, Quasiparticle properties of the quarks of the Nambu–Jona-Lasinio model. *Phys. Rev. C,* 46, 2535 – 2546.

Capitan-Valley, L.F., Alvarez de Cienfuegos-Galvez, P., Fernandez Ramos, M.D., Avidad-Castaneda, R., 2000, Determination of calcium by a single –use optical sensor, *Sensors and Actuators B* 71, 140-146.

Chadwick, D. J., and Whelan, J. (Eds)., 1992, Aluminum in Biology and Medicine, Vol. 169, Ciba Found. Symp. Wiley, New York.

Chan, W.H., Yang, R. H., Wang, K.M., 2001, Development of a mercury ion-selecive optical sensor based on fluorescence quenching of 5,10,15,20-tetraphenylporphyrin, *Anal. Chim. Acta,* 444, 261-269.

Chelly, J., Tumer, Z., Tonnesen, T., Petterson, A., Ishikawa-Brush, Y., Tommerup, N., 1993, Isolation of a candidate gene for Menkes disease that encodes a potential heavy metal binding protein. *Nature Genet.* 3**,** 14–19.

Cheng, K. L., Ueno, K., Imamura T., Ed., 1982, Handbook of Organic Analytical Reagents, CRC Press, Boca Raton.

Chenthamarakshan, C.R., Ajayaghosh, A., 1998, Enhanced sensitivity and selectivity in lithium ion recognition property of an oligometric squaraine dye based fluorescent sensor, *Tetrahedron Letters*, 39, 1795-1798.

Christiansen, T. F., 1986, The Achilles heel of the potentiometric measurements the liquid junction potential, *Trans. Biomed. Eng.,* 33, 79.

Constantini, S., and Giordano, R., 1991, *In* ‘‘Aluminum in Chemistry, Biology and Medicine’’ (M. Nicolini, P. F. Zatta, and B. Corain, Eds.), pp. 21-29. Cortina International, Verona.

Çukurovalı, A., Yılmaz, İ., Ahmedzade, M., 2000, Synthesis and characterization of a new cyclobutane-substituted Schiff base ligand and its Co(II), Cu(II), and Ni(II) complexes, *Synth. React. Inorg. Met.-Org. Chem.,* 30-5, 843-853.

Çukurovalı, A., Yılmaz, I., Ahmedzade, M., Özmen, H., 2001, A new cyclobutane-substituted Schiff base ligand and its Co(II), Cu(II), Ni(II), and Zn(II) complexes, *Synth. React. Inorg. Met.-org. Chem.,* 31-2, 255-262.

Culshaw, B. and Dakin, J. P., eds., 1996, Optical Fiber Sensors, Vols. 3 and 4, Artech House, Boston.

Deng, Z., Coudray, C., Gouzoux, L., Mazur, A., Rayssiguier, Y., and Pepin, D., 1998, Effect of oral aluminum and aluminum citrate on blood level and short-term tissue distribution of aluminum in the rat. *Biol. Trace. Elem. Res.* **63,** 139}147.

Dietzmann, K., Letko, G., Sokolowski, A., 1987, Mitochondrial membrane potential in living cells: evidence from studies with rhodamine 6G as fluorescent probe, *Exp. Pathol.,* 31 47.

Egami, C., Suzuki, Y., Sugihara, O., Fujimura, H., Okamato, N., 1997, Wide range pH fiber sensor with congored and methylred doped cladding, *Jpn. J. Appl. Phys.*, 36, 2902-2905.

Eisenrich, S. J., 1980, Atmospheric input of trace metals to Lake Michigan (USA). *Water Air Soil Pollut.* 13, 287-302.

Engelhardt, V.Q., Altenburg, W., Hoebbel, D., and Wieker, W., 1977, Si-NMR spectroscopy of silicate solutions, IV. Investigations on the condensation of monosilicic acid, *Anorg. Allg. Chem.,* 418, 43.

Ensafi, A. A. & Aboutalebi, A., 2005, A versatile stable cobalt optical sensor based on pyrogallol red immobilization on cellulose acetate film. *Sensors & Actuators, Chemicals B*, 105 (2), 479-485.

Ensafi, A. A. & Bakhshi, M., 2003, New Stable Optical Film Sensor Based on Immobilization of 2-Amino-1-Cyclopentene-1-Dithiocarboxylic Acid on Acetyl Cellulose Membrane for Ni(II) Determination, *Sensors and Actuators B: Chemicals*, 96 (1-2), 435-440.

Ertekin, K., Alp, S., Karapire, C., Yenigül, B., Henden, E., İçli, S., 2000, Fluorescence emission studies of an azlactone derivative embedded in polymer films, an optical sensor for pH measurements, *J. Photochem. Photobiol. A: Chemistry,* 137, 155-161.

Ertekin, K., Tepe, M., Yenigül, B., Akkaya, E. U., Henden, E., 2002, Fiber optic sodium and potassium sensing by using a newly synthesized squaraine dye in PVC matrix, *Talanta*, 58, 719-727.

Escriche, J. M., Cigureda, M. G., and Hernandez, F. H., 1983, Increase in the sensitivity of the fluorescent reaction of the complexing of aluminium with morin using surfactant agents, *Analyst,* 108, 1386-1391.

Fernandez-Guttierez, A. and Munoz de la Pena, A., 1985, Determination of inorganic substances by luminescence methods, *Modern Luminescence Spectroscopy, Methods and Applications,* John Wiley & Sons, New York.

Filipek, L. H., Nordstorm, D. K., and Ficklin, W. H., 1987, Interaction of acid mine drainage with waters and sediments of West Squaw Creek in the West Shasta mining district, California. *Environ. Sci. Technol.* 21**,** 388-396.

Flaten, T. P., 2001, Aluminum as a risk factor in Alzheimer's disease, with emphasis on drinking water, *Brain Research Bulletin,* 55, 187-196.

Fluhler, E., Burnham, V. G., and Loew, L.M., 1985, Spectra membrane binding, and potentiometric responses of new charge shift probes, *Biochemistry,* 24, 5749.

Francis, T. S. Y., and Shizhuo, Y., 2002, Fiber Optic Sensors, Marcel Dekker, New York, p. 494.

Frederickson, C.J., and Moncrieff, D.W., 1994 Zinc-containing neurons. *Biol. Signals,* 3,127-139.

Fromherz, P., Kotulla, R., 1984, Fluorescent dye in soap lamella as a probe of the electrical potential, *Ber. Bunsenges. Phys. Chem.,* 88, 1106.

Ganrot, P. O., 1986,Metabolism and possible health effects of aluminum. *Environ. Health Perspect.* 65**,** 363-441.

Galster, H., 1991, pH Measurements: Fundamentals, Methods, Applications, Instrumentatio, Weinhein,VCH, Germany.

Gee, K. R., Zhou, Z. L., Ton-That, D., Sensi, S. L., Weiss, J.H., 2002, *Cell.Calcium,* 35, 245–251.

Göpel, W., Schierbaum, K. D., 1995, SnO_2 sensors: Current status and future prospects, *Sensors and ActuatorsB,* 26, 1-12.

Göpel, W., Reinhardt, G. & Rösch, M., 2000, Trends in the development of solid state amperometric and potentiometric high temperature sensors. *Solid State Ionics*, 136-137 (2), *519-531.*

Grattan, K. T. V. and Meggitt, B. T. eds., 1998. Optical Fiber Sensor Technology II: Devices and Technology, Chapman and Hall, London.

Gupta, V. K., Khayat, M., Minocha, A. K., Kumar, P., 2005, Zin (II)-selective sensors based on dibenzo-24-crown-8 in PVC matrix, *Anal. Chim. Acta,* 532, 152-158.

Gupta, V. K., Jain, A. K., Maheshwari, G., 2007, Aluminum(III) selective potentiometric sensor based on morin in poly(vinyl chloride) matrix, *Talanta,* 72, 1469-1473.

Harris, W. R., Berthon, G., Day, J. P., Exley, C., Flaten, T. P., Forbes, W. F., Kiss, T., Orvig, C., and Zatta, P. F., 1996, Speciation of aluminum in biological system. *J. Toxicol. Environ. Health* **48,** 543-568.

Hernandez, F. H., and Escriche, J. M., 1984, Fluorimetric determination of aluminium with morin after extraction with isobutyl methyl ketone. Part I. Fluorescence of the aluminium-morin complex in an isobutyl methyl ketone-ethanol-water system, *Analyst,* 109, 1585-1588.

Hisamoto, H., Miyashita, N., Watanabe, K., Nakagawa, E., Yamamoto, N., Suzuki, K., 1995, Ion sensing film optodes: disposable ion sensing probes for the determination of Na^+, K^+, Ca^{2+} and Cl^- concentrations in serum, *Sens. Act. B.,* 29, 378-385.

Iler, R. K., 1979, The chemistry of Silica, Wiley, New York.

Ittel, T. H., 1993, Determinants of gastrointestinal absorption and distribution of aluminum in health and uraemia. *Nephrol. Dial. Transplant.,* 8, 17-24.

Jain, A.K., Gupta, V.K., Singh, L.P., Raisoni, J.R., 2005, Chelating ionophore based membrane sensors for copper(II) ions, *Talanta*, 66, 1355-1361.

Jeronimo, P. C. A., Araujo, A. N., Conceiçao, M., Montenegro, B. S. M., 2004, Development of a sol-gel optical sensor for analysis of zinc in pharmaceuticals, *Sensors and Actuators B,* 103, 169-177.

Katayama, Y., Fukuda, R., Iwasaki, T., Nita, K., Takagi, M., 1988, Synthesis of chromogenic crown ethers and liquid-liquid extraction of alkaline earth metal ions, *Anal. Chim. Acta,* 204, 118.

Keefer, K. D., 1990, Silicon based polymer science: a comprehensive resource, ACS Advances in chemistry ser. No.224, American Chemical Society, Washington, DC, 227-240.

Kelts, L. W., Effinger, N.J.; Melpolder, S.M., 1986, Sol-gel chemistry studied by proton and silicon-29 nuclear magnetic resonance, *J. Non-Crystalline Solids.*, 83, 353-374.

Kirkbright, G. F., Narayanaswamy, R., Welti, N. A., 1984, Fiber-optic pH probe based on the use of an immobilized colorimetric indicator, *Analyst,* 109, 1025.

Koch, K. R., Pougnet, M. A. B, Villiers, S. De., and Montegudo, F., 1988, Increased urinary excretion of aluminum after drinking tea, *Nature* 333, 122.

Kotyk, A. and Slavik, J., 1988, Intracellular pH and its measurement, CRC Press, Boca Raton.

Kurihara, K., Ohtsu, M., Yoshida, T., Abe, T., Hisamoto, H., Suzuki, K., 2001, Micrometer-sized lithium ion-selective microoptodes based on a tailed neutral ionophore and a fluorescent anionic dye, *Anal. Chim. Acta,* 426, 11-18.

Kurochkin, V. E., and Makaroa, E.D., 1996, Reflectance spectrophotometry of plasticized membranes for the design of fast optical chemosensors, *Anal. Commun.*, 33, 115-116.

Lakowicz, J. R., 1999, Principles of Fluorescence Spectroscopy, Kluwer Academic, Plenum Publishers, New York, p.698.

Lee, R. E., Jr., and von Lehmden, D. J., 1973, Trace metal pollution in the environment. *J. Air Pollut. Control Assoc.* 23, 853-857.

Lerchi, M., Bakker, E., Rusterholz, B., Simon, W., 1992, Lead-selective bulk optodes based on neutral ionophores with subnanomolar detection limits, *Anal. Chem.*, 64 (14) 1534-1540.

Levesque, L., Mizzen, C. A., McLachlan, D. R., and Fraser, P. E., 2000, Ligand specific effects on aluminum incorporation and toxicity in neurons and astrocytes. *Brain Res.* 877**,** 191-202.

Lian, H. Z., Kang, Y. F., Yasin, A., Bi, S. P., Shao, D. L., Chen, Y. J., Dai, L. M. Tian, L. C., 2003, D etermination of aluminum in environmental and biological samples by reversed-phase high-performance liquid chromatography via pre-column complexation with morin, *J. Chromatog.,* 993, 179-185.

Martin, C.M., 2006 Vitamins for the elderly: from A to zinc, *Consult Pharm.* 21:450-64

Mashraqui, S. H., Sundaram, S., Khan, T., and Bhasikuttan, A. C., 2007, Zn^{2+} selective luminescent 'off-on' probes derived from diarly oxadiazole and aza-15-crown-5, *Tetrahedron,* 63, 11093-11100.

Massaro, E. J., 2002, Handbook of copper pharmacology and toxicology, Humana Press, Totowa, New Jersey, 626 p.

Matsumoto, H., 2000, Cell biology of aluminum toxicity and tolerance in higher plants. *Int. Rev. Cytol.* 200**,** 1-46.

Mckenzie, H. A. And Smythe, L.E., 1988, Quantitative Trace Analysis of Biological Materials, Elsevier, Amsterdam.

Mei, L., Xiang, Y., Li, N., Tong, A., 2007, A new fluorescent probe of rhodamine B derivative for the detection of copper ion, *Talanta,* 72, 1717-1722.

Mercer, J. F., 2001, The molecular basis of copper-transport diseases. *Trends Mol. Med.* 7**,** 64–69.

Mercer, J. F., Livingston, J., Hall, B., Paynter, J. A., Begy, C., Chandrasekharappa, S., et al., 1993, Isolation of a partial candidate gene for Menkes disease by positional cloning. *Nature Genet.* 3**,** 20–25.

Merian E. (Ed.), Metals and Their Compounds in the Environment, VCH, Weinheim, 1991.

Moody, G.J., Saad, B.B., Thomas, J.D.R., 1998, The development of polymer matrix membranes for ion selective electrodes, *Sel. Electrode Rev.* 10, 71-78.

Mohr, G. J., 2006, A general introduction into optical sensor materials and recognition mechanism, http://www2.uni-jena.de/~c1moge/Mohr/ASCOS2002.pdf)

Motellier, S., Michels, M. H., Dureault, B., Toulhoat, P., 1993, Fibre optic pH sensor for in situ applications, *Sensors and Actuators B,* 11, 467-473.

Mukundan, R., Brosha, E. L., Brown, D.R. & Garzon, F.H., 1999, ceria-electrolyte-based mixed potential sensors for the detection of hydrocarbons and carbon monoxide, *Electrochemical and Solid State Letters,* 2(8): 412-414.

Nayak, P., and Chatterjee, A. K., 2000, Differential responses of brain phosphoesterases to aluminum in dietary protein adequacy and inadequacy. *Food. Chem. Toxicol.* **39,** 587}592.

Oehme, I., and Wolfbeis, O. S., 1997, Fundamental Rewiev: Optical sensors for determination of heavy metal ions, *Microchim. Acta,* 126, 177-192.

Oter, O., Ertekin, K., Kılıcarslan, R., Ulusoy, M., Cetinkaya, B., 2007a, Photocharacterization of a novel fluorescent Schiff Base and investigation of its utility as an optical Fe^{3+} sensor in PVC matrix, *Dyes and Pigments*, 74, 730-735.

Oter, O., Ertekin, K., Kirilmis, C., Koca, M., 2007b, Spectral characterization of a newly synthesized fluorescent semicarbazone derivative and its usage as a selective fiber optic sensor fot copper(II), *Anal. Chim. Acta,* 584, 308-314.

Ozturk, G., Alp, S., Ertekin, K.,2007, Fluorescence emission studies of 4-(2-furylmethylene)- 2-phenyl-5-oxazolone embedded in polymer thn film and detection of Fe^{3+} ion, *Dyes and Pigments,* 72, 150-156.

Peterson, J. I., Goldstein, S. R., Fitzgerald, R. V., Buckhold, D. W., 1980, Fiber-optic pH probe for physiological use, *Anal. Chem.,* 52, 864.

Pineros, M. A., and Kochian, L. V., 2001, A patch-clamp study on the physiology of aluminum toxicity and aluminum tolerance in maize: Identi7cation and characterization of Al(3_)- induced anion channels. *Plant Physiol.* **125,** 292-305.

Pohl, E. R. and Osterholtz, F. D., 1985, Molecular Characterization of Composite Interfaces, Plenum, New York, p.157.

Prassas, M., and Hench, L.L., 1984, Ultrastructure Processing of Ceramics, Glasses, and Composites, John Wiley & Sons, New York, 100-125.

Radisky, D., Kaplan, J., 1999, Regulation of transition metal transport across the yeast plasma membrane, *J. Biol. Chem.* 274, 4481-4484.

Rastegarzadeh, S., and Rezaei, V., 2008, An optical sensor for zinc determination based on zincon as sensing reagent, *Sensors and Actuators B,* 129, 327-331.

Reinhoudt, D. N., Stauthamer, W. P. R. V., Engbersen, J. F. J., Verboom, W., 1994, Influence of plasticizer on the selectivity of nitrate-sensitive CHEMFETs, *Sensors and Actuators B,* 17, 197-201.

Saleh, N., Rawashded, A.M.M., Yousef, Y.A., Al-Soud, Y.A., 2007, Structural characterization of new Cd^{2+} fluorescent sensor based on lumazine ligand: AM1 and ab initio studies, *Spectrochimica Acta Part A*, 68, 728-733.

Sali, S., Grabchev, I., Chovelon, J.M., Ivanova, G., 2006, Selective sensors for Zn^{2+} cations based on grew green fluorescent poly(amidoamine) dendrimers peripherally modified with 1,8-naphtalimides, *Spectrochimica Acta Part A*, 65, 591-597.

Seiler, K. and Simon, W., 1992, Theoretical aspects of bulk optode membranes, *Anal. Chim. Acta*, 266, 73-87.

Shamsipur, M, Alizadeh, K., Hosseini, M., Caltagirone, C., Lippolis, V., 2006a, A selective optode membrane for silver ion based on fluorescence quenching of the dansylamidopropyl pendant arm derivative of 1-aza-4,7,10- trithiacyclododecane([12]aneNS_3), *Sensors and Actuators B*, 113, 892-899.

Shamsipur, M., Poursaberi, T., Avanes, A., Sharghi, H., 2006b, Copper(II)-selective fluorimetric bulk optode membrane based on a 1-hydroxy-9,10-anthraquinone derivative having two propenyl arms as a neutral fluorogenic ionophore, *Spectrochimica Acta Part A*, 63, 9-14.

Shimizu, Y., Bartolomeo, E. D., Traversa, E., Gusmano, G., Hyodo, T., Wada, K., Egashira, M., 1999, SnO_2 sensors: Current status and future prospects, *Sensors and ActuatorsB,*60, 118-124.

Sigg, L., Xue, H., 1994, Metal speciation: concepts, analysis and effects, in: G. Bidoglio, W. Stumm (Eds.), Chemistry of Aquatic Systems: Local and Global Perspectives, Kluwer Academic Publishers, Dordrecht, p. 153.

Sorrenson, J. R. J., Campbell, I. R., Tepper, L. B., and Lingg, R. D., 1974, Aluminum in the environment and human health. *Environ. Health Perspect.* 8**,** 3-95.

Steinberg, I.M., Lobnik, A., Wolfbeis, O.S., 2003 Characterisation of an optical sensor membrane based on the metal ion indicator Pyrocatechol Violet*, Sensors and Actuators B*, 90, 230-235.

Suidan, J. S., Young, B. K., Hetzel, F. W., Seal, H. R., 1983, pH measurement with a fiber-optic tissue pH monitor and a standard blood pH meter, *Clin. Chem.,* 29, 1566.

Szöllösi, J., Damjanovich, S., Mulhern, S. A., Tron, L., 1987, Fluorescence energy transfer and membrane potential measurements monitor dynamic properties of cell membranes: a critical review, *Prog. Biophs. Mol. Biol.,* 49, 65.

Szpunar, J., Lobinski, **R.,** 1999, Species-selective analysis for metal-biomacromolecular complexes using hyphenated techniques, *Pure and App. Chem.,* 71, 899-918.

Tan, W., Shi, Z., Kopelman, R., 1992a, Development of submicron chemical fibre optic sensors, *Anal. Chem.,* 64, 2985-2990.

Tan, W., Shi, Z., Smith, S., Birnbaum, D., Kopelman, R., 1992b, Submicrometer intracellular chemical optical fiber sensors, *Science,* 258, 778-781.

Tanzi, R. E., Petrukhin, K., Chernov, I., Pellequer, J. L., Wasco, W., Ross, B., et al., 1993, The Wilson disease gene is a copper transporting ATPase with homology to the Menkes disease gene. *Nature Genet.* 5**,** 344-350.

Trautwein, A. X. (Ed.), 1997, Wiley-VCH, Weinheim, Bioinorganic Chemistry.

Turner, A. P. F., Karube, I., Wilson, G. S., 1987, Biosensors, Oxford University Press, Oxford.

U. S. Public Health Service, 1992, Toxicological Profile for Aluminum and Compounds.'' (Contact No. 205-88-0608). Prepared by Clement International Corp.

Van Gent, J., Sudhölter, E. J. R., Lambeck, P. V., Popma, T. J. A., Gerritsma, G. J., Reinhoudt, D. N., 1988, A chromophoric crown ether as a sensing molecule in optical sensors for the detection of alkali metal ions, *J. Chem. Soc. Chem. Commun.,* 893.

Vasto, S., Mocchegiani, E., Candore, G et al., 2006, Inflammation, genes and zinc in ageing and agerelated diseases, *Biogerontology,* 7,315-27.

Vasto, S., Mocchegiani, E., Malavolta, M et al., 2007, Zinc and inflammatory/immune response in aging. *Ann N Y Acad Sci.,* 1100, 111-22.

Voegelin, A., Poster, S., Scheinost, A. C., Marcus, M. A., Kretzchmar, R., 2005, *Environ. Sci. Technol.,* 39, 6616.

Vulpe, C., Levinson, B., Whitney, S., Packman, S., Gitschier, J., 1993 Isolation of a candidate gene for Menkes disease and evidence that it encodes a copper-transporting ATPase. *Nature Genet.* 3**,** 7–13.

Vulpe, C. D., Kuo, Y. M., Murphy, T. L., Cowley, L., Askwith, C., Libina, N., et al., 1999, Hephaestin, a ceruloplasmin homologue implicated in intestinal iron transport, is defective in the *sla* mouse. *Nature Genet.* 21, 195–199.

Williams, A. T. R., Winfield S. A., Miller, J. N., 1983, Relative fluorescence quantum yields using a computer controlled luminescence spectrometer, *Analyst*, 108, 1067.

Wolfbeis, O. S. (Ed.), 1991, Fiber Optic Chemical Sensors and Biosensors, Vol. 1, CRC Press, London, p. 385.

Wolfbeis, O. S. (Ed.), 1991, Fiber Optic Chemical Sensors and Biosensors, Vol. 2, CRC Press, London, p. 341.

Wolfbeis, O. S., and Offenbacher, H., 1984, Preconcentration and semi-quantitative determination of aluminum (III) with immobilized morin, *Frez. Anal. Chem.,* 319, 282-285.

Wolbeis, O. S., and Schaffar, B. P. H., 1987, An ion-selective optrode for potassium, *Anal. Chim. Acta,* 198, 1-12.

World Food and Nutrition Study, 1977, Supporting papers, Vol. 11, pp. 74-84. Natl. Acad. Sci., Washington, DC.

Yamazoe, N. & Miura, N., 1996, Prospect and problems of solid electrolyte-based oxygenic gas sensors, *Journal of Solid State Ionics*, 86-88 (Part II), 987-993.

Yang, L., and Saavedra, S. S., 1995, Chemical sensing using sol-gel derived planar waveguides and indicator phases, *Anal. Chem.,* 67, 1307-1314.

Yang, X., Wang, K., Xiao, D., Guo, C., Xu, Y., 2000, Development of a fluorescent optode membrane for sodium ion based on the calix[4]arene and tetraphenylporphine, *Talanta,* 52, 1033-1039.

Yılmaz, I. and Çukurovalı, A., 2003, Salicylaldehyde thiazolyl hydrazones as ligands, *Heteroatom Chem.,* 14 (7), 617-621.

Yokel, R. A., 2000, The toxicology of aluminum in the brain: A review. *Neurotoxicology* 21**,** 813-828.

Zhang, X.B., Peng, J., He, C.L., Shen, G.L., Yu, R.Q., 2006, A highly selective fluorescent sensor for Cu^{2+} based on 2-(2'-hydroxyphenyl)benzoxazole in a poy(vinyl chloride) matrix, *Anal. Chim. Act,* 567,189-195.

Zhujun, Z., and Seitz, W. R., 1988, Ion-selective sensing based on potential sensitive dyes, *Proc. SPIE,* 906, 74.

CURRICULUM VITAE

Name	**:** Nur ERDEM AKSUNER
Citizenship	**:** Turkish Republic
Date of Birth	**:** 02.01.1976
Place of Birth	**:** İzmir
Private Address	**:** Mithatpaşa Cad. No: 889 D: 3 Göztepe-İZMİR
Occupation	**:** Chemist at Ege University, Faculty of Science, Department of Chemistry, 35100, Bornova-İZMİR
Marital Status	**:** Married
Foreign Languages	**:** English

Academic Status	**Department/Branch**	**Universty**	**Period**
B.Sc.	Chemistry	Ege	1992-1996
M.Sc.	Chemistry	Ege	1997-2001
Ph.D.	Chemistry	Ege	2001-2008